12-2013

Functional Stroke Recovery through Tissue Engineered Niche Neural Constructs

Natasha Topoluk
Clemson University, ntopolu@clemson.edu

FUNCTIONAL STROKE RECOVERY THROUGH TISSUE-ENGINEERED NICHE NEURAL CONSTRUCTS

A Thesis
Presented to
The Graduate School of
Clemson University

In Partial Fulfillment
Of the Requirements for the Degree
Master of Science
Bioengineering

By
Natasha Topoluk
December 2013

Accepted by:
Dr. Dan Simionescu, Committee Chair
Dr. Alfred Nelson Jr.
Dr. Jeremy Mercuri
Dr. Ken Webb

ABSTRACT

According to the Centers for Disease Control and Prevention, stroke is statistically responsible for 1 in every 19 deaths of American citizens.[5] Stroke is the leading cause of permanent disability due to the fact that it compromises both cellular and tissue components of the brain, leading to the formation of a physical void within the tissue.

Current research approaches address the cellular component by injecting stem cells into this void; however, extremely low cell engraftment, high injected cell death, and overall no matrix regeneration are observed. Additionally, these stem cells do not remain committed to a neural lineage. We propose to overcome these obstacles by incorporating a tissue engineered niche matrix component to the delivery of such stem cells. We hypothesize the implantation of this construct will lead to brain regeneration with complete sensory and motor functional recovery.

Niche neural constructs were successfully created and characterized in vitro. In addition to maintaining and supporting the life of induced neural-like cells, seeding HADSCs onto these scaffolds yielded spontaneous differentiation and overall extended cell viability.

After implantation into MCAO stroke-afflicted rats for 4 weeks, rats treated with niche neural constructs showed significant recovery when compared to stroked controls ($P<0.05$) as early as 2 weeks post-stroke culminating in 98% recovery. Histological evidence showed integration of the construct with host tissue, an absence of reactive astrocytes, widespread neovascularization, and significant tissue remodeling.

Additionally after 4 weeks the implanted cells were still committed to a neuron lineage and have remained engrafted to the construct area. Additionally, numerous non-human neurons were observed within the construct area, further indicating integration with host tissue and overall, validating this approach towards functional brain tissue regeneration.

ACKNOWLEDGEMENTS

First and foremost, I would like to thank Drs. Dan and Aggie Simionescu for their constant support and guidance. It is impossible for me to properly acknowledge all they have done for me and to further this research in this small space. I am forever indebted to them for their mentorship, trust, and patience.

Second, I would like to thank my committee members: Dr. Alfred Nelson Jr., Dr. Ken Webb, Dr. Jeremy Mercuri, and Dr. Dan Simionescu for their time and dedication to the successful progression of this research.

The research within this thesis could not have been completed without the cooperation and endless efforts of Godley-Snell Research Center. I deeply appreciate the dedication and commitment of their staff throughout all stages of this research.

Additionally, I would like to recognize Dr. Jeffrey Gimble for his promptness in his critiques and responses to my questions. I am humbled by the generosity LaCell LLC has shown as a provider of human adipose derived stem cells for this research.

Lastly, I would like to recognize Clemson Bioengineering for all they have done to ensure my professional development and success. Particularly, I would like to recognize all members of the Biocompatibility and Tissue Regeneration Laboratory. My colleagues provided an endless support network and were always willing to provide a helping hand. Specifically, my undergraduate mentor and current lab mate, James Chow, continues to go above and beyond: providing advice, constructive criticism, and protocol assistance.

TABLE OF CONTENTS

Page

TABLE OF CONTENTS (Continued) Page

TABLE OF CONTENTS (Continued) Page

LIST OF TABLES Page

LIST OF FIGURES Page

CHAPTER 1: INTRODUCTION AND BACKGROUND

1.1 Neural Anatomy and Physiology

The brain is divided into two almost completely symmetric hemispheres. Additionally, the brain can be divided into four lobes. Each lobe controls different bodily functions, but a complete map of the brain shows that different functions are associated with specific anatomical structures. These structures differ in their comprising matrix as well as the number and types of neural cells observed.

1.1.1. Matrix

Brain matrix can be divided into two categories, grey and white matter. Grey matter contains cell bodies, glial cells, and vessels. It is termed “grey” due to the lack of myelinated axons, which are characteristically white in color. White matter, then, is primarily composed of these myelinated axons as well as glial cells. Functionally, white matter is associated with action potentials and thus cognition via intra brain communication and body-brain communication. These structural differences allow for distinct histological identification between brain regions. Most notably, white mater will stain very heavily for myelin while grey matter will not stain. Additionally, white matter characteristically appears fragmented compared to grey mater. This fragmentation is largely due to the heavy lipid concentration within the matrix.

Glycosaminoglycans (GAGs) are one of the most well-characterized neural extracellular matrix (ECM) components.[1] GAGs are proteoglycans composed of a protein core with repeated disaccharide units. The polar nature of these molecules makes them extremely hydrophilic, functioning as a shock-absorbing material.

Additionally, GAGs within the brain function in cell signaling, tissue morphogenesis, neuronal cell migration, and axon regeneration.[1, 2] Though GAGs are widely present in healthy brain tissue, the up-regulation of chondroitin sulfate proteoglycans is a direct result of glial scar formation.[2] Thus any newly formed neural tissue with both a strong GAG presence and activated astrocytes should undergo further phenotypic examination as potential glial scarring.

Collagen and Laminin are notable fibrous components in the brain. Collagen IV is the dominating collagen type due to its presence in the basement membrane. Overall, fibrous components are not heavily present in the brain.[1] However they serve numerous functional roles including providing structure, directing cell differentiation and proliferation, and aiding in development.[1, 3]

1.1.2. Cellular Components

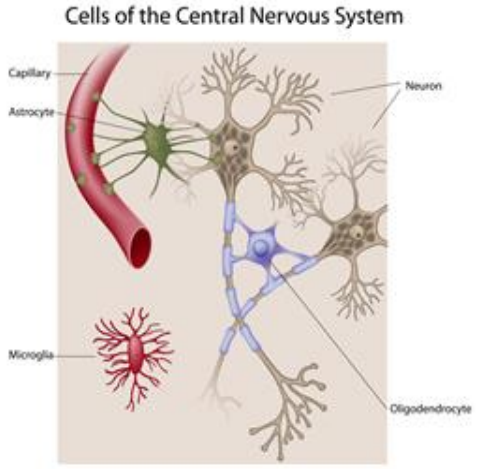

Figure 1: Astrocytes, microglia, and oligodendrocytes are all considered accessory cells to the neurons, which are the primary neural cell and function as chemical and electrical transport cells.

There are four main neural cell types, three of which are categorized as accessory cells to the neuron: astrocytes, microglia, and oligodendrocytes. Inactivated astrocytes are known for their maintenance of the blood-brain barrier through interactions with capillaries. The function of microglia is similar to that of leukocytes. Oligodendrocytes are the myelin producing cells within the brain, sheathing axons with electrical insulation. Lastly, the neuron is the chemical and electrical signaling cell responsible for the transmission of information to and from the brain and all other parts of the body.

1.2 Stroke

Cerebral ischemia, more commonly known as stroke, is responsible for 11.1% of all deaths worldwide.[4] According to the Centers for Disease Control and Prevention (CDC), stroke is statistically responsible for 1 in every 19 deaths of American citizens, costing over $38.6 billion in medical expenses.[5] The most alarming statistic of stroke comes from a 2011 study conducted by the CDC reporting that over the past 10 years, stroke prevalence has increased 40% in those aged under 30, leaving a larger and larger population debilitated for a longer period of time.[6]

1.2.1 Pathology

Just this year, the stroke council of the American Heart Association met to create what they termed a "working definition of stroke for the 21st century," and they determined stroke is brain cell death resulting from oxygen deprivation.[7] There are two main ways this can occur. In hemorrhagic stroke a cerebral blood vessel leaks or bursts. Secondly, in ischemic stroke a blood clot forms within a cerebral vessel. Ischemic stroke

is by far the more common, but regardless of type, due to nerve tract decussation, stroke symptoms occur contralateral to the damaged tissue.

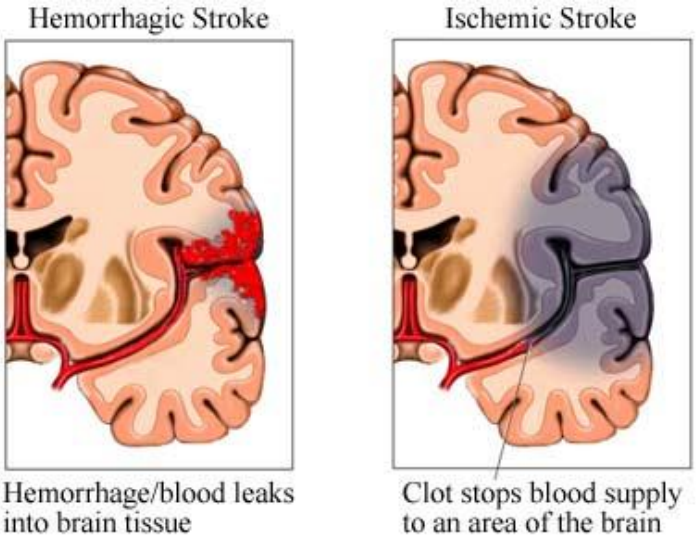

Figure 2: There are two main types of stroke. In the first, hemorrhagic, blood leaks into brain tissue after the bursting of a vessel. In ischemic stroke, there is actual blood clot formation within the cerebral vasculature.

Such clots produce both physical and functional damage. When this damage is left untreated extensive tissue necrosis occurs, leading to the formation of a tissue void within the neural cavity, as seen in figure 3.[8] This extreme body response is largely due

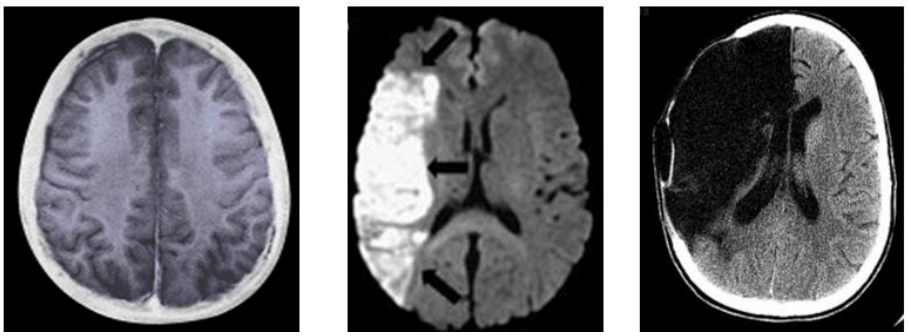

Figure 3: Stroke Progression. CT images showing the progression of lesion formation within the neural cavity. Left: the healthy brain. Middle: the brain shortly after stroke. Right: the lesion resulting from the necrosis of stroked tissue areas.

to the fact that the previously mentioned neural cell types, most notably the neuron, have limited to no regenerative capacity. When a neuron becomes damaged, the neural immune response is initiated which leads to the up-regulation of numerous cytokines and the disabling of cell adhesion molecules causing further cell death. Moreover, these events activate the astrocytes, initiating the cascades heralded as the inhibitors of neural regeneration, the most pressing example being the formation of the glial scar.[9]

1.2.2 Clinical Interventions

Tissue Plasminogen Activator (tPA) is the only drug approved for clinical use in treating stroke, and even its use is extremely confined by administration restrictions. Additionally, tPA is only effective in the treatment of ischemic stroke. As seen below in the current clinical scenario for a stroke patient, the most pressing piece of information is if it has been less or greater than three hours since the onset of symptoms.

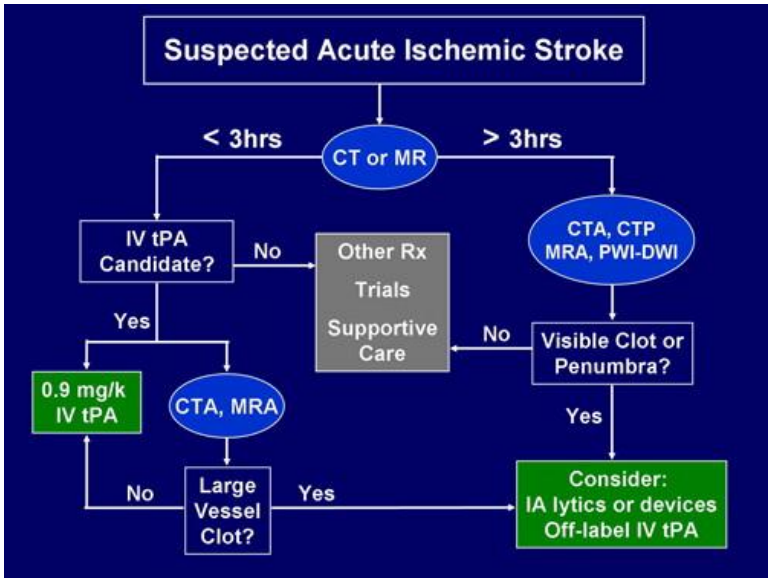

Figure 4: Current clinical scenario for a stroke patient highlighting the limitations of the only FDA approved stroke treatment, tPA, as well as demonstrating the significance of the three hours immediately following the onset of stroke symptoms.

tPA can only be administered if it has been less than three hours since symptom onset and the patient meets the drug use indications. If it has been more than three hours and there is visible damage on a CT or MRI, clot retrieval devices can by employed to restore blood flow. However, if it has been more than three hours and there is no visible damage, patients are simply moved to supportive care. In all of these cases, it is important to recognize that these clinical interventions treat the clot, not the functional damage the clot already caused. There is a dire need for solutions that aim to restore this physical and functional damage.

1.3 Treatment Approaches

Though tPA is the only FDA approved stroke treatment, there are promising research initiatives in all stages of development. Most of these methods aim to restore cell numbers to pre-ischemic levels through the administration of cells or pre-conditioned stem cells.

1.3.1 Cellular-Focused Approaches

Cell-focused stroke therapies typically employ neural progenitor cells or non-embryonic stem cells. The traditionally hypothesized mechanism of action is that these cells would migrate to damaged brain areas, and re-populate the area with viable cells by differentiating into various neural cell types.

Neural Progenitor Cells (NPCs)

Utilizing NPCs is very promising, because they have been proven to differentiate into all neural cell types.[10] Though recent studies have discovered new sources of NPCs in the adult brain, particularly in the sub-ventricular zone, these cells have limited

differentiation potential.[11] The only true source of neural progenitors is the fetal brain, shrouding NPC use in ethical concerns.[10]

Stem Cells

Non-embryonic stem cells, particularly bone marrow derived stromal cells and adipose derived stem cells do not have these ethical concerns. They have proven neural differentiation potential, and they can be donor specific to avoid rejection via the generation of an immune response.[12] Strong arguments favoring the use of human adipose derived stem cells (HADSCs) are the vast abundance of adipose tissue (compared to bone marrow), more tissue can be removed per procedure generating a higher stem cell yield, and the procedure to obtain the stem cells is far less invasive.[12-15]

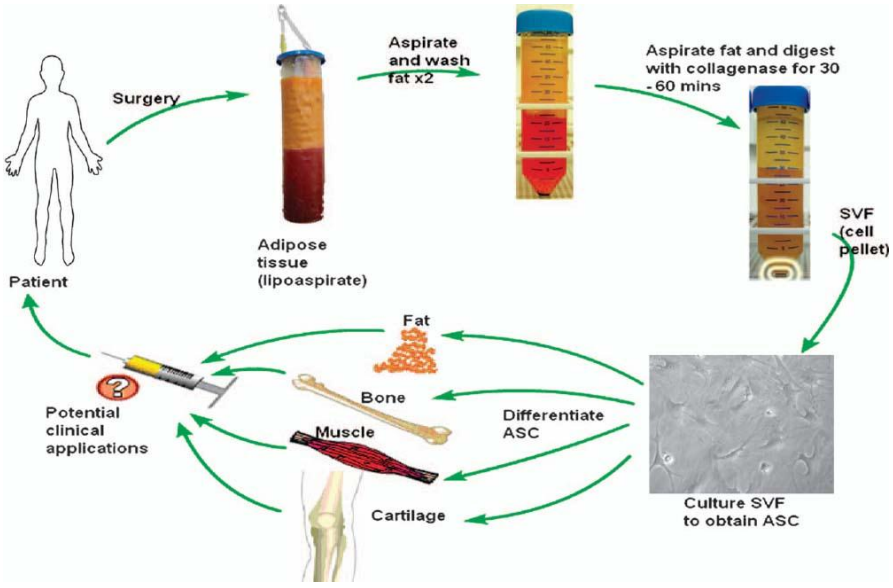

Figure 5: Human Adipose Derived Stem Cells. Lipoaspirate is obtained from the patient, this is enzymatically processed to obtain the stromal vascular fraction, and this fraction is plated and cultured to obtain the adipose derived stem cells. These stem cells have numerous proven differentiation lineages including neural applications.

As illustrated above, removed adipose tissue can be enzymatically processed yielding a stromal derived fraction, and this fraction can be cultured to obtain the HADSCs.

The testing of these stem cells in vivo has been widely documented. There are two main methods of administration, intravenous and intracranial injection. In both cases, stem cell therapies increase the treatment window from 3 hours to 7 or more days. Moreover, the behavioral testing results indicate varying degrees of functional recovery.[16-19] However, overall there is minimal cell retention to the target tissue. One of the most notable studies showed only a 1% retention rate to the brain.[18] There are also reports of extensive cell death, little to no decrease in the size of the lesion cavity, and overall poor differentiation. [16-20]

Evaluation of Differentiation

Unfortunately there is no one marker for neural cells, but there are a handful of commonly used markers indicating successful differentiation. The first such marker is

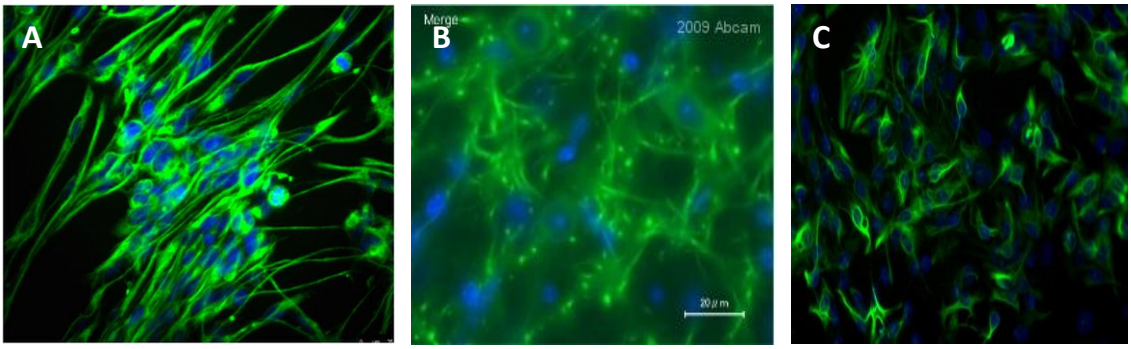

Figure 6: Commonly used markers of neural differentiation. A) Nestin, a cytoskeletal neural progenitor marker. B) Map-2, a cytoskeletal neuron marker. C) GFAP, a cytoskeletal astrocyte marker. Note: GFAP is regularly expressed by astrocytes, but it is heavily up regulated post neural injury.

Nestin which is a neural progenitor marker.[13-15] As figure 6A illustrates it is a cytoplasmic marker, and it is known to be minimally expressed by HADSCs.[14] Map-2 (figure 6B) is

also cytosolic as it is the protein responsible for the creation and maintenance of neural cell projections.[14, 15, 21] It is widely accepted in the literature that Map2 expression indicates a cell committed to a neuron lineage. Lastly, GFAP (figure 6C) is a structural cytoskeletal marker, and it is widely accepted that GFAP expression indicates an astrocyte or astrocyte-like cell.[14, 22]

1.3.2 Conditioning-Focused Approaches

In an effort to enhance the expression of such neural markers, researchers have begun chemically treating stem cells through a process known as neural induction.[13-15, 22, 23] It is impossible to reference neural induction without mentioning Woodbury, specifically his 2000 publication which is the foundation of all neural induction approaches (see figure 7). [24]

The medium used to induce differentiation is referred to as neural induction medium (NIM). Neural induction protocols typically differ in the chemical base of the NIM utilized for induction. Unfortunately, there is an inverse relationship between induced cell viability and success of differentiation.[25] Harsh chemicals yield extensive cell death with promising differentiation potential, while less intense chemicals yield strong, relatively undifferentiated cell populations. A balance of sustained neural differentiation and cell viability has yet to be attained.[23] As such, in vitro neural induction has a finite life calling any in vivo or clinical efficacy of the process into question. To date, neural induction has not been replicated in animal stroke models.[10]

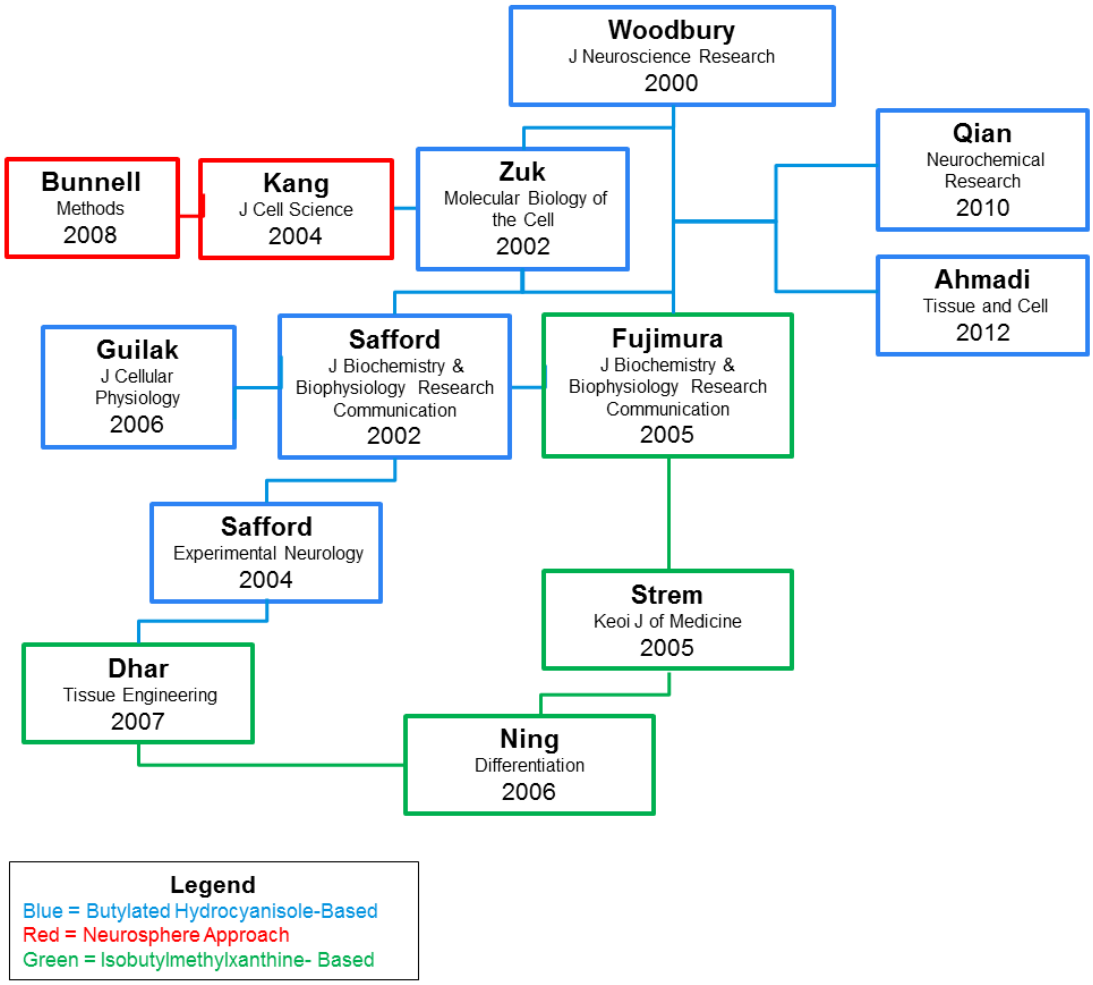

Figure 7: Neural Induction. Woodbury's 2000 publication can be seen as the gold standard for neural induction, as his neural induction medium is the chemical cocktail upon which all subsequent neural induction approaches have been based.

1.3.3 Extracellular Matrix-Focused Approaches

Overall, there is no investigation into the incorporation of a matrix component in the stroke-treatment field. This is surprising for a two main reasons. Firstly, as previously described, stroke compromises neural cells and neural tissue, so an effective treatment would need to address both of these components. Secondly, the benefits of the incorporation of a matrix are extremely well documented.[21, 26-28]

The extracellular matrix is the secretion products of resident cells.[26, 27] It is biomolecularly tissue-specific, so any slight change in the microstructure can alter resident cell phenotype and function. The ECM is a natural niche environment, meaning it contains the cues for cellular migration, proliferation, and differentiation.[21, 26-28] More notably, it has been proven to induce host tissue remodeling.[26]

For these reasons, extracellular matrix is incorporated into an array of regenerative approaches including the skin, kidney, lung, as well as other neural fields in the form of a gel.[21, 29, 30] Figure 8 shows a collagen gel used in traumatic brain injury models, and figure 9 illustrates a tissue engineered gel both loaded into the syringe and in reconstituted form after subcutaneous implantation.

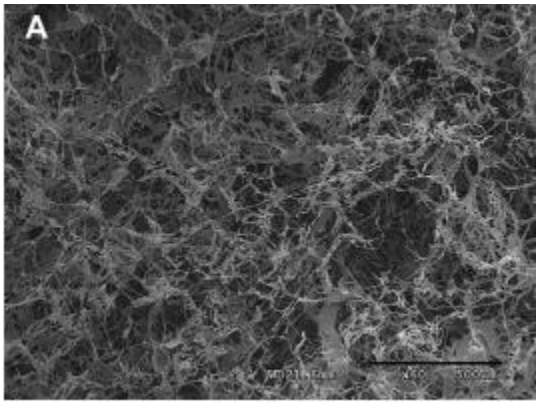

Figure 8: Scanning electron microscopy image of a collagen gel utilized in traumatic brain injury models.

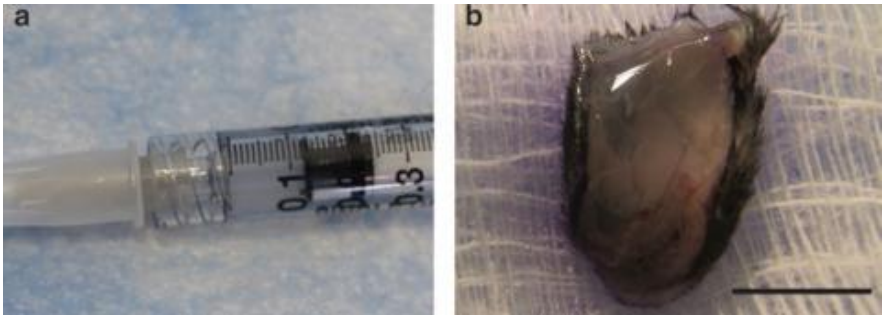

Figure 9: A tissue engineered gel loaded for delivery (left) and reconstituted (right).

The appeal of these gels is that their delivery would be minimally invasive.[29] However, gels are only approximations of the target tissue.[21] Therefore, in traumatic brain injury models, no real reduction in lesion cavity size and again no proven matrix regeneration are observed.[16, 30]

CHAPTER 2: PROJECT APPROACH

2.1 Overview

The creation of a matrix component that more closely mimics native brain tissue and its combination with the previously investigated cellular and induction will create a new platform for stroke treatment. For this reason, tissue engineering is the most appealing approach to further stroke treatment investigations.

The goal of tissue engineering is commonly described as creating functional substitutes for damaged tissues.[31] As illustrated below, the tissue engineering paradigm usually involves harvesting target xenogeneic tissues and chemically treating them through a process known as decellularization to obtain a matrix component, referred to as the scaffold.[26, 31-33] Simultaneously, adipose tissue is removed from the patient, and the tissue is processed to isolate the HADSCs. These HADSCs are then cultured and chemically treated through neural induction producing neural-like cells. These neural-like cells can then be seeded back onto the scaffold, and this resulting construct (cells + scaffold) can be implanted into the patient, ultimately returning living viable tissue to the damaged areas.

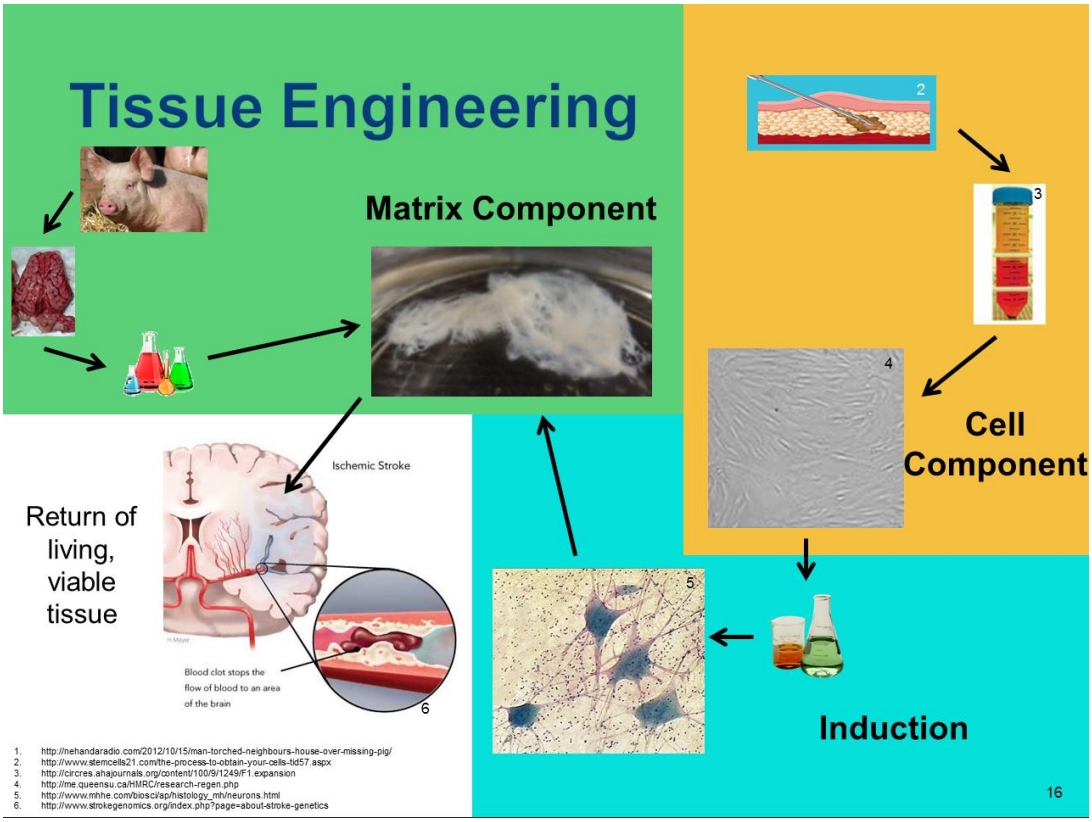

Figure 10: The tissue engineering paradigm: Porcine brains are chemically treated to obtain a matrix component referred to as a scaffold. Simultaneously, adipose tissue is removed from the patient and this tissue is processed to obtain the adipose derived stem cells. These cells are chemically treated through neural induction and seeded onto the scaffold. The resulting construct is then implanted into the stroke patient ultimately retuning living tissue and overall function to the area.

The long-term goal for this project is the creation of a clinical alternative for patients suffering from stroke that yields complete functional recovery. Ultimately such a recovery involves regeneration of viable native neural tissue in areas compromised by stroke. This regenerated tissue will not be immunogenic, will fully integrate with host tissue, will maintain properties necessary for neural cell growth and maintenance, and will ultimately lead to complete restoration of lost function. The hypothesis being examined is that niche tissue-engineered scaffolds reseeded with adipose derived stem

cells will, upon implantation, return living neural tissue and restore overall function to area compromised by stroke.

2.2 Specific Aims

Validating the hypothesis that neural tissue regeneration and therefore functional stroke recovery can be achieved through this tissue engineering approach requires the successful completion of three specific aims.

2.2.1 Aim I: Create and Characterize a Tissue-Engineered Neural Scaffold

Our goal is to utilize tissue engineering methods to create a neural scaffold that will efficiently serve as a biomimetic stem cell niche for the next generation of stroke treatment investigations. Through decellularization, we can utilize the native architecture of porcine brains to generate niche neural scaffolds. This scaffold should contain an intact matrix, be free of cells and DNA, have retained basement membrane proteins.

2.2.2 Aim II: Analyze Stem Cell Niche Potential of Scaffold In Vitro

Our goal is to determine if the novel scaffold created and characterized in Aim 1 is in fact a stem cell niche. Therefore, our scaffold must ultimately mimic native neural tissue by producing un-aided neural differentiation and providing a suitable environment for sustained neural-like cell survival and maintenance. Most notably, this involves retaining high levels of viable cells and ensuring that these cells are retaining their neural-like characteristics through protein expression analyses. Additionally, neural cell morphologies and alignments must be considered.

2.2.3. Aim III: Establish Preliminary Efficacy of Niche Constructs In Vivo

Our goal is to employ the niche neural construct developed in specific aim 2 as a stroke treatment that upon implantation, returns living neural tissue and therefore overall function to areas compromised by stroke. Short-term, this involves improved motor and sensory control; long-term, this involves brain tissue regeneration.

CHAPTER 3: MATERIALS AND METHODS

3.1 Experimental Methods

The following protocols were used in the creation and in vitro and in vivo testing of our niche neural scaffolds and constructs.

3.1.1 Decellularization

Porcine brains were ordered from Animal Technologies Inc. (Tyler, Texas). The brains were collected from animals aged 2+ years, and were removed leaving the carotid arteries intact. The experimental protocol for immersion decellularization was modified from DeQuach, Jessica A., et.al. and is as follows.[21] There were no deviations from this protocol.

Decellularization Process:

1. Remove cerebellum, and cut cerebrum in half. Place each half of the brain in a separate decellularization container
2. Immerse brains in fresh decellularization solution overnight under agitation
3. Repeat step number 2 until brain is decellularized (appears transparent with no residual cream/tan colored matrix and the solution is clear). This takes approximately 14 days
4. Initiate washing procedure

Washing Process:

1. Rinse in 1x PBS for 20 minutes under agitation
2. Rinse in 70% Ethanol for 20 minutes under agitation
3. Rinse in 70% Ethanol overnight under agitation

Remaining step should be completed using aseptic technique

4. Place in 70% Ethanol for 20 minutes under agitation
5. Rinse in 1x sterile PBS for 20 minutes under agitation
6. Rinse in 1x sterile PBS overnight under agitation
7. Rinse in 1x sterile PBS for 20 minutes under agitation
8. Immerse scaffolds in DNase/RNase rinse (1L 1x PBS + 3.7mg RNase + 1.015g $MgCl_2$ + 100µL of 1.8mg DNase/1mL ddH_2O solution) for 72 hours
9. Rinse in 1x sterile PBS for 20 minutes under agitation (3x)
10. Rinse in 1x sterile OBS overnight

Sterilization Treatment:

1. Rinse scaffolds in peracetic acid (250µL peracetic acid + 250mL 1x PBS) for 3 hours
2. Rinse in 1x sterile PBS for 20 minutes under agitation (2x)
3. Rinse in 1x sterile PBS overnight under agitation
4. Rinse in 1x sterile PBS for 20 minutes under agitation (3x)
5. If scaffolds will not be used immediately, store at 4° C in storage buffer

<u>Solution Preparation</u>

1. Decellularization Solution
    a. Combine 0.99 g Sodium dodecyl sulfate (wear mask) in 990mL 1x PBS
    b. Stir in 10mL penicillin/streptomycin
    Result: 100mL 0.1% wt/vol SDS in PBS with 1% antibiotic/antimitotic
2. Storage Buffer
    a. Combine 20mg Sodium azide in 100mL 1x PBS
    b. Stir in 10µL protease inhibitor cocktail
    Result: 100mL 0.2% wt/vol Sodium azide in PBS with 1% protease inhibitor cocktail

Total decellularization protocol takes approximately 22 days.

3.1.2. Histological Tissue Fixation

All tissues to be histologically processed were first fixed in 10% neutral buffered formalin. Porcine scaffolds were cut as illustrated in figure 11A prior to tissue to processing, embedding in paraffin wax, and sectioning at 5μm. Explanted rat brains were cut into coronal thirds such that the implanted materials were confined to the middle portion (as illustrated in figure 11B) prior to processing, embedding in paraffin wax, and sectioning at 5μm.

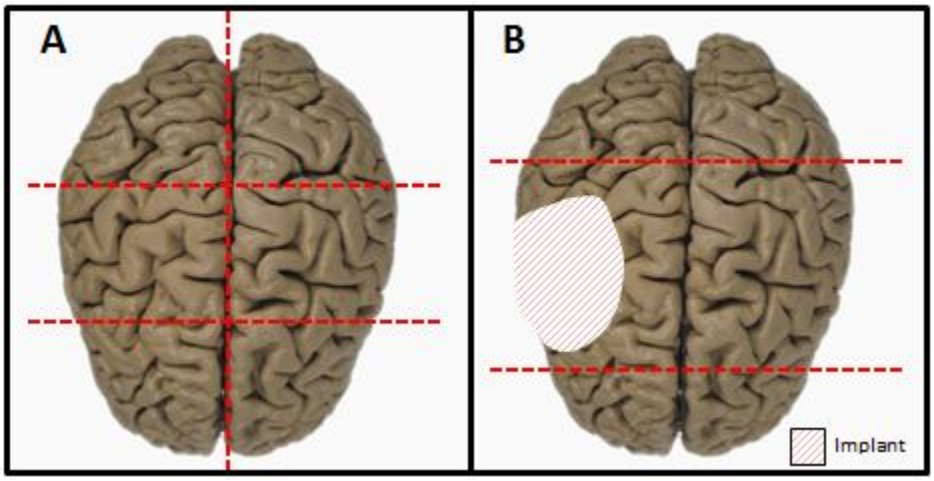

Figure 11: Orientation of tissues prior to processing. Left, porcine scaffolds and fresh samples were cut into 6 relatively equal sections. Right, rat explants were cut such that the implants were confined to the middle section.

3.1.3 Hematoxylin and Eosin Sections

Hematoxylin and Eosin (H&E) staining is a commonly employed method of generic cellular and matrix staining. The hematoxylin stains nuclei and other basophilic substances blue, while the eosin stains cytoplasm and tissue elements various shades of pink. Slides were stained according to the Richard-Allan™ H&E protocol listed below.

1. Xylene _____ 10 dips
2. Xylene _____ 5 min
3. 100% EtOH _____ 10 dips
4. 100% EtOH _____ 1 min
5. 95 % EtOH _____ 10 dips
6. 95% EtOH _____ 1 min
7. Running H_2O _____ until clear
8. Distilled H_2O _____ 1 min
9. Hematoxylin _____ 5 min
10. Running H_2O _____ until clear
11. Clarifier _____ 10-15 dips
12. Running H_2O _____ until clear
13. Bluing _____ 1 min
14. Running H_2O _____ 30 sec
15. 95% EtOH _____ 10 dips
16. Eosin _____ 45 sec
17. 95% EtOH _____ 10 dips
18. 95% EtOH _____ 10 dips
19. 100% EtOH _____ 10 dips
20. 100% EtOH _____ 10 dips
21. 100 % EtOH _____ 2 min
22. Xylene _____ 10 dips
23. Xylene _____ 5 min

3.1.4 Masson's Trichrome Sections

Masson's Trichrome is a staining method typically employed to clearly differentiate between collagen, blue, and muscle and fibrous components, red, (cell nuclei stain black). Slides were stained according to the Poly Scientific Masson's Trichrome Method listed below. Note that the sections were left in Aniline Blue solution for 20 minutes.

1. Deparaffinize and hydrate to distilled water
    a. Xylenes 10 Dips
    b. Xylenes 5 Minutes
    c. 100% Ethanol 10 Dips
    d. 100% Ethanol 1 Minute
    e. 95% Ethanol 10 Dips
    f. 95% Ethanol 1 Minute
    g. Tap Water Until "sheeting" action occurs
    h. Distilled Water 1 Minute
2. Mordant Bouins Fixative for 1 hour at 56°C or overnight at room temperature, if formalin fixed
3. Cool and wash in running water until yellow color disappears
4. Rinse in distilled water
5. Place in Weigert's Iron Hematoxylin Working Solution for 10 minutes
6. Wash in running water for 10 minutes
7. Rinse in distilled water
8. Place in Biebrich Scarlet – Acid Fuchsin for 2 minutes
9. Rinse in distilled water
10. Place in Phosphotungstic – Phosphomolybdic Acid for 10 minutes
11. Place in Aniline Blue Solution for 5 minutes (For central nervous system, leave for 15-20 minutes)
12. Rinse in distilled water
13. Place in Acetic Acid 1% Aqueous for 3 minutes.
14. Dehydrate in 95% Alcohol, Absolute Alcohol, and clear in Xylene, two changes each

*Note: To ensure proper mordanting, Bouins Fixative should be pre-heated

3.1.5 Bielschowsky Neural Stain Sections

The Bielschowsky Lester-King method is a silver staining technique employed in the diagnosis of Alzheimer's disease due to its deep brown staining of senile plaques. In this case the stain was employed, because it clearly stains nuclei and neuronal axons black (This allows analysis of cellular interactions as well as serves as an additional decellularization assessment). White and gray matter stain yellow to brown. Sections were stained according to the Newcomer Supply Lest-King method which is listed below. Note that all glassware was cleaned using Hydrochloric Acid, 0.15% Aqueous Solution and rinsed in at least six changes of distilled water prior to use. Sections were developed for 6 minutes.

1. Deparaffinize and hydrate to distilled water
    a. Xylenes 10 Dips
    b. Xylenes 5 Minutes
    c. 100% Ethanol 10 Dips
    d. 100% Ethanol 1 Minute
    e. 95% Ethanol 10 Dips
    f. 95% Ethanol 1 Minute
    g. Tap Water Until "sheeting" action occurs
    h. Distilled Water 1 Minute
2. Place slides in preheated 37°C Solution A, Silver nitrate Solution, 20% Aqueous for 15 minutes
3. Take slides out of solution A and place in distilled water
4. Add solution B, Ammonium Hydroxide, 28-30% drop by drop into the heated Solution A until precipitate disappears (Approximately 10mL). Stir with glass rod
5. Place slides back in to this ammoniacal silver solution in 37°C environment
6. Place slides in distilled water bath
7. Add 1 drop of solution C, Developer to the ammoniacal silver solution. Stir with glass rod
8. Return slides to the solution for 5-15 minutes in 37°C environment. Inspect slides in 3 minute intervals under the microscope
9. Rinse thoroughly in distilled water for 5 minutes
10. Put slides in Solution D, Sodium Thiosulfate, 5% Aqueous Solution for 5 minutes
11. Rinse thoroughly in tap water
12. Dehydrate through graded ethyl alcohols, clear in xylene

*Note: All glassware used in this staining method should be acid washed prior to use

3.1.6 Alcian Blue Sections

Alcian Blue is a staining method for glycosaminoglycans (GAGs) where cell nuclei stain red, cytoplasm stains pink, and GAGs stain blue. Though concentrations and types of GAGs change with development, the mature brain retains a large amount of GAGs. The below protocol was utilized to visualize this GAG composition.

1. Deparaffinize and hydrate to distilled water
    a. Xylenes 10 Dips
    b. Xylenes 5 Minutes
    c. 100% Ethanol 10 Dips
    d. 100% Ethanol 1 Minute
    e. 95% Ethanol 10 Dips
    f. 95% Ethanol 1 Minute
    g. Tap Water Until "sheeting" action occurs
    h. Distilled Water 1 Minute
2. Mordant in Acetic Acid 3% Aqueous for 3 minutes
3. Place in Alcian Blue 1% in 3% Acetic Acid (pH 2.5) for 30 minutes
4. Wash in running water for 10 minutes
5. Rinse in distilled water
6. Counter-stain in Nuclear Fast Red 0.1% for 5 minutes
7. Wash in running water for 1 minutes
8. Dehydrate in 95% ethanol, 100% ethanol, and xylene (reverse order of steps a-h above).
9. Mount and coverslip

3.1.7 Movat's Pentachrome Sections

Movat's pentachrome is an efficient stain utilized to clearly differentiate between five common matrix components. This stain is particularly useful in scaffold characterization and analysis of tissue development. Cellular nuclei stain black, elastin fibers stain purple-black, collagen stains yellow, ground substance (GAGs) stains blue, and muscle/fibrinoid stain red.

1. Deparaffinize and hydrate to distilled water
    a. Xylenes 10 Dips
    b. Xylenes 5 Minutes
    c. 100% Ethanol 10 Dips
    d. 100% Ethanol 1 Minute
    e. 95% Ethanol 10 Dips
    f. 95% Ethanol 1 Minute
    g. Tap Water Until "sheeting" action occurs
    h. Distilled Water 1 Minute
2. Rinse thoroughly in distilled water
3. Place in Alcian Blue 1% in 1% Acetic Acid for 20 minutes
4. Wash in running water for 3 minutes
5. Place in Alkaline Alcohol (pH must be over 8) for 2 hours
6. Wash in running water for 10 minutes
7. Rinse in 70% Alcohol
8. Place in Fuchsin Working solution for 16 hours
9. Wash in running water for 10 minutes
10. Rinse in distilled water
11. Place in Weigert's Hematoxylin Working solution for 15 minutes
12. Rinse in dunning water
13. Rinse in distilled water
14. Place in Woodstain Scarlet – Acid Fuchsin solution for 5 minutes
15. Rinse in Acetic Acid 0.5% Aqueous
16. Differentiate in Phosphotungstic Acid 5% Aqueous for 10-20 minutes
17. Rinse in Acetic Acid 5% Aqueous
18. Rinse thoroughly in 3 changes of Absolute Alcohol
19. Place in Saffron Du Gratinais 3% Alcoholic for 5-15 minutes
20. Dehydrate in graded alcohols, clear in Xylene

3.1.8 Luxol Fast Blue Staining

Luxol Fast Blue is a prominent method for staining myelin and Nissil substances in neural and spinal tissue sections. In this method, myelinated fibers stain blue and Nissil substances and nerve cells stain violet.

1. Deparaffinize sections if necessary and hydrate in distilled water
2. Incubate slide in Luxol Fast Blue Solution for 24 hours at room temperature or 2 hours at 60°C.
3. Rinse slide thoroughly in distilled water.
4. Differentiate the section by dipping in Lithium Carbonate Solution several times (up to 20 seconds).
5. Continue differentiation by repeatedly dipping in Alcohol Reagent until gray-matter is colorless and the white-matter remains blue.
6. Rinse slide in distilled water.
7. Incubate slide in Cresyl Echt Violet for 2-5 minutes.
8. Rinse quickly in distilled water.
9. Dehydrate quickly in 3 changes of absolute alcohol.
10. Clear and mount in synthetic resin

3.1.9 Immunohistochemical Examination

Immunohistochemistry (IHC) is a popular staining method for protein expression. Positive staining, indicative of matrix or cellular expression of the targeted protein, appears brown. All antibody preparations were made at the manufacturer (Abcam) recommended dilution.

Table 1: List of Antibodies		
Antibody Name	Serum Source	Antigen Source
Anti Nestin	Rabbit	Human, rat, porcine
Anti Map-2	Rabbit	Human, rat, porcine
Anti GFAP	Rabbit	Human, rat, porcine
Anti Mitochondria	Mouse	Human
Goat anti Rabbit	Goat	Rabbit
Donkey anti Mouse	Donkey	Mouse

Table 1: List of all antibodies including serum and antigen source.

3.1.9.1 Manual Method

Table 1 lists all antibodies used during IHC assays. These same antibodies were utilized in immunofluorescence staining (see section 3.1.15).

1. Deparaffinize and hydrate sections to water.
2. Place slides in 10mM citric acid monohydrate (pH 6.0)
3. Place in histology lab microwave and put power setting to 5. Microwave for 5 minutes, check temperature at 2.5 minutes. Repeat for a total of 20 minutes, the last 10 minutes of microwaving will yield a citric acid solution temperature between 90 - 100°C (monitor for evaporation)
4. Allow buffer and slides to cool to room temperature (~30-60 minutes).
5. Rinse slides twice in TBS for 5 min each
6. Circle sections with a Vector "immedge pen"
7. Rinse twice in 0.025% Triton for 5 min
8. Rinse once in TBS for 5 min
9. Incubate sections in normal blocking serum for 45 min at room temperature
10. DO NOT RINSE SLIDES. WICK THEM WELL (blot excess serum from sections)
11. Apply primary antibody made in TNB buffer. USE TBS FOR NEGATIVE CONTROL. Incubate at room temperature for 1 hour or overnight at 4°C in humidified chamber.
12. Following incubation, rinse twice in TBS for 5 minutes each.
13. Block the endogenous peroxidase with 0.3% H_2O_2 in 0.3% normal serum in TBS for 30 min
14. Rinse twice in TBS for 5 min each
15. Apply secondary biotinylated antibody for 30 minutes at room temperature
16. Rinse twice in TBS for 5 min
17. Apply R.T.U. ABC complex for 30 min at room temperature
18. Rinse twice in TBS for 5 min
19. Develop with DAB
20. Rinse in tap water for 5 min
21. Counterstain in diluted hematoxylin (50% hematoxylin, 50% water) for 1 minute
22. Rinse in water
23. Dehydrate, clear, and mount

Solution Preparation:

Tris Buffer Saline (TBS) → 6.05 g TRIS, + 8.95 g NaCl + 1L water, pH to 7.5

0.3% H_2O_2 in 0.3% normal serum in TBS → 1.8 mL TBS + 6ul normal serum + 200ul 3% H_2O_2

0.025% Triton → 25ul Triton + 100mL TBS

Normal blocking serum (1.5%) (Vectastatin kit) → 30uL horse normal serum + 2mL TBS

TNB buffer → 1mL blocking reagent solution from Western Blot kit) + 19mL TBS

Secondary antibody → 30uL normal horse blocking serum + 2mL TBS + 10uL biotinylated IgG

ABC complex → provided as Ready To Use from Vector

DAB substrate solution → 5mL water + 2 drops Buffer Stock Solution, mix well, then add 4 drops DAB stock solution, mix well, then add 2 drops H_2O_2, mix well

3.1.9.2 Automated Method (Using the Leica Bond System)

The Leica Bond Max instrument preforms automated IHC using the highly specific Leica polymer detection system. This method of IHC was used for all explant IHC analyses.

3.1.10 Qiagen DNA Purification

The Qiagen DNeasy Blood and Tissue Kits is a silica-based DNA purification system which prepares DNA samples for both qualitative and quantitative analysis. This research employed the protocol for purification of total DNA from animal tissue, listed below.

1. Cut up to 25mg tissue into small pieces and place in a 1.5mL microcentrifuge tube. Add 180µL Butter ATL
2. Ensure a hole is punctured in the top of the cap
3. Place samples in -80°C freezer overnight
4. Lyophilize tissues for 24 hours
5. Remove from lyophilizer, and replace punctured cap with a new cap.
6. Add 20µL proteinase K and mix thoroughly by vortexing. Incubate at 56°C until tissue is completely lysed
7. Vortex for 15s. Add 200µL Buffer AL and mix thoroughly by vortexing. Add 200µL 100% ethanol and mix again by vortexing
8. Pipet the mixture from step 3 into the DNeasy Mini spin column placed in a 2mL collection tube. Centrifuge at 8000rpm for 1 minute. Discard flow-through and collection tube
9. Place in DNeasy Mini spin column in a new collection tube. Add 500µL Buffer AW1 and centrifuge at 8000rpm for 1 minute. Discard flow-through and collection tube
10. Place in DNeasy Mini spin column in a new collection tube. Add 500µL Buffer AW2 and centrifuge at 14000rpm for 3 minute. Discard flow-through and collection tube
11. Place the DNeasy Mini spin column in a clean 2mL microcentrifuge tube. Pipet 200µL Buffer AE directly onto the DNeasy membrane. Incubate at room temperature for 1 minute prior to centrifugation at 8000rpm for 1 minute
12. Repeat step 7 once for maximum DNA yield

3.1.11 Ethidium-Bromide DNA Agarose Gel Electrophoresis

Gel electrophoresis separates molecules (in this case DNA) by size and or charge. An electric field is applied, and the negatively charged DNA molecules move away from the edge of the gel producing bands. The below protocol was used for gel preparation and analyses.

Gel Preparation:

1. Prepare Agarose gel by combining 0.5x TBE with 1g Agarose
2. Microwave gel for 1.5 minutes, pausing every 30 seconds to stir. Allow cooling to 60°C prior to pouring into mold
3. Add 5µL Ethidium bromide to Agarose gel. Mix
4. Pour the gel in the mold and place the comb(s)

Sample and Standard Preparation:

1. Samples
    a. Add 4µL loading dye to 16µL purified DNA sample
    b. Spin down prior to loading
    c. Load 20µL into 1st well
2. Standards:
    a. Add 4µL of DNA Sodium salt standard (500µg/mL, Sigma) to 4µL loading dye and 12µL ddI water
    b. Spin down prior to loading
    c. Load 20µL into 1st well
3. Run gel at 100V for 60 minutes

Solution Preparation:
10X TBE Buffer: Combine 21.8g TRIS + 11g Boric Acid + 0.93g EDTA in 200mL ddI water. pH to 8.3
Electrode Buffer: Combine 75mL of 10x TBE buffer with 1475mL of ddI water

3.1.12 Nano Drop 200C Analysis

Nano Drop 200C utilizes very low volumes of purified DNA to generate quantitative DNA measurements through UV absorbance. DNA absorbs light of wavelength 260nm. The amount of light absorbed indicates increasing amounts of DNA in the sample.

1. Establish a blank using the appropriate buffer (For samples that have been purified through Qiagen Kit, use AE buffer)
    a. Pipette 2µL buffer onto lower pedestal
    b. Carefully lower the top arm
    c. Record measurement
2. Wipe away the blank (wipe both top and bottom pedestals)
3. Enter the sample ID
    a. Pipette 2µL sample onto lower pedestal
    b. Carefully lower the top arm
    c. Record Measurement

3.1.13 Cellular Maintenance and Seeding

HADSCs

HADSCs (Invitrogen) were maintained with the manufacture recommended media, MesenPRO. Cells were expanded until passage 3-6 prior to use in these studies. HADSCs utilized during the in vivo studies were donated from LaCell LLC, and maintained according to the previously described conditions.

Rat Cortical Astrocytes

Astrocytes (Invitrogen) were maintained with the manufacture recommended medium, the Astrocyte Growth Medium Bulletkit ®. Astrocytes were expanded up to passage 7 prior to use in these studies.

Cell Seeding

All cell types underwent the same drop-wise cell seeding method using their respective mediums. Briefly, prior to seeding, cells were re-suspended in the total volume of media necessary such that 2mL suspension/well (cells seeded onto plastic) or 105µL suspension/well (cells seeded onto scaffolds) was pipetted slowly over the top of each lyophilized scaffold.

3.1.14 Live/Dead Staining

Live/Dead staining is a common qualitative assessment of cell viability. Calcein stains live cells a vibrant green via the enzymatic conversion of Calcein AM within cells to Calcein. Ethidium homodimer enters damaged cell membranes and binds to any remaining nucleic acids, producing red fluorescence.

1. Rinse cells/scaffolds with warm (37°C) PBS (3x)
2. Add enough dye solution to cover cells/scaffolds
3. Incubate in the dark at room temperature for 30 minutes

Dye Solution Preparation:

1. Transfer 10µL of 2mM EtdD stock solution to 5mL sterile PBS
2. Vortex yielding 4mM Eth-1 solution
3. Transfer 2.5µL Calcein stock solution to solution from step 1
4. Vortex
5. Protect from light until use

3.1.15 Immunofluorescence

Immunofluorescence is a popular staining method for protein expression. Cells that are expressing the protein will fluoresce light at a wavelength dictated by the emission spectra of the secondary antibody, in this case green. All antibody preparations were made at the manufacture (Abcam) recommended dilution.

1. Rinse cells with warm (37°C) PBS
2. Fix cells with warm (37°C) paraformaldehyde for 20 minutes
3. Rinse cells with PBS (3x)
4. Permeabilize with 0.2% Triton in PBS for 10 minutes
5. Block with 5% Bovine Serum Albumin and 0.05% Triton in PBS for 45 minutes
6. Apply 1° antibody for 2 hours at room temperature or overnight at 4°
7. Rinse with PBS (3x)
8. Apply 2° Alexa Fluor antibody for 1 hour at room temperature. Protect from light
9. Rinse with PBS
10. Mount in DAPI

Solution Preparation:
Triton: 998mL ddH_2O + 2mL Triton
Blocking Solution: 5gBSA + 50µL Triton + 100mL 1xPBS
Anti-Nestin 1°: 40µL primary + 7960µL blocking solution
Anti-Map-2 1°: 32µL primary + 7968µL blocking solution
Anti-GFAP 1°: 8µL primary + 7992µL blocking solution
Anti-Synapsin I 1°: 8µL primary + 7992µL blocking solution
2° antibody: 24µL primary + 11976µL blocking solution

3.1.16 DAPI Staining

4', 6-diamidino-2-phenylindole (DAPI) is a popular counterstaining method in fluorescent techniques. DAPI binds strongly to certain nucleic acid residues fluorescing blue, making it a strong cell nucleus marker. DAPI counterstaining validates positive immunofluorescence staining by co-localizing the staining with a cell nucleus. DAPI was applied directly onto samples prior to fluorescent imaging.

3.1.17 2,3,5-triphenyltetrazolium chloride (TCC) Staining

TCC staining is a common method of confirming tissue infarction. TCC salts react with dehydrogenase enzymes in cells resulting in a red-purple stain. Infarcted tissues lack these enzymes, leaving the tissue a pale-cream color.

Staining Procedure:

1. Immerse brains in saline to facilitate cutting. Cut brains into 3mm coronal sections
2. Completely immerse brains into TCC solution
    a. Completely protect from light
    b. Incubate at 37°C for 15 minutes
3. Carefully aspirate TCC and fix brain sections in warm 4%pFA

TCC Solution Preparation:

1. Prepare 2% TCC Staining Solution
    a. Make Saline (9g NaCl in 1L ddH_2O)
    b. Dissolve 20g TCC salt into 1L saline
2. Protect solution from light before and during use
3. Warm prior to use in 37° C water bath

3.2 Scaffold Creation and Characterization

Neural scaffolds were created following the previously described decellularization protocol. Prior to use, all scaffolds were rinsed 3x with sterile PBS, followed by an overnight rinse in sterile PBS, and 3x rinse with sterile PBS to ensure removal of storage buffer prior to use in any assay or histological process.

Scaffold characterization involved histological examination to ensure removal of cellular and DNA containing components as well as confirm the presence of an intact extracellular matrix. Additionally, more specific stains were employed to determine the matrix composition of the scaffolds and compare this composition with that of native brain.

Lastly, retention of key basement membrane proteins was examined. Collagen IV and Laminin are commonly assessed basal lamina proteins, because as previously described, they facilitate cell proliferation, differentiation, adhesion, and viability. Additionally, Laminin is a known promoter of neural differentiation and GABAergic cell proliferation.[3] Retention of these proteins is key in the effort to produce a niche neural scaffold, meaning a scaffold that acts as a stem cell niche by promoting unaided differentiation of stem cells into neural cells and maintaining the viability and neural-likeness of these cells.

3.3 In Vitro Experimentation

The in vitro experimentation focused on determining the niche stem cell potential of our scaffolds. Studies were devised such that potential niche stem cell groups were directly compared to induced stem cells groups of similar conditions. Initial studies were completed in plastic culture wells to establish base measurements of cell viability and successful differentiation. Most preliminarily, the method of inducing cells via neural induction was replicated to ensure our results would be comparable to the current literature.

3.3.1 Cells Seeded onto Plastic

<u>In Vitro Study 1</u>

To confirm the efficacy of neural induction, human adipose derived stem cells (HADSCs, Invitrogen) were seeded into tissue culture well plates at a seeding density of 1500cells / mm^3. Cells were allowed 48 hours to adhere before replacing the MesenPRO culture media with NIM. The NIM remained for 4hour, 24 hour, or 5 day time points after

which time protein expression for neural markers and cell viability were analyzed through immunofluorescence and Live/Dead staining, respectively. Controls for this study included HADSCs with no induction step and rat cortical astrocytes (Lonza). All controls were seeded at the same density as the test group and allowed 48 hours to adhere. After 48 hours, protein expression for neural markers and cell viability were analyzed through immunofluorescence and Live/Dead staining, respectively. An outline of the study can be seen in figure 12.

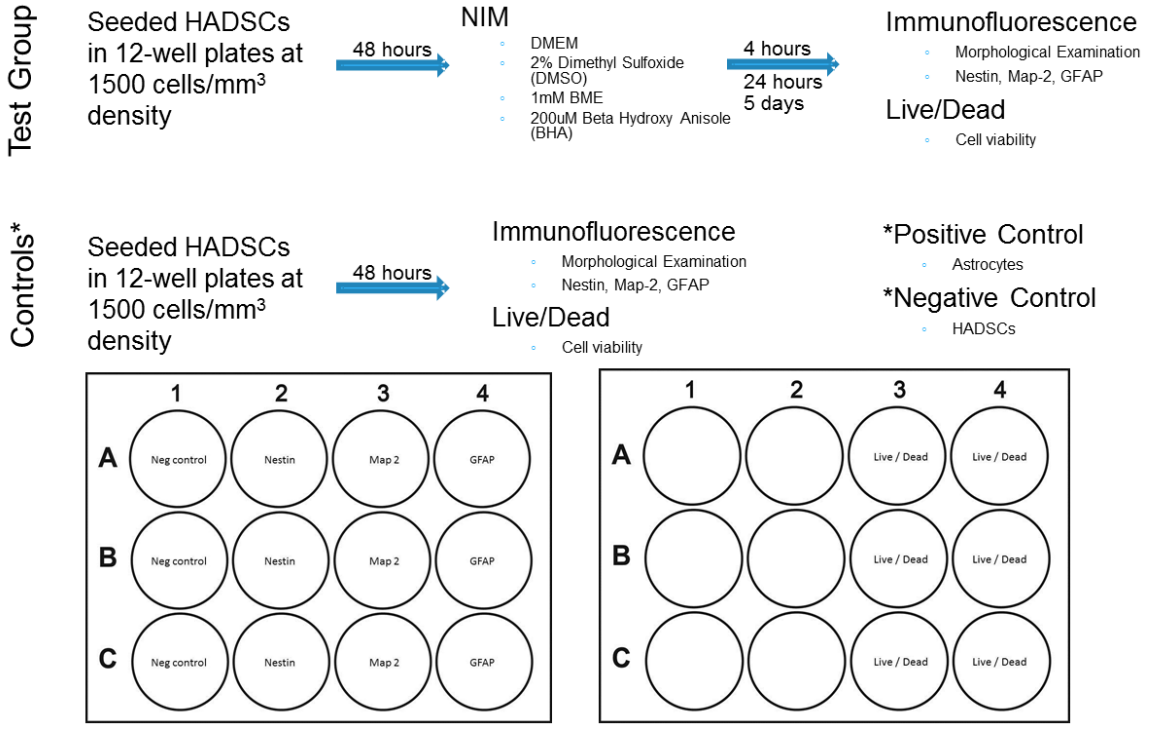

Figure 12: Detailed explanation of study 1: cells seeded onto plastic.

In Vitro Study 2

In an effort to determine if the low viability associated with neural induction results from a lack of nutrient supply, study 2 was completed following the exact

methods described for the treatment group in study 1, except the NIM was replaced daily.

3.3.2 Cells Seeded onto Scaffolds

In preparation for cell seeding, sterile scaffolds were cut into 5mm diameter punches and spread throughout the base of one 96-well tissue culture plate well. Scaffolds were frozen in -80°C overnight prior to lyophilization for 24 hours.

To allow direct comparisons between groups, the methods of studies 3 and 4 exactly mirror those of in vitro studies 1 and 2, respectively. A schematic of methods for scaffold preparation and study 3 can be seen in figure 13.

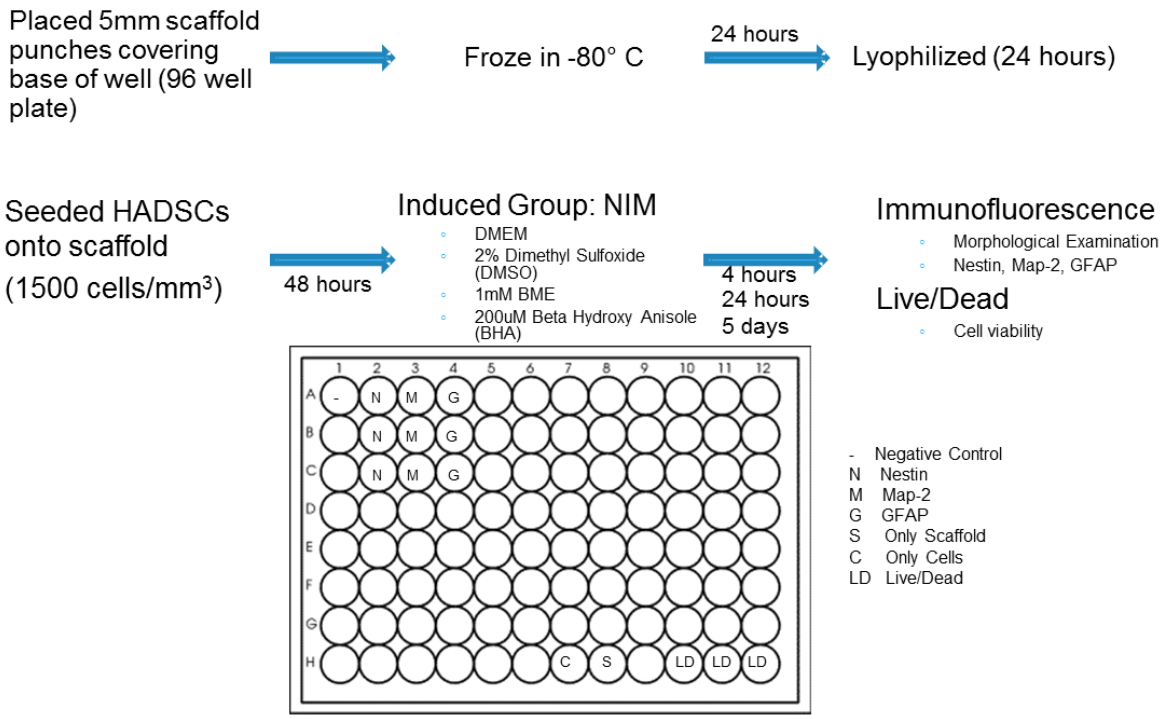

Figure 13: Detailed explanation of study 3: cells seeded onto scaffolds.

Study 5

To determine the stem cell niche potential of the scaffolds, HADSCs were seeded into tissue culture well plates at a seeding density of 1500cells / mm^3. Cells were allowed 48 hours to adhere before replacing the MesenPRO culture media. This culture media remained for 4hour, 24 hour, or 5 day time points after which time protein expression for neural markers and cell viability were analyzed through immunofluorescence and Live/Dead staining, respectively. The positive control for this study was rat cortical astrocytes (Lonza). Astrocytes were seeded at the same density as the test group and allowed 48 hours to adhere. After 48 hours, protein expression for neural markers and cell viability were analyzed through immunofluorescence and Live/Dead staining, respectively. A schematic of the test group methods can be seen in figure 14.

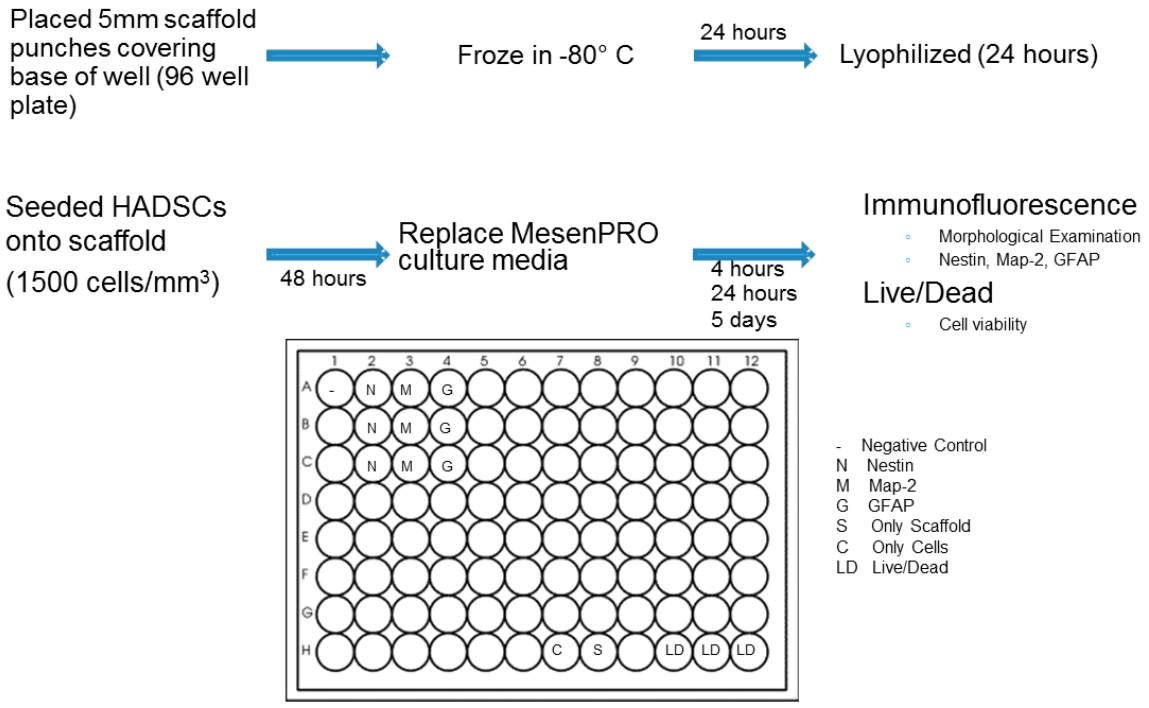

Figure 14: Detailed explanation of study 5: cells seeded onto scaffolds.

Study 6

In an additional effort to determine if the viability of HADSCs was being affected by a lack of nutrient supply, study 6 was completed following the exact methods described for the treatment group in study 5, except the MesenPRO was replaced daily.

3.4 In Vivo Experimentation

3.4.1 Overview

The goal of the in vivo experimentation was to confirm the niche neural construct's efficacy in stroke treatment. There is no in vitro model for stroke. Rodents, more specifically rats, are the most commonly used animal models for stroke due to the similarities between their intracranial circulation system and that of humans, the abundance of available neurochemical data, and the lack of *rete mirabile.*[34, 35]

The most widely used animal stroke model is middle cerebral artery occlusion (MCAO). This method most commonly involves a mid-line neck incision to expose the internal and external carotid arteries followed by suture introduction through the external into the internal thereby blocking blood flow through the middle cerebral artery. Transient introduction of the suture for a 2-hour period yields the most reproducible infarct while minimizing animal death. [25, 36-38] The general schematic of this procedure can be seen in figure 15.

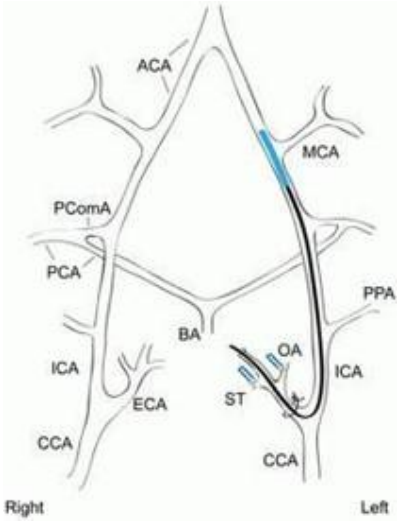

Figure 15: Intraluminal suture method of middle cerebral artery occlusion to induce stroke.

Functional recovery in rodent stroke models has been seen as a result of the intracranial administration or intravenous administration of stem cell therapies. Intravenous administration tends to fuel cell death as well as lead to unwanted side effects in other areas.[19] However, both delivery methods show the most promise with administration 1 day post-stroke and 7 days post stroke.[19, 39] Functional recovery can be evaluated through a variety of testing methods, but certain tests such as the "rotarod" and "water maze" are known to yield a larger percentage of false positives due to their target of very specific brain regions, while the neural severity scoring system, adhesive-removal, food grabbing, and limb placement tests have yielded more positive results, especially during long-term animal monitoring.[17, 19, 40-44] Due to the immune-privileged location of the stroked brain, a growing number of studies are employing the use of human cells in rodent models without antigenic concerns; this approach also supports the eventual adoption of the treatment in a translational research scenario.[16, 17, 20, 40, 45]

The in vivo study methods employed in this research were designed to confirm our ability to successfully induce stroke in our rodent model, to validate a method for

niche neural construct delivery, and to evaluate animals' functional recovery post-treatment. All components of the in vivo study were completed in accordance with Clemson University AUP2013-032 and IBC2010-28.

3.4.2 Stroke Induction

22 middle-aged female Wistar rats underwent 2 hour transient MCAO via the intraluminal suture method (described in detail below). The sutures employed for occlusion were 3-0 monofilament nylon sutures coated with silicon (Docool Corp.) that were blunted via introduction into flame prior to insertion.

1. Anesthetize rats with 1-5% isoflurane in O_2 in a chamber; maintain with 1-3% isoflurane (nose cone)
2. Maintain body temperature throughout procedure with an external heating source
3. Using aseptic techniques, make a midline incision through the neck that will expose the right common carotid artery (RCA), external carotid artery (ECA), and internal carotid artery (ICA)
4. Identify the first bifurcation of CCA, and then clear the soft tissues around the ECA and ICA without harming the artery
5. Place two knots at the distal part of the ECA to prevent the backflow of blood and cut the ECA between the knots. (The tied section attached proximal to the CCA junction can be straightened to allow the filament to enter the ICA, and then, the second bifurcation is cleared to obtain a good view of the MCA.)
6. Place a microvascular clip in the ICA temporarily proximal to the CCA junction. Incise the tied section of ECA using microscissors.
7. Place a knot below the arteriotomy in the ECA once the tip of the monofilament reaches the CCA junction. Remove the microvascular clip that was placed in the ICA to allow filament insertion
8. Straighten the ECA stump and advance the filament carefully until it reaches the MCA (~18.5-19.5mm depending on animal weight)
9. Staple the animal closed and wake up for the 2 hour occlusion period (Note: To assist in waking, rats will be placed in an O_2 chamber for approximately 10 minutes before being returned to separate caging with access to food and water for the duration of the 2 hour period).
10. After 2 hours, re-anesthetize rats and remove staples. Again, place a in the ICA and loosen the knot in the ECA stump below the arteriotomy.
11. Perform reperfusion by removing the suture until the tip clears the lumen of the External Carotid.
12. Suture animals closed (Note: To assist in waking, rats will be placed in an O_2 chamber for approximately 10 minutes before being returned to separate caging with access to food and water for the duration of the 2 hour period).

Immediately after closing, 6 rats were euthanized and their brains collected for TCC Staining to confirm infarction and to determine an average infarct area. The

location of the craniotomy incisions and tissue removal were based off of this average infarcted area.

3.4.3 Niche Neural Construct Delivery (Craniotomy)

One day post-MCAO, 8 rats underwent niche neural construct implantation via craniotomy. Briefly, the top of the head of each rat was shaved prior to making an incision in the top of the head. The skin was peeled back, and a 5mm square of bone was removed from the skull using a dental drill. Then, light suction was introduced, removing the damaged tissue from the brain.

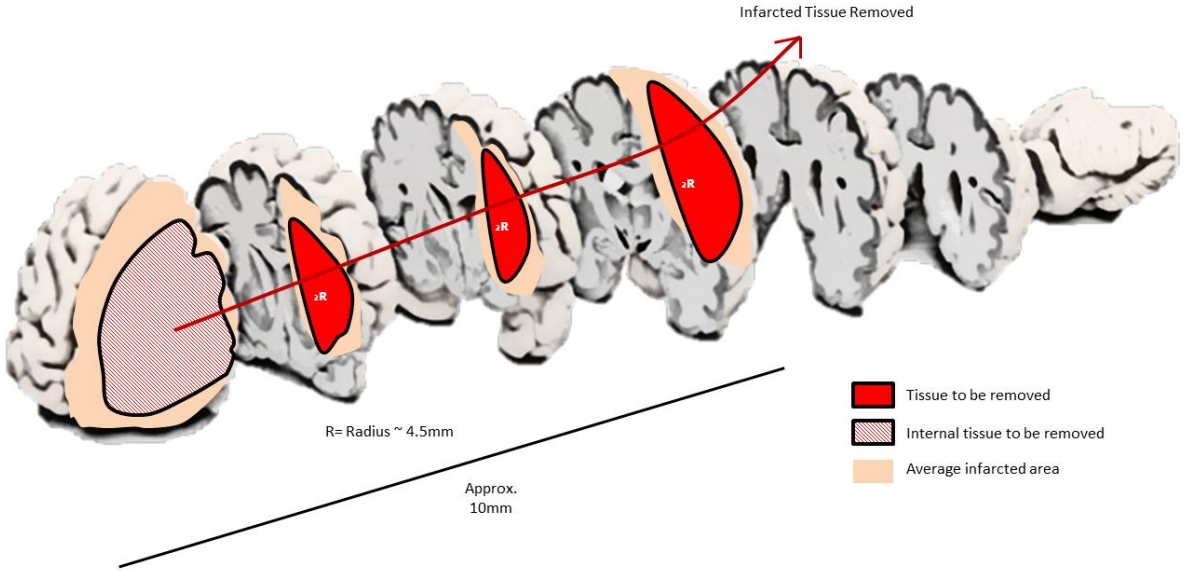

Figure 16: Diagram of average infarcted area as determined by TCC staining and tissue intended to be removed prior to construct delivery.

Niche neural constructs were then inserted filling the created void. A piece of Surgicel (Ethicon) was placed over the top of the brain. The skin was folded back over the skull, and each rat was sutured closed.

These niche neural constructs were prepareed according to the methods described in section 3.3.2. The constructs are representitive of the study 6 group at a 4 day timepoint. The only deviation from the previously cited methods was that the hunman adipose stem cells were verified to be from male donors and were obtained from LaCell LLC.

3.4.4 Behavioral Testing

To assess functional recovery post-stroke, all rats underwent behavioral testing which consisted of modified neural severity scoring (mNSS). The mNSS is a combination of sensory and motor analyses where one point is awarded for abnormal function (i.e. a score of 0 indicates perfect function). This examination required no training prior to administration. The mNSS was administred the night prior to stroke induction, 1 hour post-stroke, and weekly thereafter to obtain baseline measuremets, assess immediate functional damage, and monitor functional recovery, respectively. The mNSS protocol utilized in these assessments is listed below.

One point is awarded for abnormal function

Muscle Status-Hemiplegia

Raising rat by the tail
- Flexion of forelimb
- Flexion of hindlimb
- Head movement >10° to vertical axis within 30 seconds

Placing rat on floor
- Inability to walk straight
- Circling toward paretic side
- Falling down to paretic side

Abnormal Movements

- Immobility or Staring
- Tremor (wet dog shakes)
- Irritability, seizures

Sensory Tests

- Placing Test
- Proprioceptive Test

Reflexes

- Pinna
- Corneal
- Startle

Total Possible Score: 14

Explanation of Terms

Placing Test: Holding rat by tail, slowly bring rat such that the front paws can contact the floor. Observe proper or improper placement at contact

Proprioceptive Test: Push front paws again the edge of table. Observe rat response to stimulus (indicating proper or improper sensory function)

3.4.5 Animal Sacrifice

Animals were euthanized via deep isoflurane anesthesia followed by exsanguination. Death was confirmed through bilateral pneumothorax. Rat brains were carefully removed via post-mortem craniotomy and immediately placed in formalin. (Note: n=6 brains required for TCC staining were not placed in formailn).

3.4.6 Explant Analysis

Explants were prepared for histology and stained as previously described in sections 3.1.2-3.1.9.

CHAPTER 4: RESULTS

4.1 Scaffold Creation and Characterization

Fresh porcine brains were decellularized according to the methods described in section 3.1.1. Macroscopic changes from fresh to decellularized specimens are observed in figure 17. The decellularized scaffold appeared transparent and showed significant mass loss 95.97% ± 0.28 (n=3).

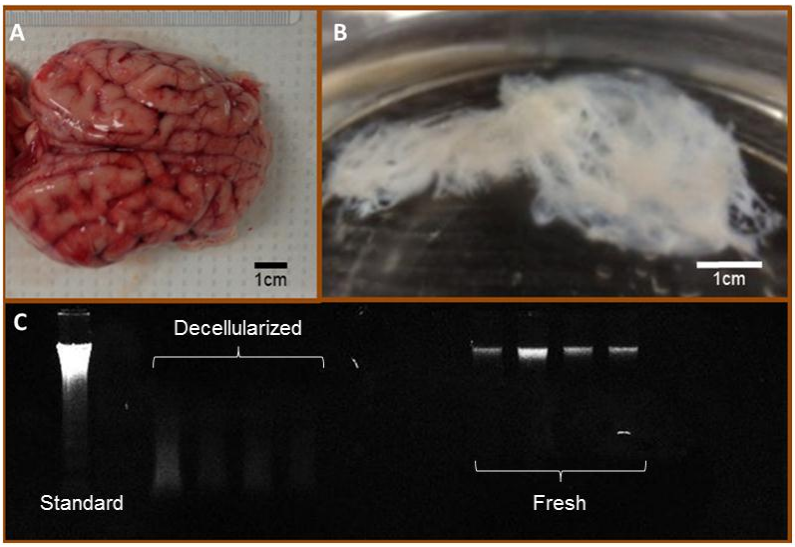

Figure 17: Qualitative Scaffold Analysis. A) Fresh porcine brain. B) Decellularized scaffold. C) DNA gel indicating significant reduction from fresh tissue to scaffolds.

Qualitative DNA analysis through Ethidium-Bromide DNA Agarose Gel Electrophoresis (figure #17C) shows a significant reduction in DNA from fresh to decellularized scaffolds. As seen in figure 18, analysis utilizing the Nanodrop 200C quantified this reduction from 818.5 ± 66.4 ng/mg in fresh tissue to 4 ± 4.0 ng/mg in the scaffolds ($P<0.005$).

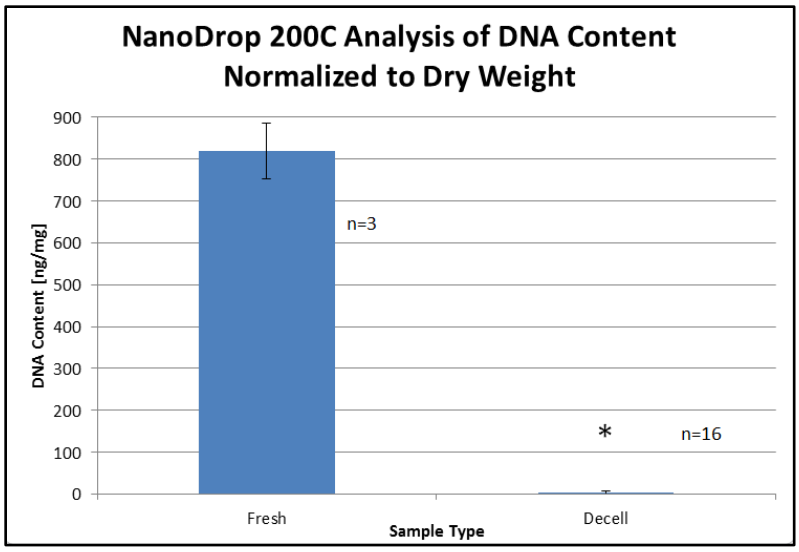

Figure 18: Quantitative DNA Analysis via Nanodrop 200C indicating >99% reduction in DNA content from fresh to decellularized tissues.

IHC for neural proteins was employed as an additional measure of successful decellularization. Figure 19 illustrates the complete removal of all Nestin, Map-2, and GFAP staining after decellularization.

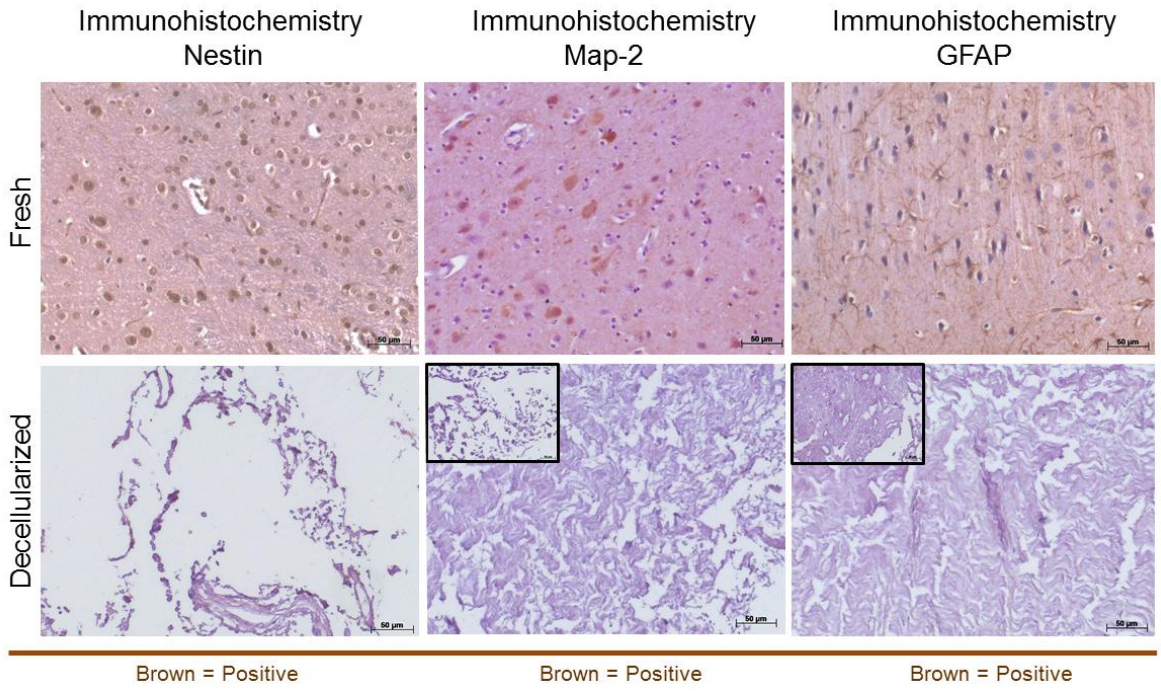

Figure 19: Histological Decellularization Confirmation. Complete removal of key neural cell proteins is observed in decellularized scaffolds.

Further characterization was accomplished through histological staining (figure 20-22). Through H&E, it was clear the scaffold consisted of an intact matrix and was free of all cellular components. Masson's Trichrome staining indicated the scaffold was primarily composed of collagen. The presence of what appeared to be intact blood vessels was also observed. Additionally through Bielschowsky staining, complete removal of neural fibers was observed.

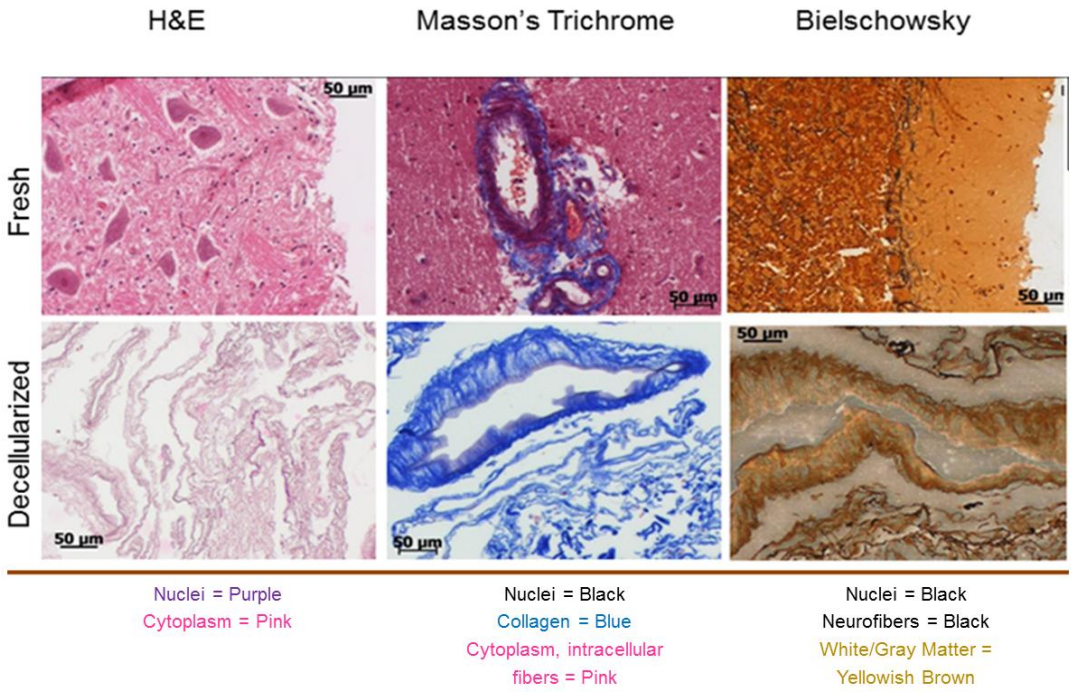

Figure 20: Preliminary Histological Characterization. Left, H&E staining indicating scaffolds contained an intact matrix with no cellular remnants. Middle, Masson's Trichrome staining indicating this matrix was primarily collagen. Right, Bielschowsky neural stain confirming scaffolds did not contain neural fibers.

A more in depth understanding of the scaffold composition was obtained through Movat's Pentachrome and Alcian Blue staining. Movat's Pentachrome staining was consistent with Masson's Trichrome indicating the scaffold is primarily composed of collagen. However, significant portions of the scaffold also appeared to stain for ground substance, supposedly GAGs, and elastin (figure 21). Alcian blue confirmed the

presence of GAGs intermixed with other matrix components in fresh tissue. Consistent with the Movat's staining, limited GAG fractions, primarily near the outer edges of the scaffold, were retained through decellularization.

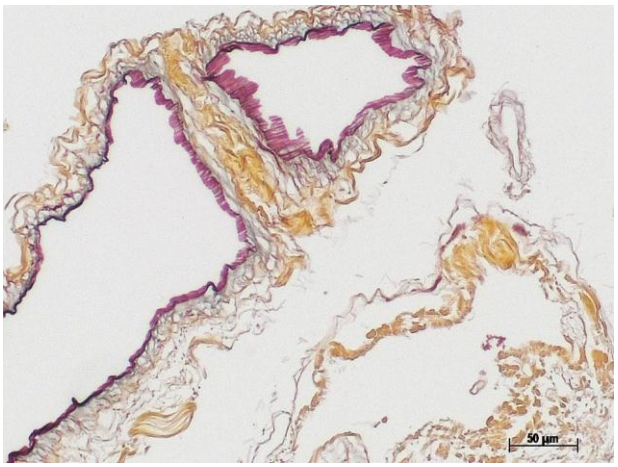

Figure 21: Movat's Pentachrome Staining indicating the scaffold, though primarily collagen, had retained elastin and ground substance (GAGs).

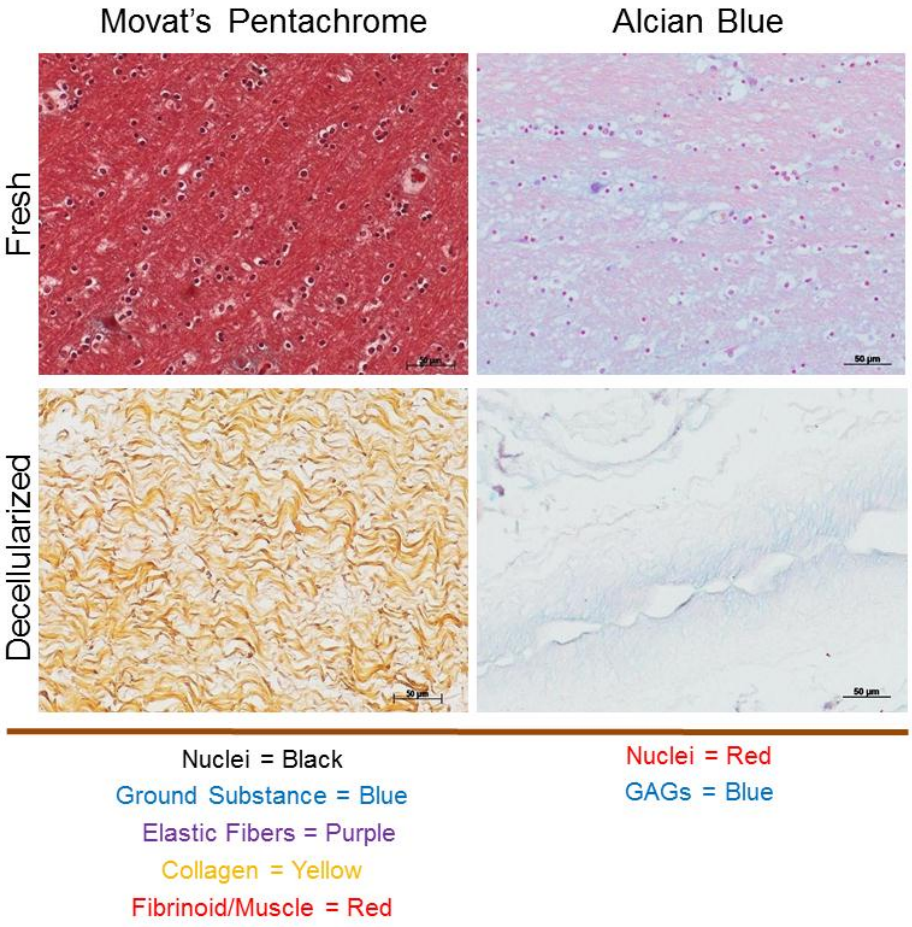

Figure 22: Histological Examination Continued. Left, Movat's Pentachrome staining confirming the scaffold was primarily collagen matrix. Right, Alcian blue staining indicating there was minimal retention of GAGs near scaffold edges.

Lastly, the scaffold was examined for retention of key basement membrane proteins. Figure 23 shows the successful retention of both collagen IV and Laminin.

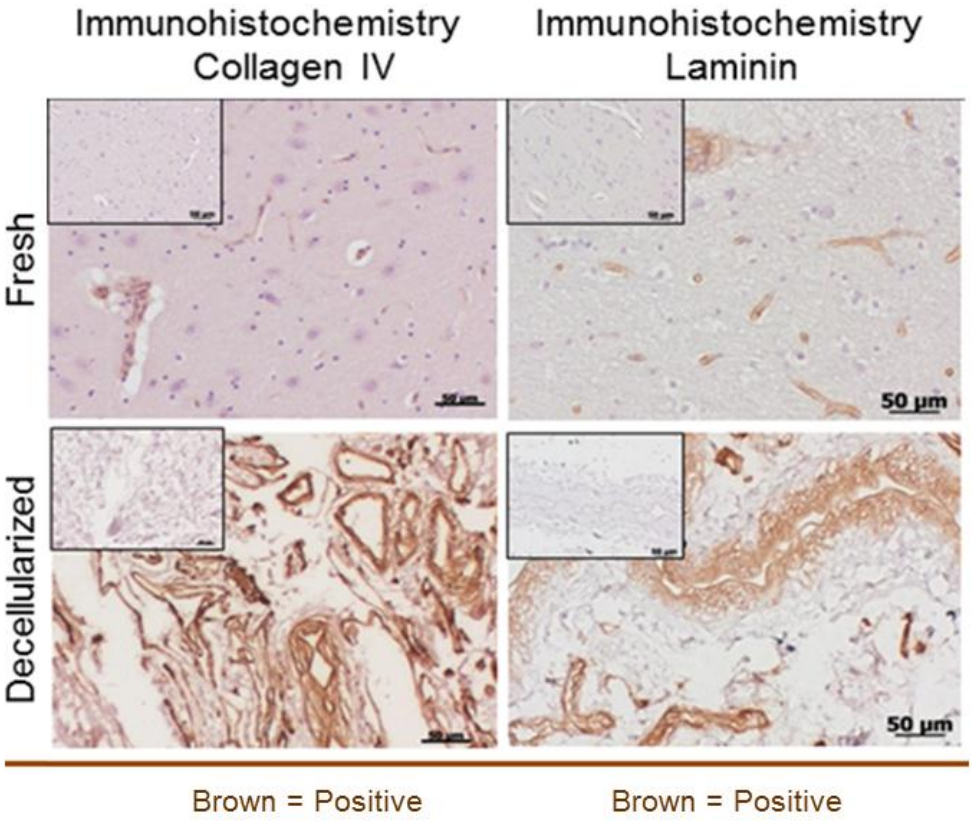

Figure 23: Basement Membrane Analysis. Left, IHC for collagen IV and right, IHC for Laminin confirming retention of both these key basement membrane proteins within the scaffolds.

4.2 In Vitro Experimentation

4.2.1 Viability Assessment

Qualitative assessment of cell viability through Live Dead staining of the positive control, astrocytes, showed predominantly viable cells (Figure 24). Quantitative analysis

indicated 87% viable cells after 24 hours of culture in well plates compared to 95% viability when astrocytes were seeded onto scaffolds.

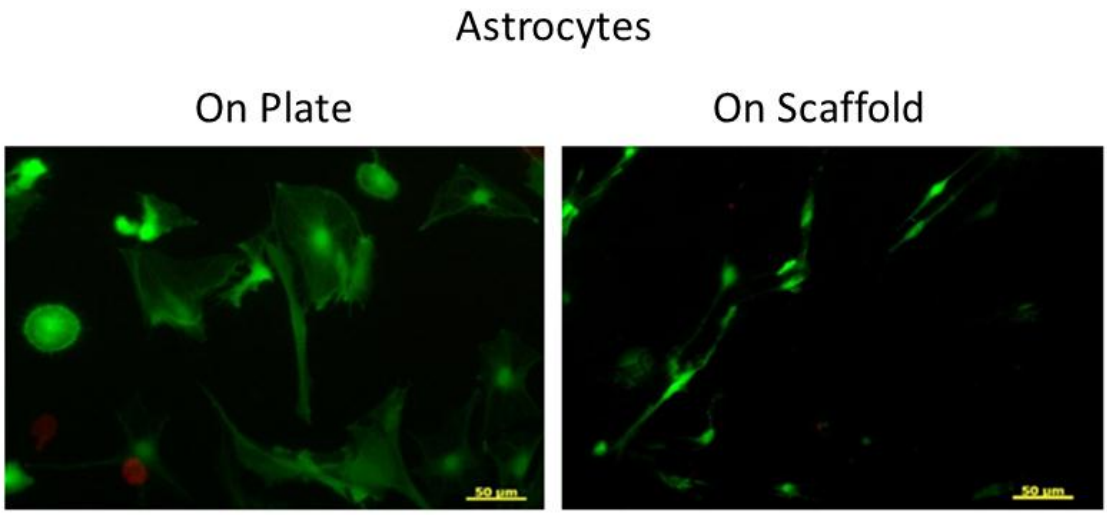

Figure 24: Astrocyte Viability Assessment through Live Dead staining indicating 87% viable cells seeded onto plastic compared to 95% viability when seeded onto scaffolds.

Similar assessment of cell viability in the test groups of NIM treated HADSCs at 4 hours showed a significant population of live cells (figure 25).

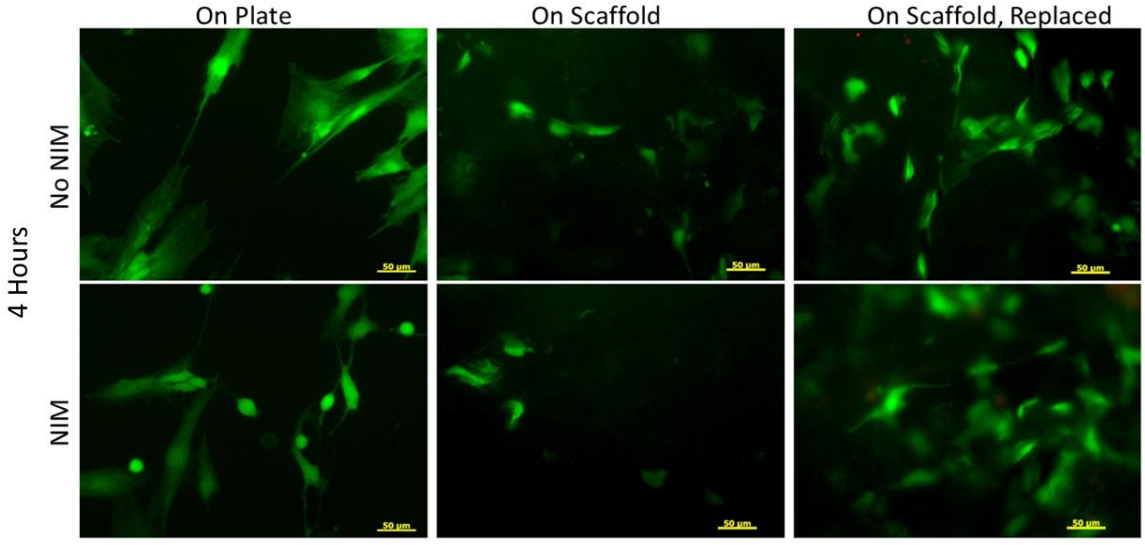

Figure 25: 4 Hour Viability Assessment. Live Dead staining indicated significant populations of viable cells across all test groups.

Quantitative assessment of this viability is seen in table 2.

Table 2: Viability Comparison at 4 Hours			
Experiment	% Live	Experiment	% Live
No Nim On Plate	99	NIM On Plate	95
No NIM On Scaffold	98	NIM On Scaffold	96
No NIM On Scaffold, Replaced	98	NIM On Scaffold, Replaced	97

Table 1: 4 Hour Quantitative Viability Assessment. There was comparable viability between No NIM and the respective NIM groups. Overall, strong viability was observed across all groups.

By 24 hours, the remaining cells were almost all viable. However, overall there were fewer cells observed throughout the specimens, particularly the NIM groups seeded into well plates.

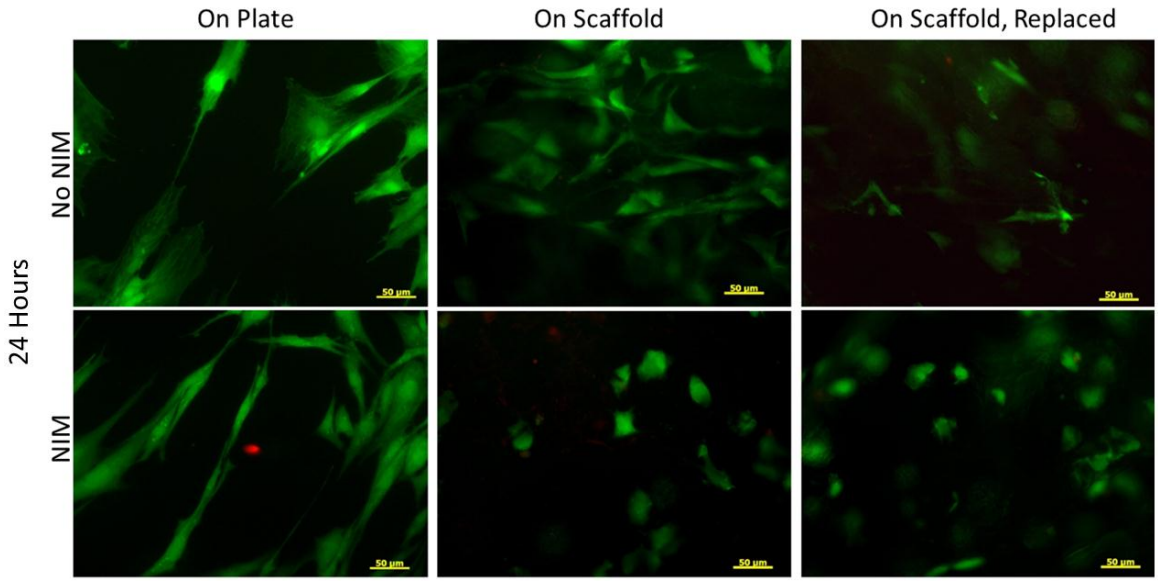

Figure 26: 24 Hour Quantitative Viability Assessment. There was an increase in viability between No-NIM and the respective NIM groups. Overall, strong viability was observed with the exception of the NIM treated group seeded into well plates.

Quantitative assessment of this viability is seen in table 3.

Table 3: Viability Comparison at 24 Hours			
Experiment	% Live	Experiment	% Live
No Nim On Plate	99	NIM On Plate	66
No NIM On Scaffold	97	NIM On Scaffold	92
No NIM On Scaffold, Replaced	98	NIM On Scaffold, Replaced	94

Table 2: 24 Hour Quantitative Viability Assessment. There was an increase in viability between No-NIM and the comparable NIM groups. Overall, strong viability was observed with the exception of the NIM treated group seeded into well plates.

Finally by day 5, all NIM groups were greatly compromised compared to non-NIM treated groups. In the NIM groups seeded onto plastic, almost no viable cells were observed; whereas NIM groups seeded onto scaffolds retained populations of viable cells.

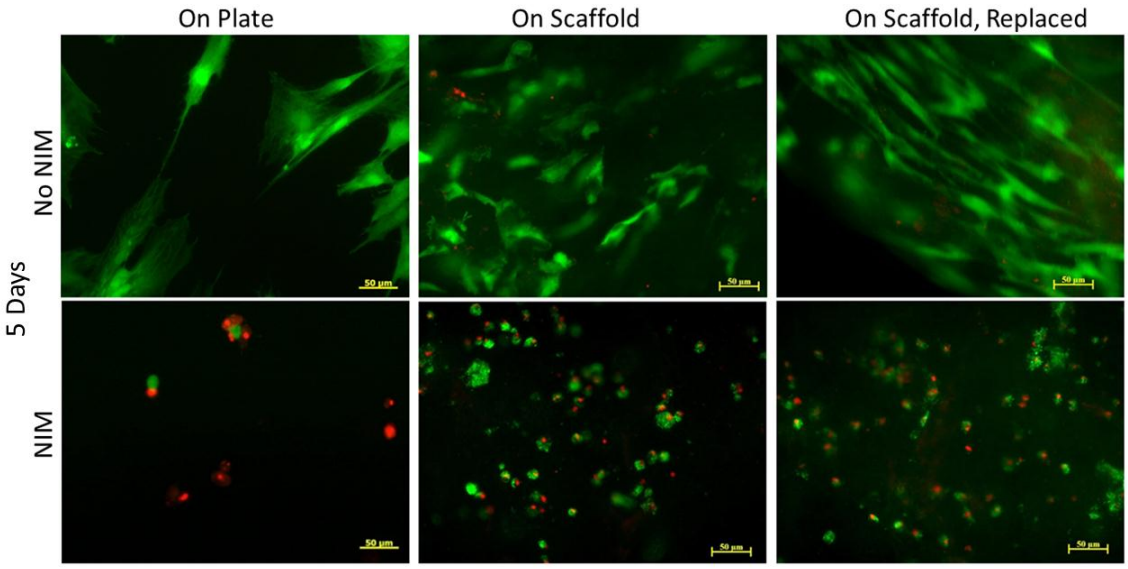

Figure 27: 5 Day Quantitative Viability Assessment. All NIM groups showed extremely compromised viability. Non-NIM treated groups showed significant populations of viable cells.

Quantitative assessment of this viability is seen in table 4.

Table 4: Viability Comparison at 5 Days			
Experiment	% Live	Experiment	% Live
No Nim On Plate	99	NIM On Plate	5
No NIM On Scaffold	84	NIM On Scaffold	49
No NIM On Scaffold, Replaced	93	NIM On Scaffold, Replaced	36

Table 4: 5 Day Quantitative Viability Assessment. All NIM groups were extremely compromised. However, the NIM groups seeded onto scaffolds showed significantly increased viability compared to cells seeded into well plates. All scaffold seeded groups had strong viability, with a clear increase in viability for the group where the culture media was replaced.

The quantitative viability for NIM groups is summarized in the below graph. All NIM groups where cells were seeded onto scaffolds showed greater cell viability than their counterparts seeded onto plastic. Significantly, by 24 hours there was statistical difference between scaffold and both plate groups. However, no statistical difference was observed between groups seeded onto scaffolds. By day 5 there was a clear increase in viability, 36-49% compared to 0-5%, between scaffold-seeded and well plate-seeded groups. Additionally, the statistical difference between scaffold and both plate groups still holds. Most notably, by 5 days regardless of environment, replacing the NIM resulted in statistically different (lower) viability.

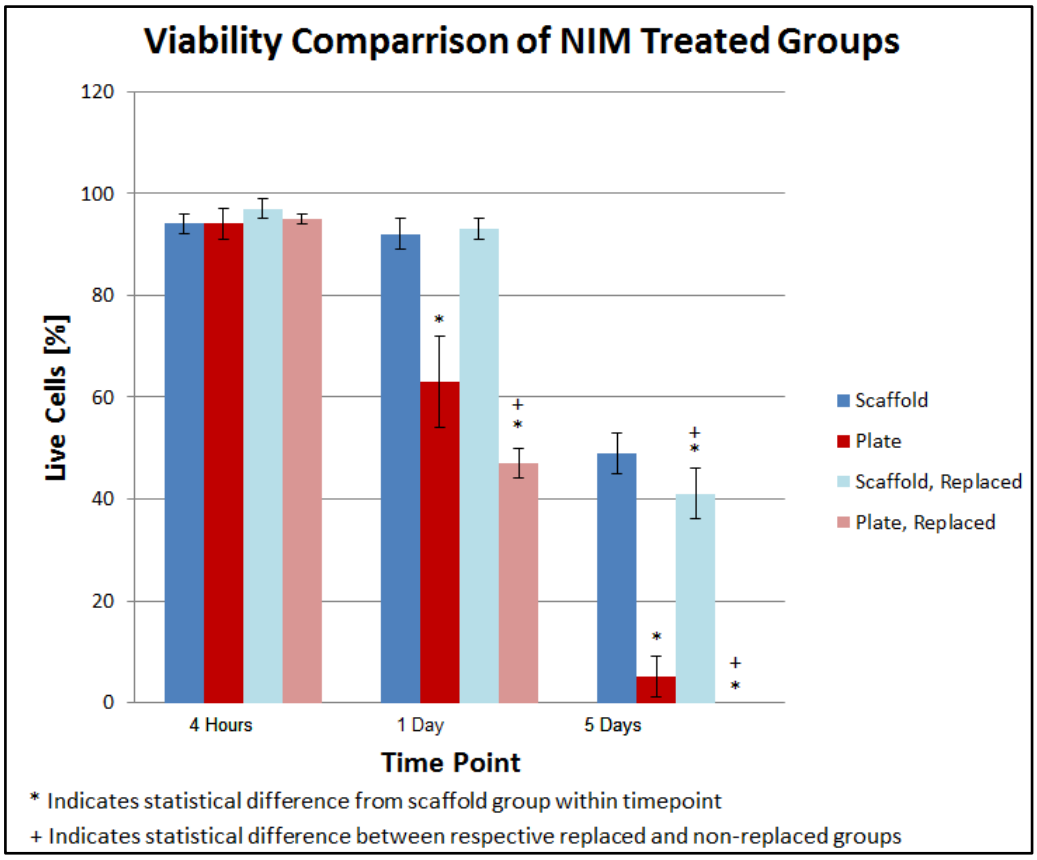

Figure 28: NIM Viability Summary. By 24 hours there was statistical difference between scaffold and both plate groups. This statistical difference held at 5 days with the addition of statistical difference between the scaffold and scaffold replaced group. Significantly, regardless of environment, replacing the NIM yielded statistically different (lower) viability.

4.2.2 Cells Seeded onto Plastic

Quality of differentiation was assessed though immunofluorescence for neural proteins Nestin, Map-2, and GFAP. Negative controls for all immunofluorescence studies are provided in the top left corner of each image.

The negative control, HADSCs, seeded into well plates very minimally expressed Nestin, expressed nuclear Map-2, and did not express GFAP (See Appendix A).

The positive control, astrocytes, seeded into well plates very minimally expressed Nestin, did not express cytosolic Map-2, and vibrantly expressed GFAP.

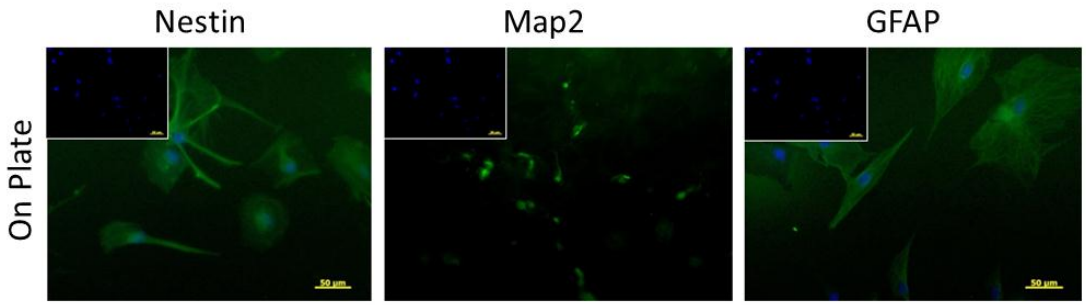

Figure 29: Astrocyte Protein Expression on Plastic. Astrocyte controls expressed small amounts of Nestin, no cytosolic Map-2, and significant amounts of GFAP.

Study 1

At 4 hours, NIM induced cells seeded onto plastic minimally expressed Nestin, Map-2 expression was beginning to transition from nuclear to cytosolic, and no GFAP expression was observed.

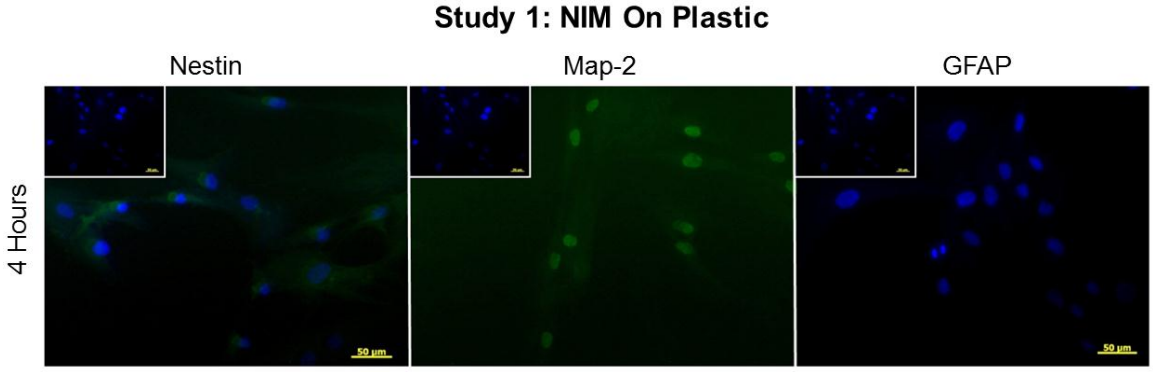

Figure 30: Study 1 – Protein Expression at 4 hours. Nestin and Map-2 were minimally expressed by test group cells. No GFAP expression was observed.

By 24 hours, expression of both Nestin and Map-2 had significantly increased. Additionally, cells began to express GFAP. Notably, all expression was co-localized with

a cell nucleus. There were also indications of morphological changes including the development of cytosolic processes.

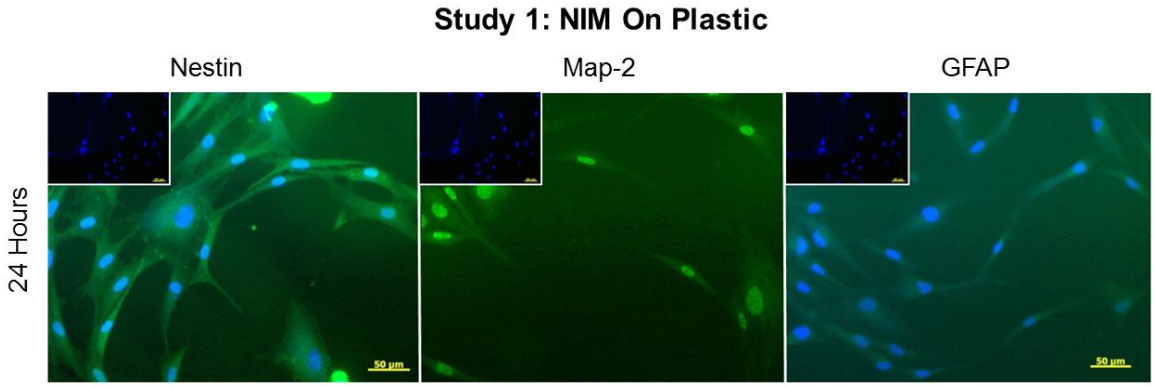

Figure 31: Study 1 – Protein Expression at 24 hours. Expression of all markers was observed. Map-2 expression had transitioned from nuclear to cytosolic. Additionally, the development of cytosolic processes was observed.

By 5 days, expression was virtually non-existent. Additionally, there were almost no intact nuclei indicating no viable cells.

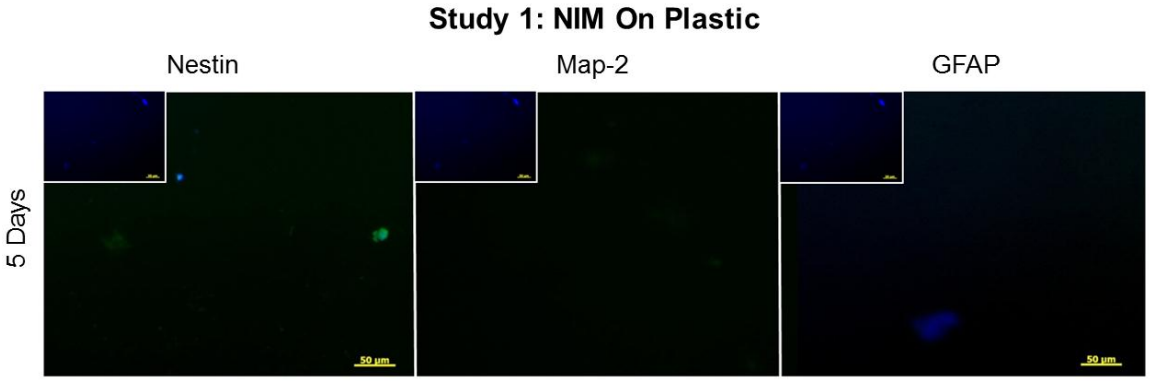

Figure 32: Study 1 – Protein Expression at 5 Days. No expression was observed. Additionally, very few viable cell nuclei were observed.

Study 2

By 4 hours, NIM induced cells where the NIM was replaced daily expressed Nestin and cytosolic Map-2. However, no GFAP expression was observed.

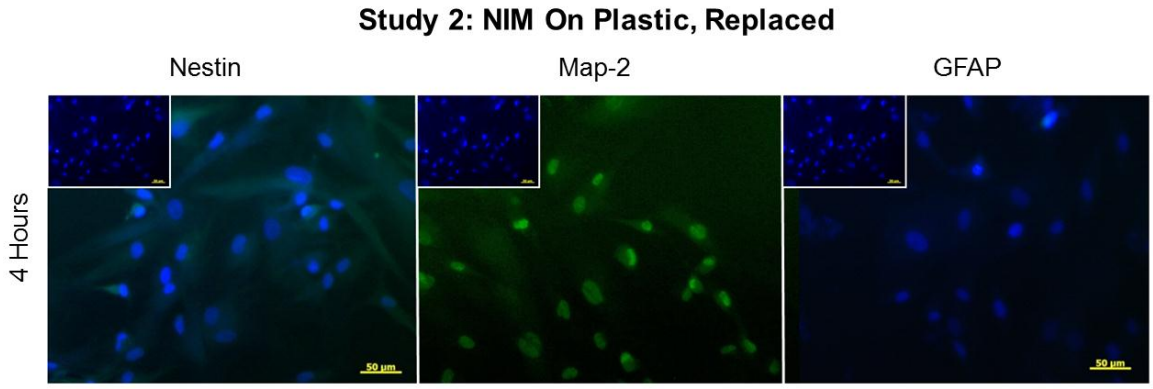

Figure 33: Study 2 – Protein Expression at 4 Hours. Nestin and cytosolic Map-2 expression were observed. However, no GFAP expression was observed.

By 24 hours, expression of Nestin and Map-2 lessened, but GFAP expression was now observed. Across all markers, unfavorable morphological changes were observed.

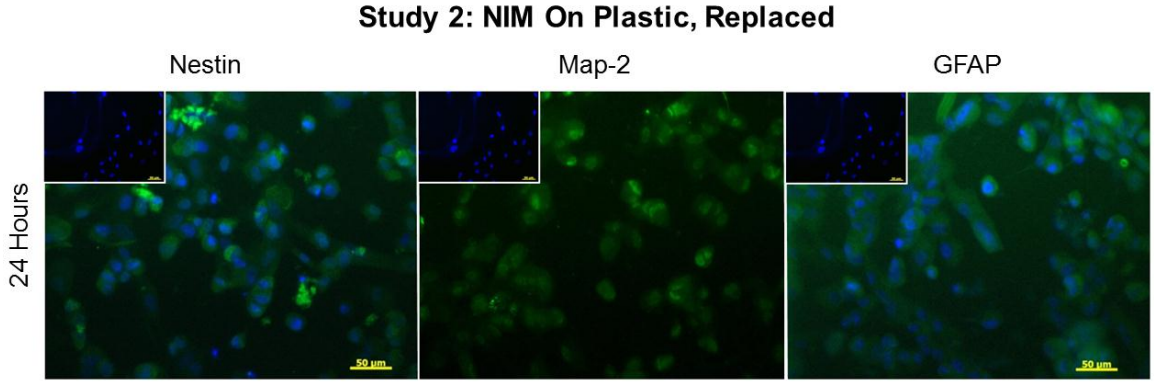

Figure 34: Study 2 – Protein Expression at 24 Hours. Expression of all markers was visible. No favorable morphological changes were observed.

By 5 days, neither marker expression nor viable nuclei were observed.

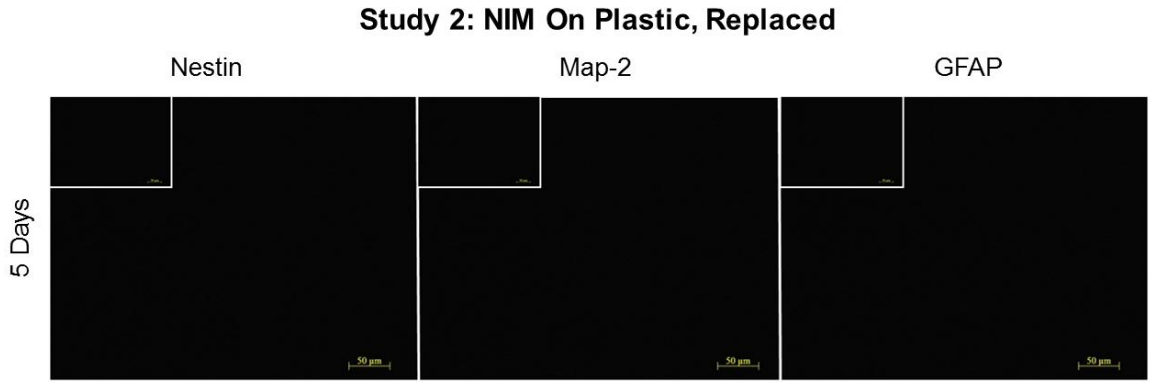

Figure 35: Study 2 – Protein Expression at 5 Days. Neither marker expression nor viable nuclei observed.

4.2.3 Cells Seeded onto Scaffolds

The positive control, astrocytes, seeded onto scaffolds very minimally expressed Nestin, did not express Map-2, and vibrantly expressed GFAP.

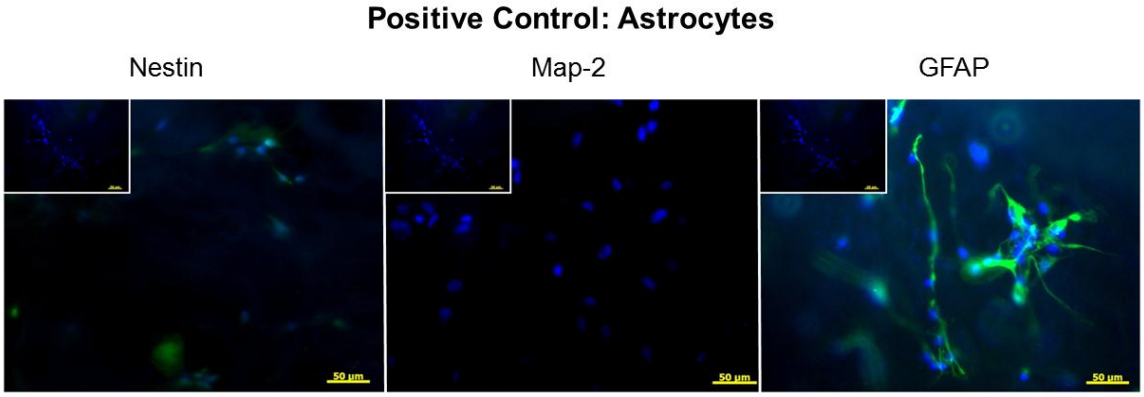

Figure 36: Astrocytes Seeded onto Scaffolds. Minimal Nestin, no Map-2, and significant GFAP expression were observed.

Study 3

For NIM induced cells seeded onto scaffolds at 4 hours, expression of all markers was observed. Significantly, MAP-2 expression transitioned from nuclear to cytosolic.

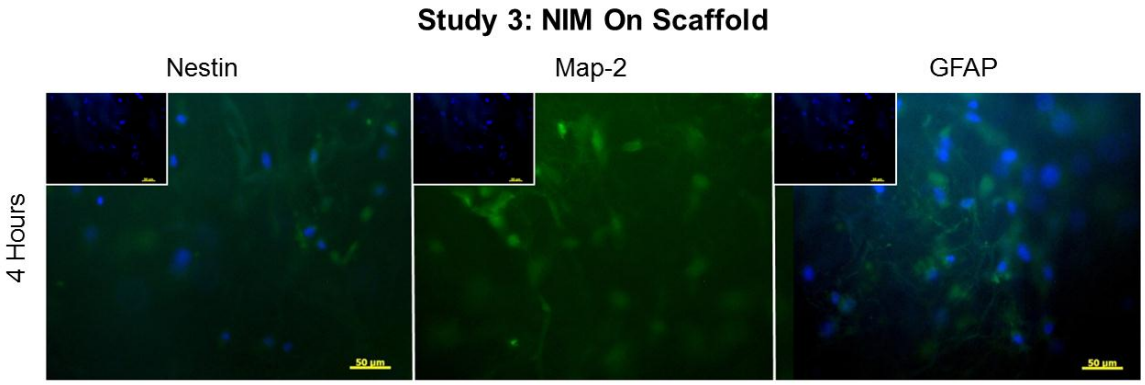

Figure 37: Study 3 – Protein Expression at 4 Hours. Expression of all markers was observed.

By 24 hours, expression of all markers had been maintained. Significantly, cytosolic Map-2 expression was still observed.

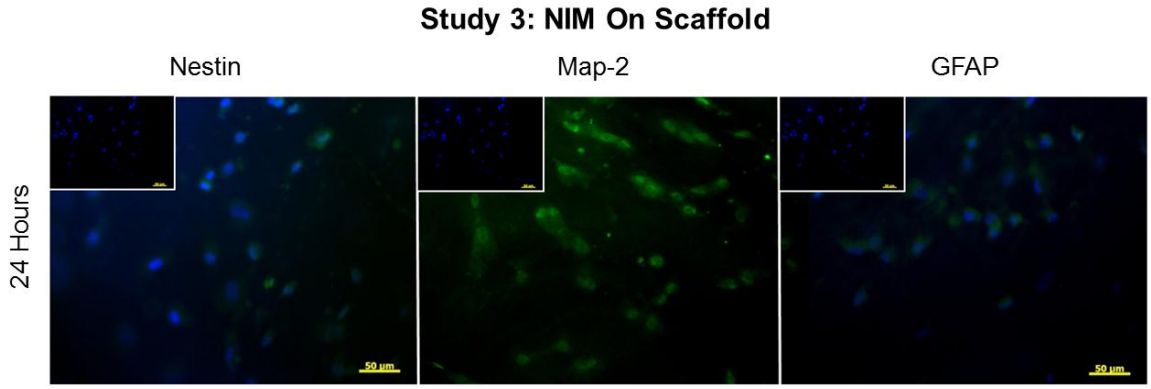

Figure 38: Study 3 – Protein Expression at 4 Hours. Expression of all markers was maintained.

At 5 days, there was still fluorescence indicating expression of all markers. Though the fluorescence appeared very faintly, there was cytosolic Map-2 expression.

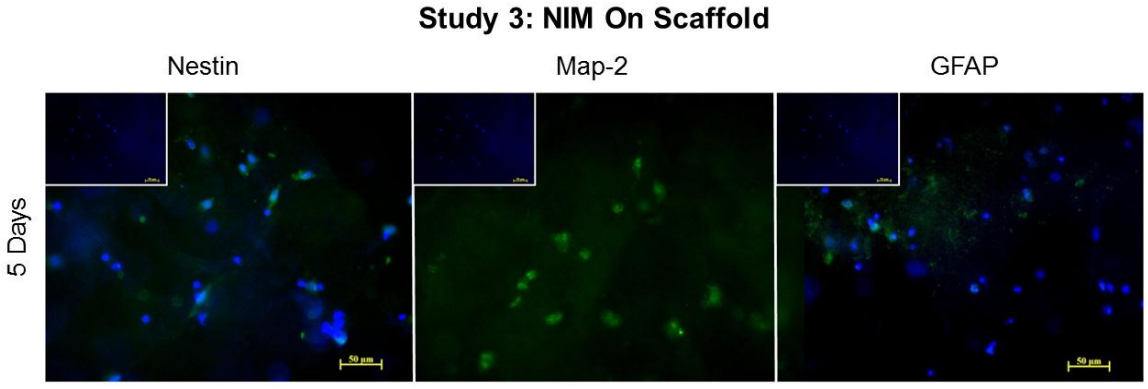

Figure 39: Study 3 – Protein Expression at 5 Days. Expression of all markers was still observed.

Study 4

For NIM induced cells seeded onto scaffolds where the NIM was replaced daily, expression of all markers was observed at 4 hours. Significantly, MAP-2 expression transitioned from nuclear to cytosolic.

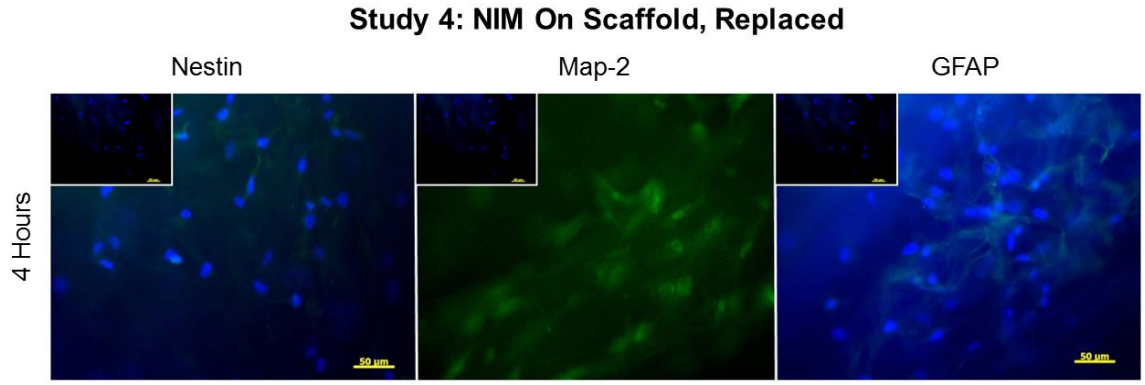

Figure 40: Study 4 – Protein Expression at 4 Hours. Expression of all markers was observed. Significantly, Map-2 expression was cytosolic.

By 24 hours, expression of GFAP appeared to increase. However, the morphological changes and alignment observed in the Nestin and Map-2 staining at 4 hours were no longer present. Additionally, it is unclear if cytosolic Map-2 expression was maintained.

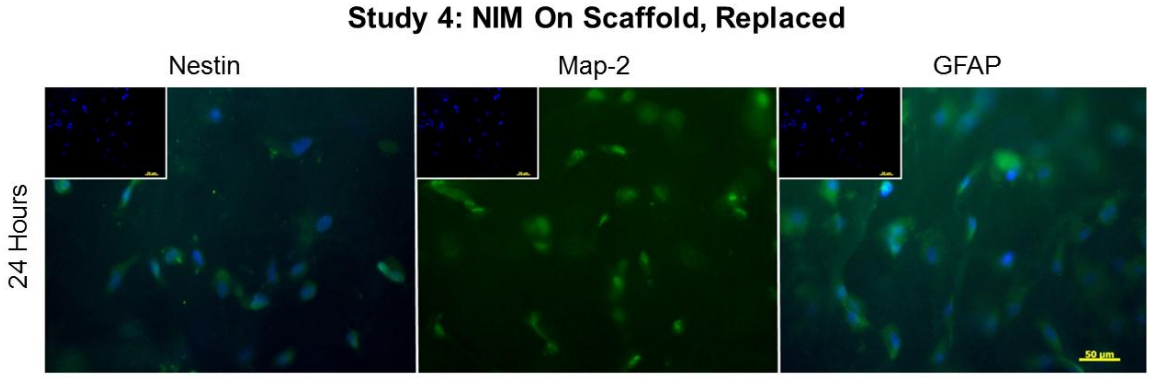

Figure 41: Study 4 – Protein Expression at 24 Hours. Expression of all markers was observed. It is unclear if cytosolic Map-2 expression was maintained.

By 5 days, very minimal Nestin and GFAP expression were observed. No distinct cytosolic Map-2 staining was present.

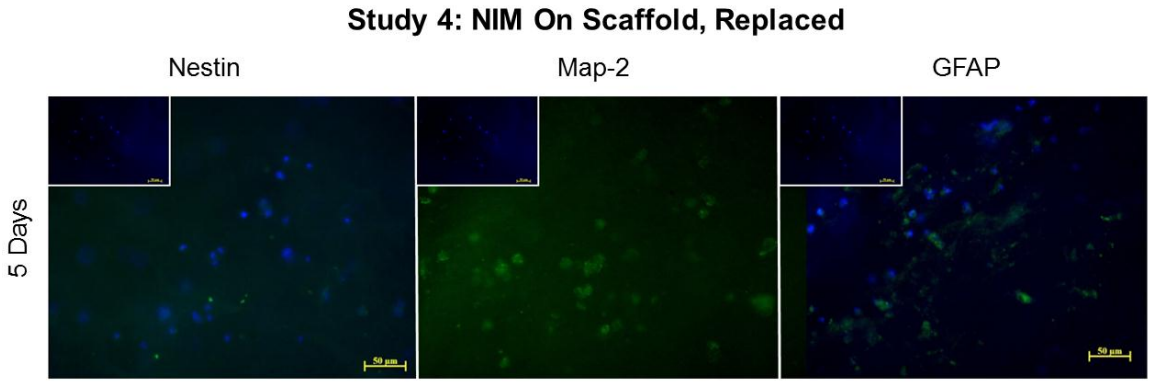

Figure 42: Study 4 – Protein Expression at 5 Days. Minimal expression of Nestin, nuclear Map-2, and GFAP was observed.

Study 5

At 4 hours, HADSCs seeded onto scaffolds with no induction step expressed Nestin, nuclear Map-2, and minimal GFAP. Additionally, there were clear morphological changes demonstrating the development of numerous cytoplasmic processes.

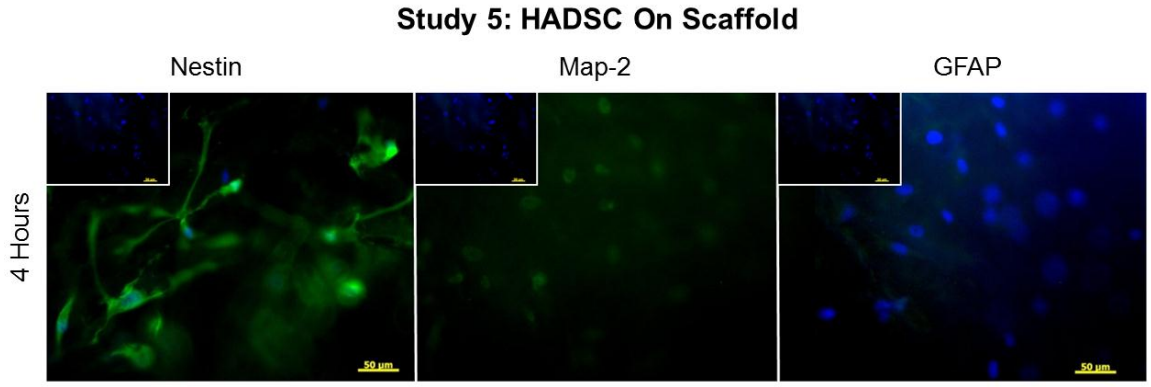

Figure 43: Study 5 – Protein Expression at 4 Hours. HADSCs seeded onto scaffolds expressed Nestin, nuclear Map-2, and minimal GFAP. Significant morphological changes had occurred, as illustrated by the development of numerous cytoplasmic processes in cells staining for Nestin.

By 24 hours, HADSCs were expressing all neural markers (Map-2 expression had transitioned to cytoplasmic expression). Significant cytoplasmic processes and cellular interactions were also noted.

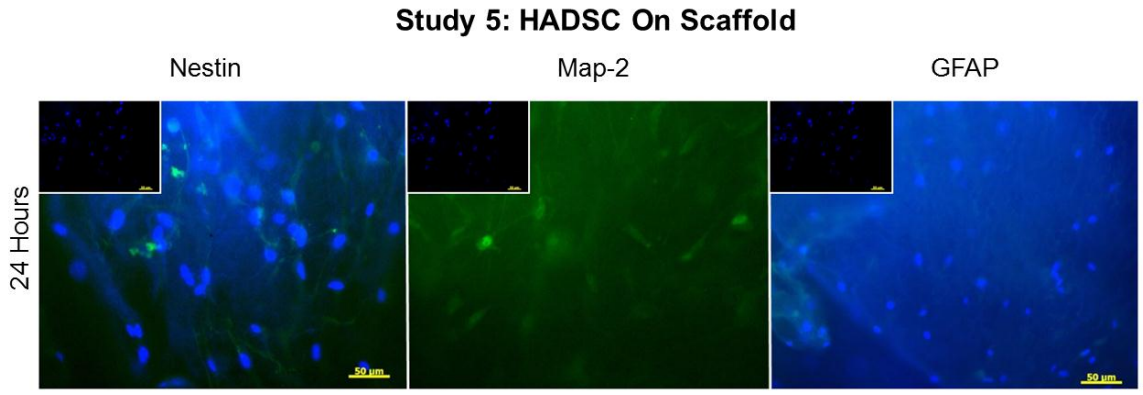

Figure 44: Study 5 – Protein Expression at 24 Hours. HADSCs seeded onto scaffolds expressed all markers and continued to show morphological characteristics of neural-like cells.

By 5 days, expression of all markers was maintained and even increased. Additionally, cellular processes continued to develop and cells began to align tip-to-tail.

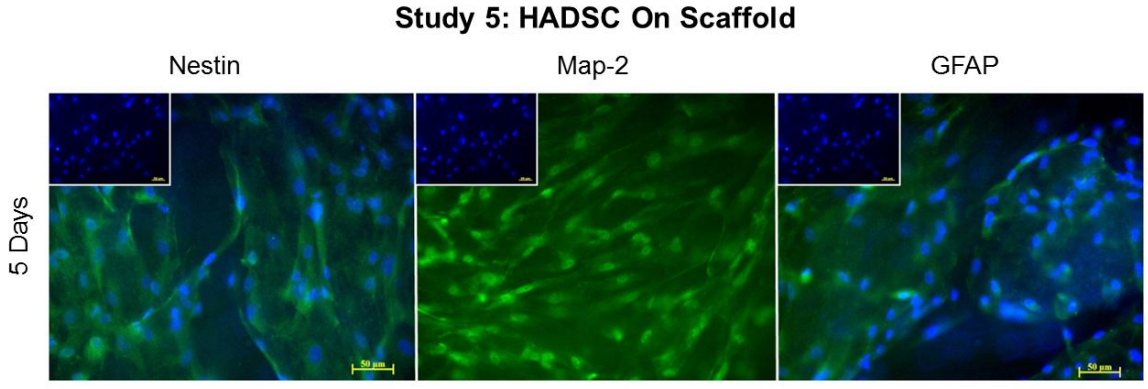

Figure 45: Study 5 – Protein Expression at 5 Days. HADSCs seeded onto scaffolds exhibited heightened expression of all markers. Additionally, cellular alignment is observed and morphological changes were maintained.

Study 6

At 4 hours, HADSCs seeded onto scaffolds where the MesenPRO cell culture media was replaced daily expressed Nestin, nuclear Map-2, and minimal GFAP. As in study 5, there were morphological changes demonstrating the development of numerous cytoplasmic processes.

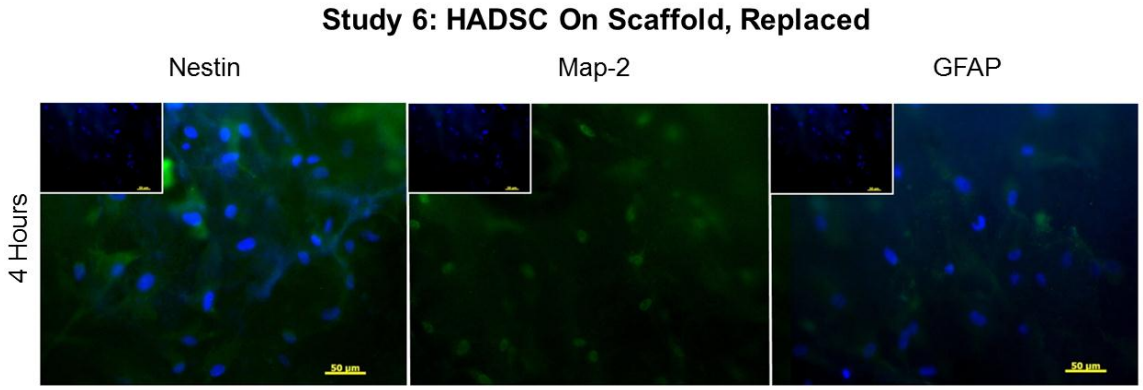

Figure 46: Study 5 – Protein Expression at 4 Hours. HADSCs seeded onto scaffolds expressed Nestin, nuclear Map-2, and minimal GFAP.

By 24 hours, cells were expressing all markers. Map-2 staining had transitioned from nuclear to cytosolic expression. Additionally, morphological changes were maintained.

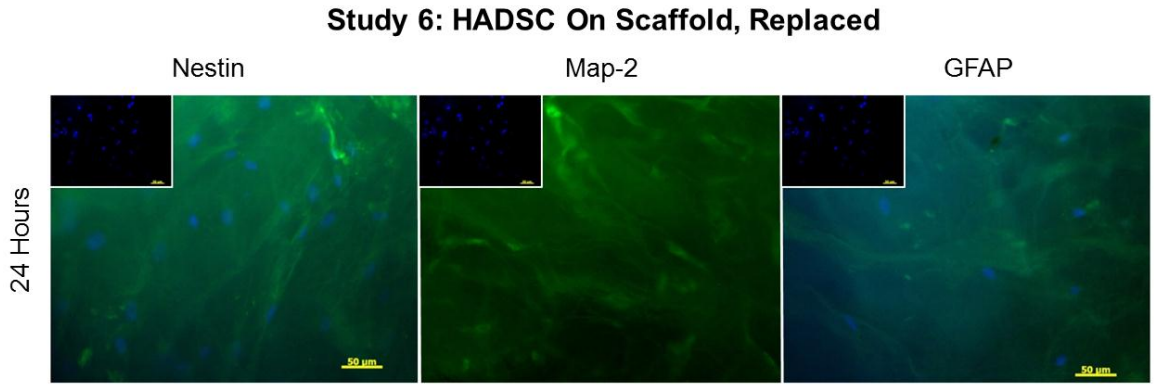

Figure 47: Study 5 – Protein Expression at 24 Hours. Cells expressed all markers and had maintained morphological changes.

Expression of all markers was not only maintained but appeared to increase by day 5. Significant cellular alignment as well as maintenance of developed projections was observed.

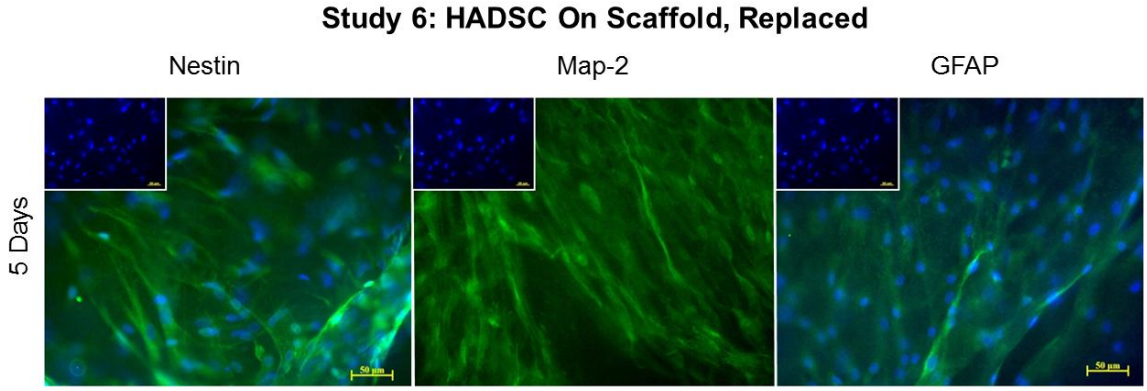

Figure 48: Study 5 – Protein Expression at 5 Days. An increase in expression of all markers was observed. Additionally, cells began to align and maintained morphological changes.

Phase contrast images overlayed with the calcein portion of a Live Dead stain highlighted these maintained morphological features. Cell bodies as well as cellular projections were aligning to the fibers within the scaffold.

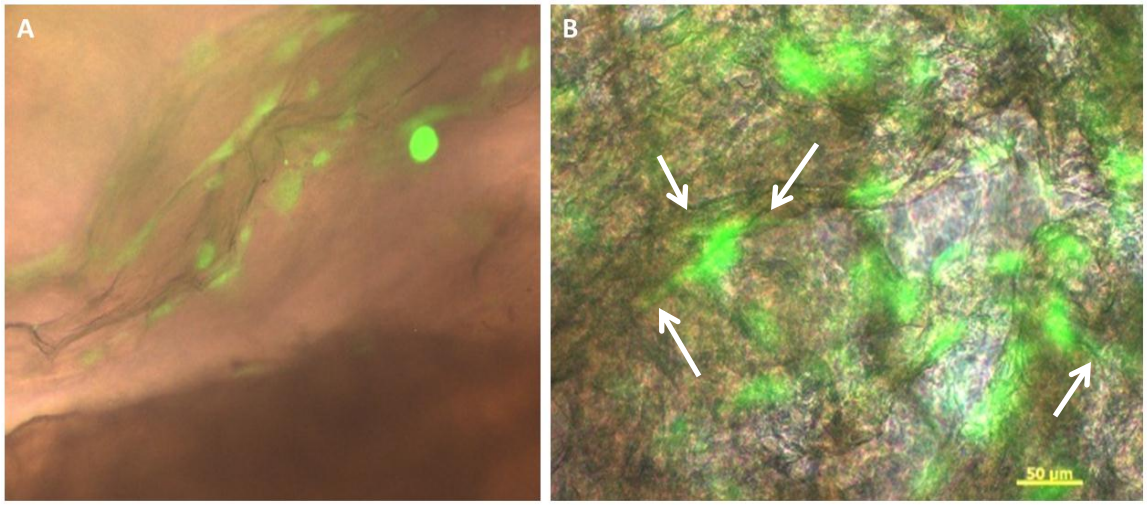

Figure 49: Cellular Alignment to Scaffold Fibers. Phase contrast images overlayed with the calcein portion of a Live Dead stain clearly indicated cells (A) and cellular projections (B) were aligning to scaffold fibers.

4.3 In Vivo Experimentation

4.3.1 Stroke Induction

The two hour transient MCAO procedure described in section 3.4.2 was completed on all 22 rats. A summary of the operation is seen in figure 50. Briefly, the rats were anesthetized, a mid-line neck incision was made, and the glandular tissue was retracted to reveal the common, external, and internal carotid arteries. The internal carotid artery was clamped and the external carotid was ligated. An incision was made into the external carotid and the suture was introduced into the internal carotid via the external carotid artery. The clamp was removed and the rat was stapled closed for the two hour occlusion period. After 2 hours, the rat was re-anesthetized and opened, the suture was removed to allow reperfusion, and the rat was sutured closed (not pictured).

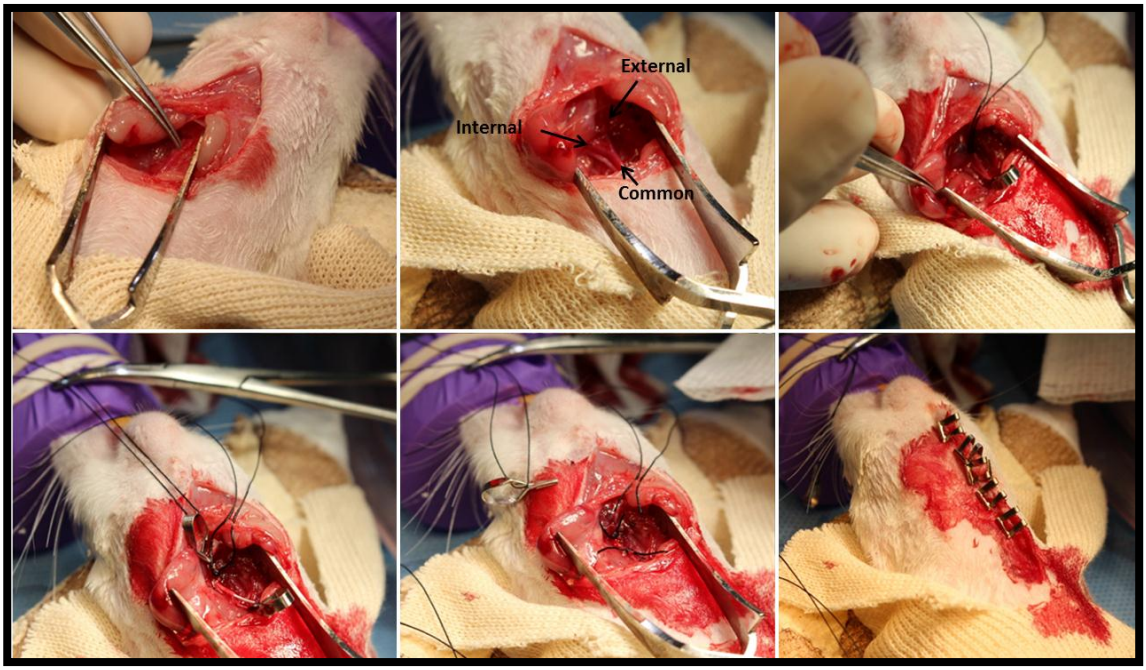

Figure 50: MCAO Operation. Two hour transient MCAO was performed on all 22 rats as described in section 3.4.2. Briefly, a midline neck incision was made and the common, external, and internal carotid arteries were isolated. After ligating the external carotid, a small incision was made and the suture was introduced for a two hour period. After two hours the suture was removed to allow reperfusion.

Following MCAO stroke induction, 6 rats were euthanized and their brains collected for TCC staining. Figure 51 shows a representative TCC stained brain section. The pale cream color of the brain visible through TCC staining indicated successful stroke induction. These staining results yielded the average infarcted area and therefore the anticipated location of construct implantation illustrated in figure 16.

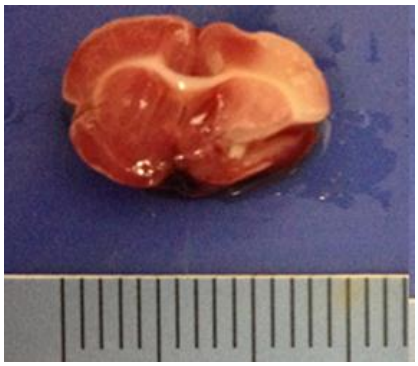

Figure 51: TCC Staining. The cream color in the upper right indicated successful stroke induction.

The remaining 16 rats were divided into 2 groups, MCAO control (n=8) and treatment (n=8). N=4 control rats and N=2 treatment rats died either during or as a result of complications from surgery.

4.3.2 Niche Neural Construct Delivery (Craniotomy)

The remaining N=6 treatment group rats underwent niche neural construct implantation. N=1 rats experienced an anesthesia related death. Niche neural construct delivery was successfully accomplished as described in section 3.4.3. Figure 52 illustrates this process. Briefly, rats were anesthetized, an incision was made on the top of the head, and the skin was retracted. Next, a small ~25mm^2 section was removed from the skull using a dental drill. Damaged brain tissue was identified, as it was texturally different from the healthy tissue. Light suction was introduced to these brain areas removing the necrotic tissues. The pre-prepared sterile niche neural constructs were introduced into this void. Surgicel was placed over the operated area, and the rat was sutured closed. This method allowed for the creation of an injury specific void and thus maximal treatment delivery.

Figure 52: Niche Neural Construct Delivery via Craniotomy. Construct delivery was accomplished as described in section 3.4.3. Briefly, a small ~25mm^2 skull fragment was removed and light suction was introduced to the damaged brain areas. A Niche neural construct was placed into the created void, Surgicel was placed over this area, and the rat was sutured closed.

4.3.3 Behavioral Testing

Behavioral testing was completed as described in section 3.4.4. Figure 53 shows the baseline (week -1), post-stroke (week 0), and recovery (up to 4 weeks) of each rat surviving to the 4 week time point. Each rat began with perfect function, but this function decreased from 4-10 points post-stroke, another indication the rats were successfully

stroked. Over the four week period, the treatment group (purple colors) had an overall more consistent and better recovery than the stroke controls (orange colors).

Figure 53 shows the average mNSS score of each group over the 6 time points. Post stroke scores between groups were not statistically different. Over the 4 week recovery period, the control group exhibited what appeared to be minimal improvement eventually plateauing; however, there is no statistical difference between week 0 and any recovery week time point (P>0.1). The treatment group exhibited rapid and consistent improvement over 4 weeks. This improvement is statistically different from week 0 beginning at the 2 week time point (P<0.05). Similarly, the improvement of the treatment group is statistically different from that of the control group beginning at the 2 week time point (P<0.05).

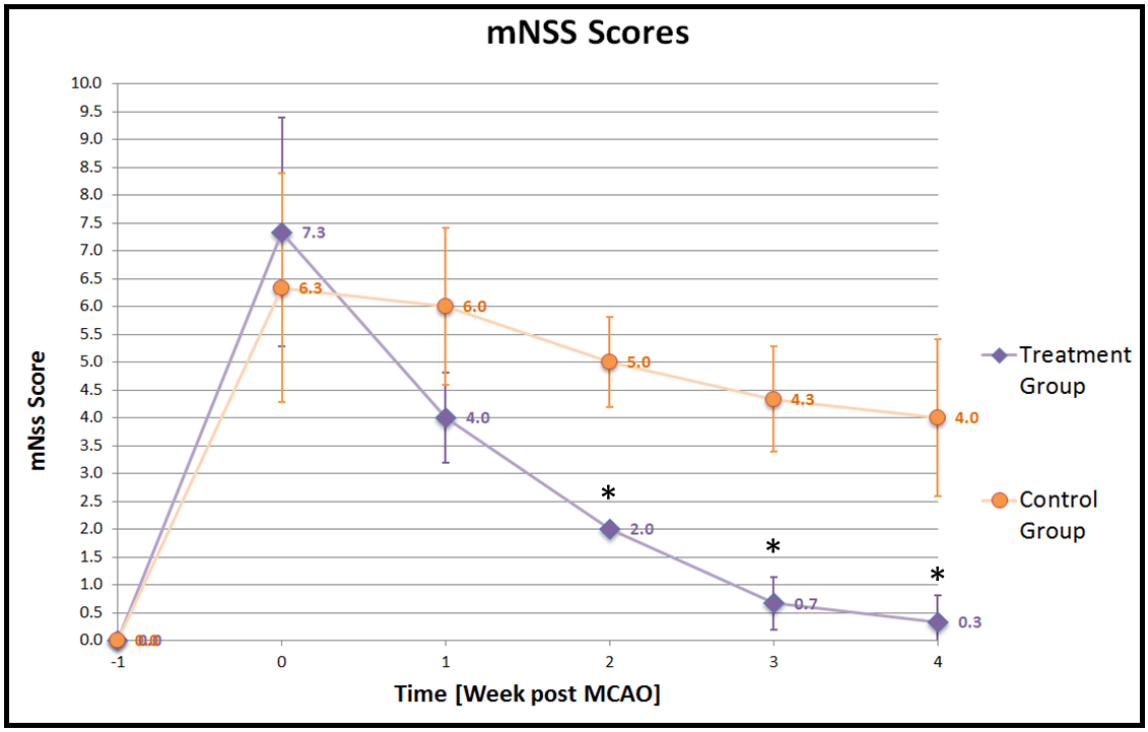

Figure 53: mNSS Scores by group. The treatment group is statistically different from the control group beginning 2 weeks post stroke (P<0.05). Additionally, though the control group appeared to improve, there is no statistical difference between control group scores at any time point (P>0.1). Contrastingly, the treatment group scores became statistically different from the week 0 score at the 2 week time point (P<0.05).

4.3.4 Explant Analysis

Control (Stroke) Group

Histological analysis showed that at 1 week post stroke, rat brain tissue was extremely damaged. The tissue did not stain well, and it showed initial signs of degradation. By 4 weeks, most of the tissue had been degraded leaving a void of tissue within the rat brain.

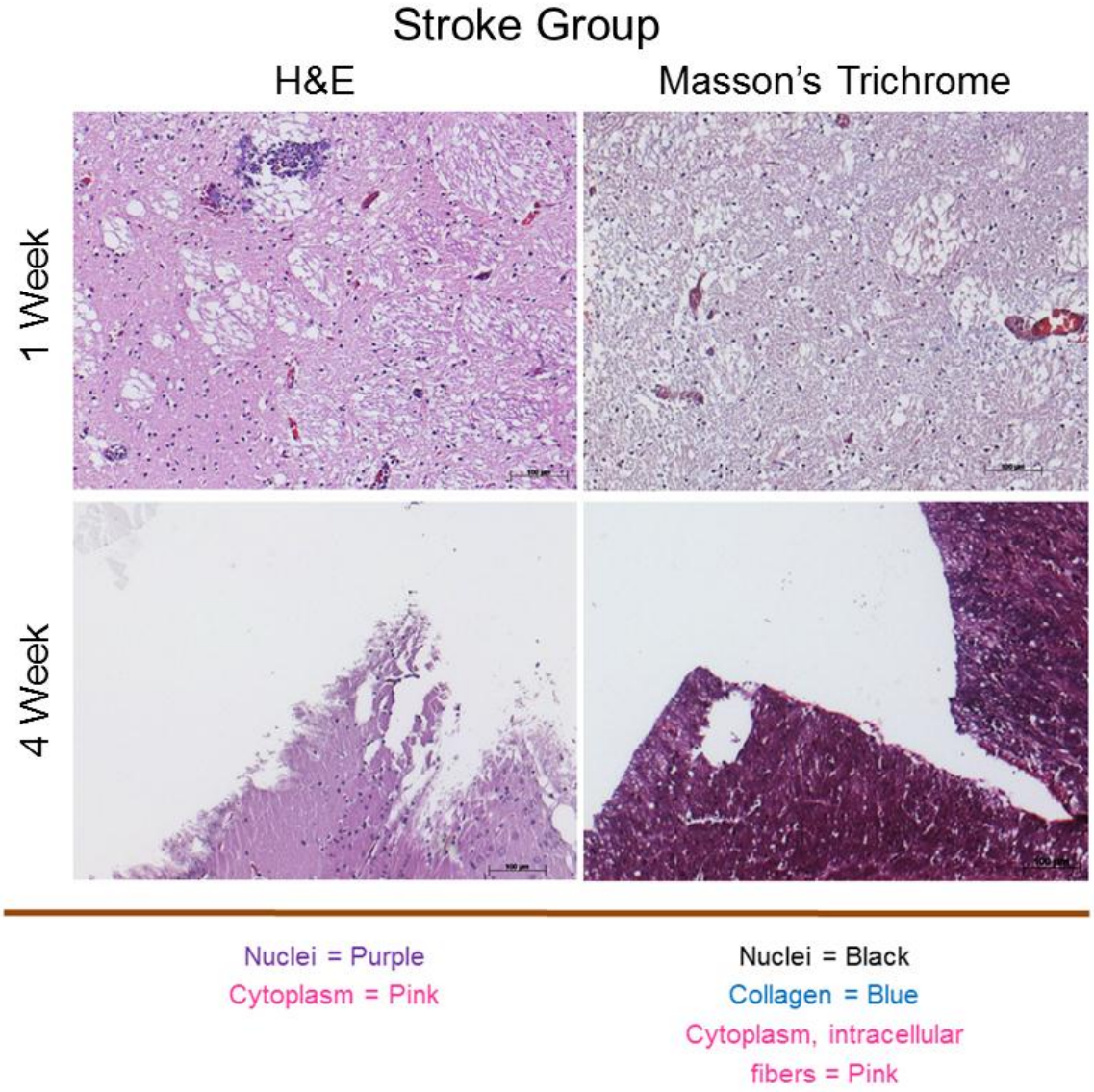

Figure 54: Control Group Histology. Overall, the tissue looked extremely damaged and stained poorly compared to healthy tissues. At 1 week, there were signs of degradation, and by 4 weeks most of the tissue had degraded leaving a void.

Figure 55 shows more matrix component specific staining. A similar trend of degradation is observed.

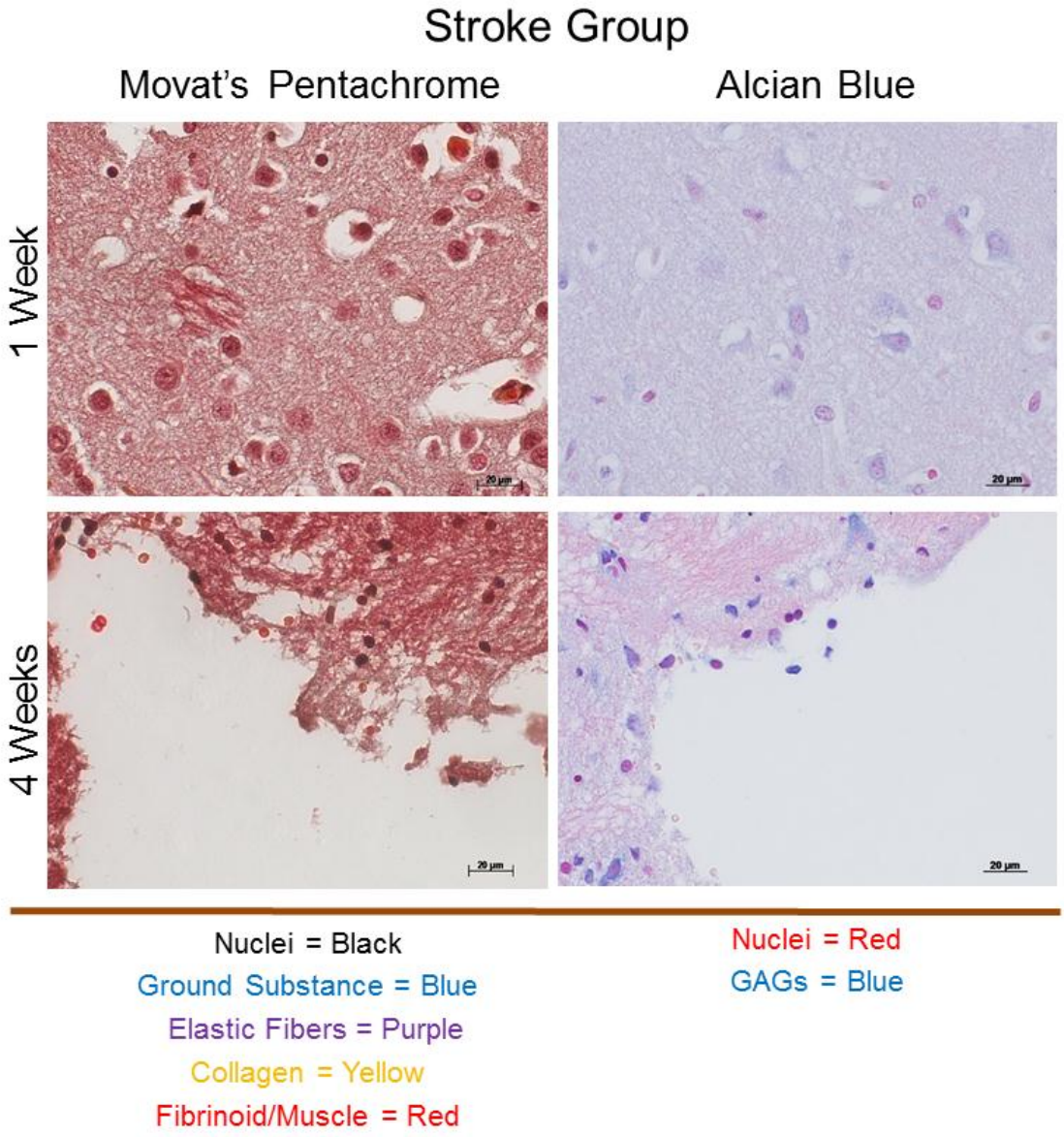

Figure 55: Control Group Histology Continued. At 1 week, there were signs of degradation, and by 4 weeks most of the tissue had degraded leaving a void.

Treatment Group – 1 Week Matrix Analysis

At one week, the implanted niche neural constructs did not show significant degradation or change in overall matrix composition.

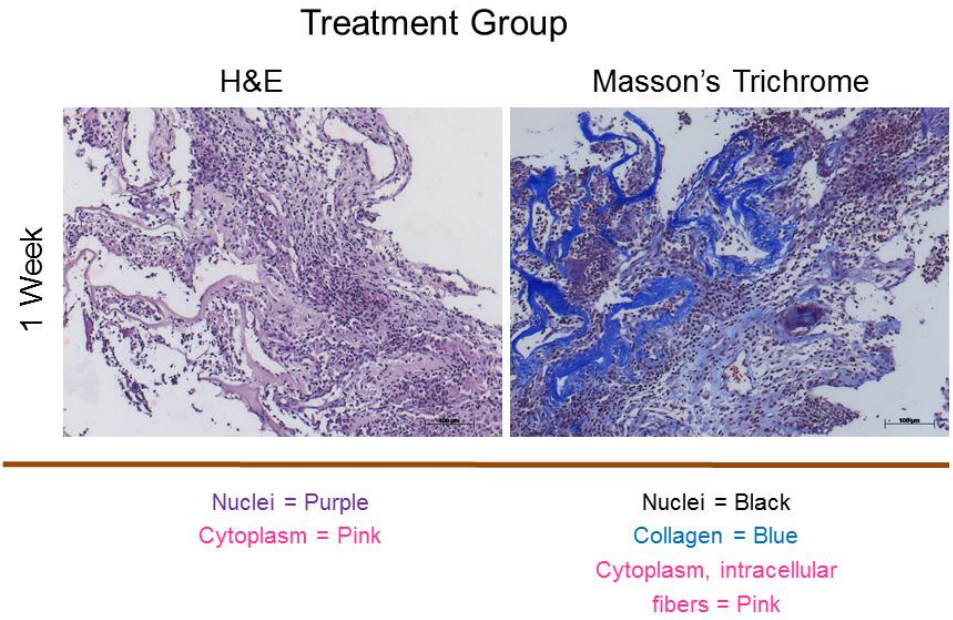

Figure 56: Week 1 Treatment Group – Matrix Analysis. Niche neural constructs did not show significant degradation. Additionally, the matrix remained almost entirely collagen.

Movat's Pentachrome staining revealed the matrix still contained elastin. Alcian Blue staining indicated that GAG formation was occurring between scaffold edges.

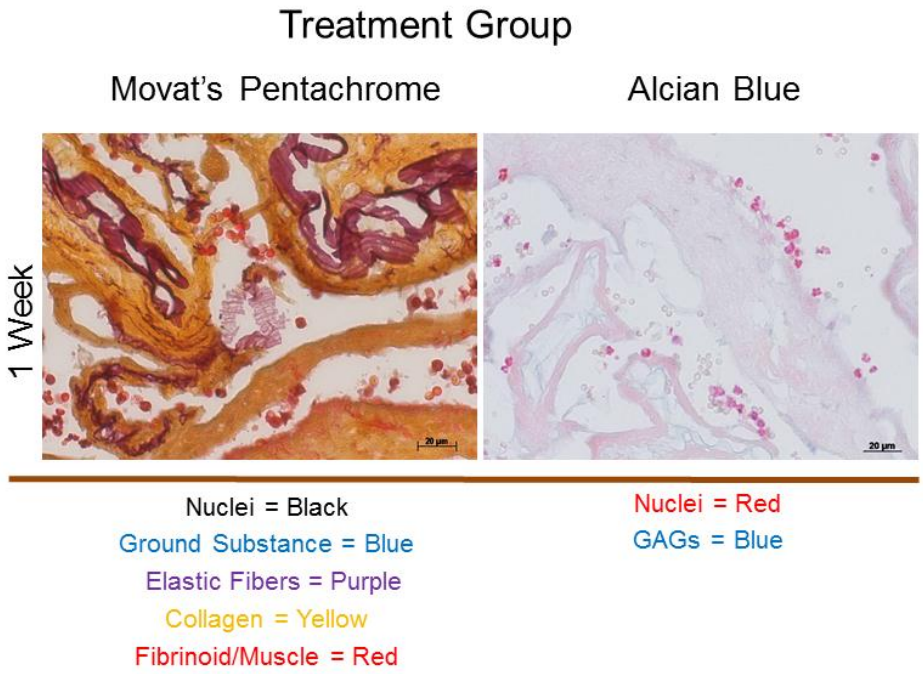

Figure 57: Week 1 Treatment Group – Matrix Analysis Continued. Niche neural constructs had retained elastin, left. At right, new GAG formation was occurring between scaffold edges.

Treatment Group – Week 4 Matrix Analysis

As seen in H&E staining, by 4 weeks, the constructs had large amounts of tissue ingrowth. This tissue appeared extremely disorganized, and it was not primarily composed of collagen.

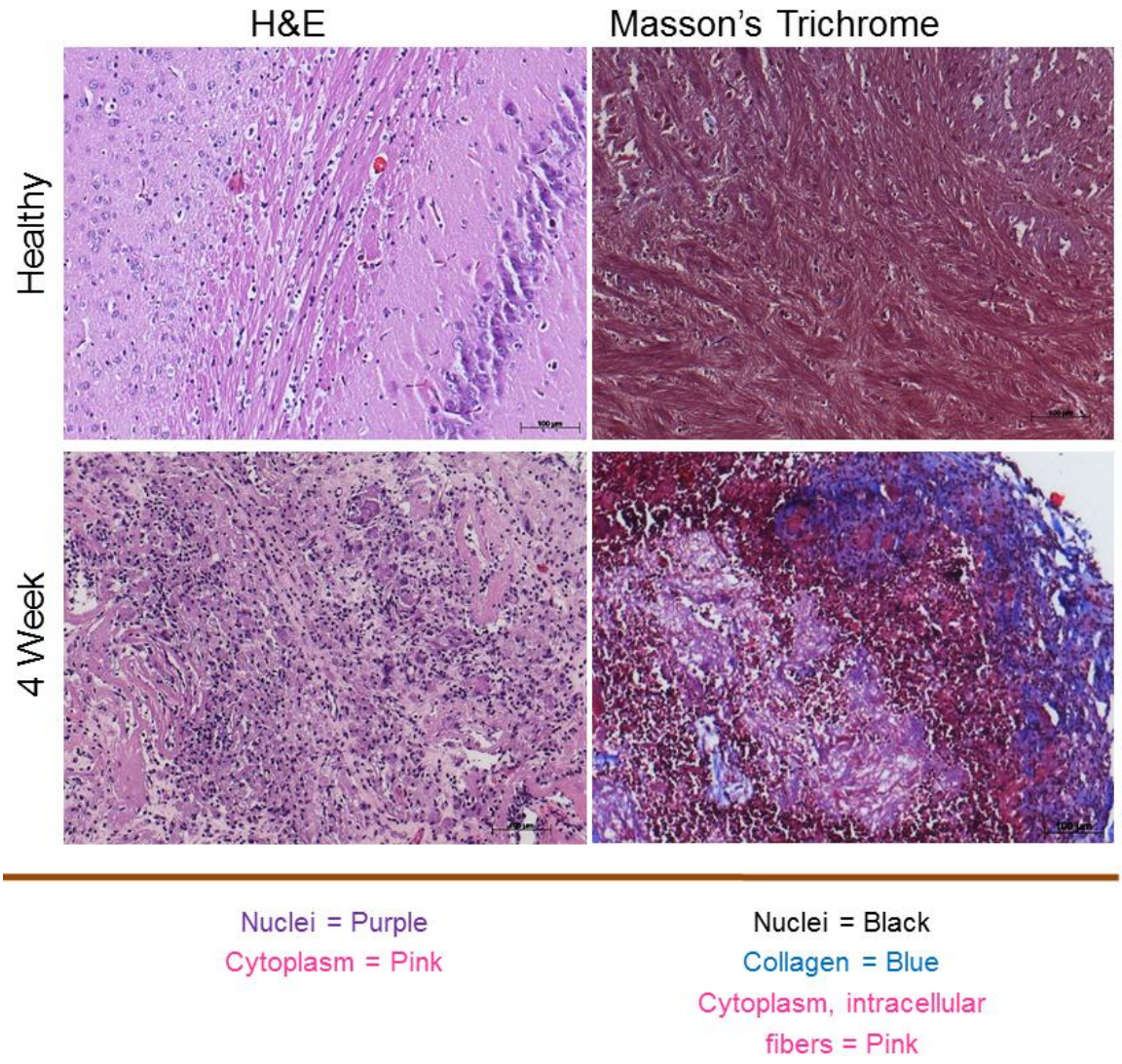

Figure 58: Week 4 Treatment Group – Matrix Analysis. There was extensive tissue ingrowth within the constructs. This tissue growth did not appear organized, and it was not primarily composed of collagen.

Staining with Movat's Pentachrome confirmed that the tissue ingrowth was not collagen. Staining with Alcian blue indicated GAGs comprised a significant portion of this new matrix.

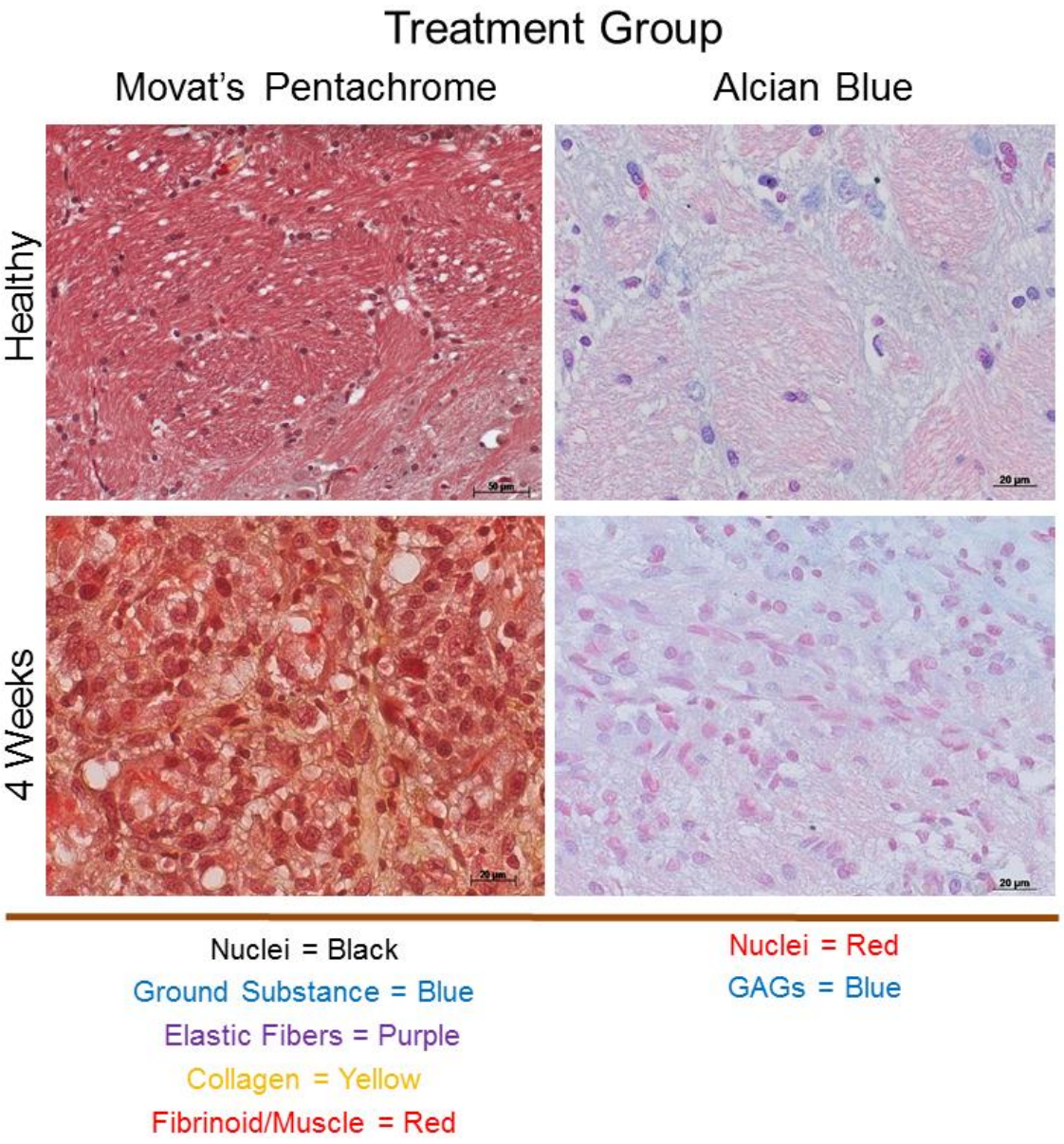

Figure 59: Week 4 Treatment Group – Matrix Analysis Continued. Movat's Pentachrome staining confirmed the lack of collagen in the newly formed tissue. Alcian Blue staining confirmed a large portion of this tissue was GAGs.

Vascular Assessment

Embedded in healthy brain matrix are numerous small blood vessels. As seen in figure 60, these vessels are typically 20μm in diameter.

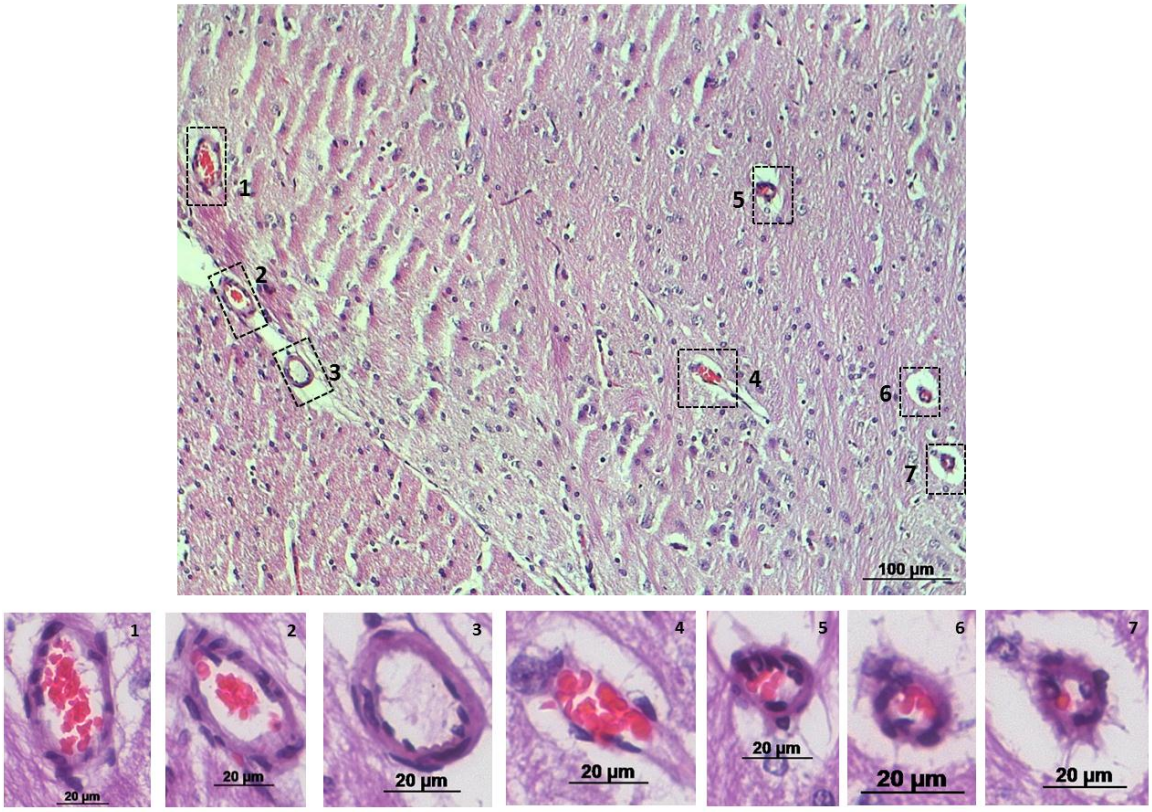

Figure 60: Healthy Brain Vasculature. Cerebral blood vessels differ in size and orientations, but they are primarily 20μm in diameter.

H&E staining of 4 week explants showed a similar network of small diameter vessels. Similar to the vasculature of healthy brain tissue, these vessels were 20μm in diameter on average. These vessels were distributed rather evenly across the construct, and contained red blood cells; no leukocytes were visible within the lumen of these vessels.

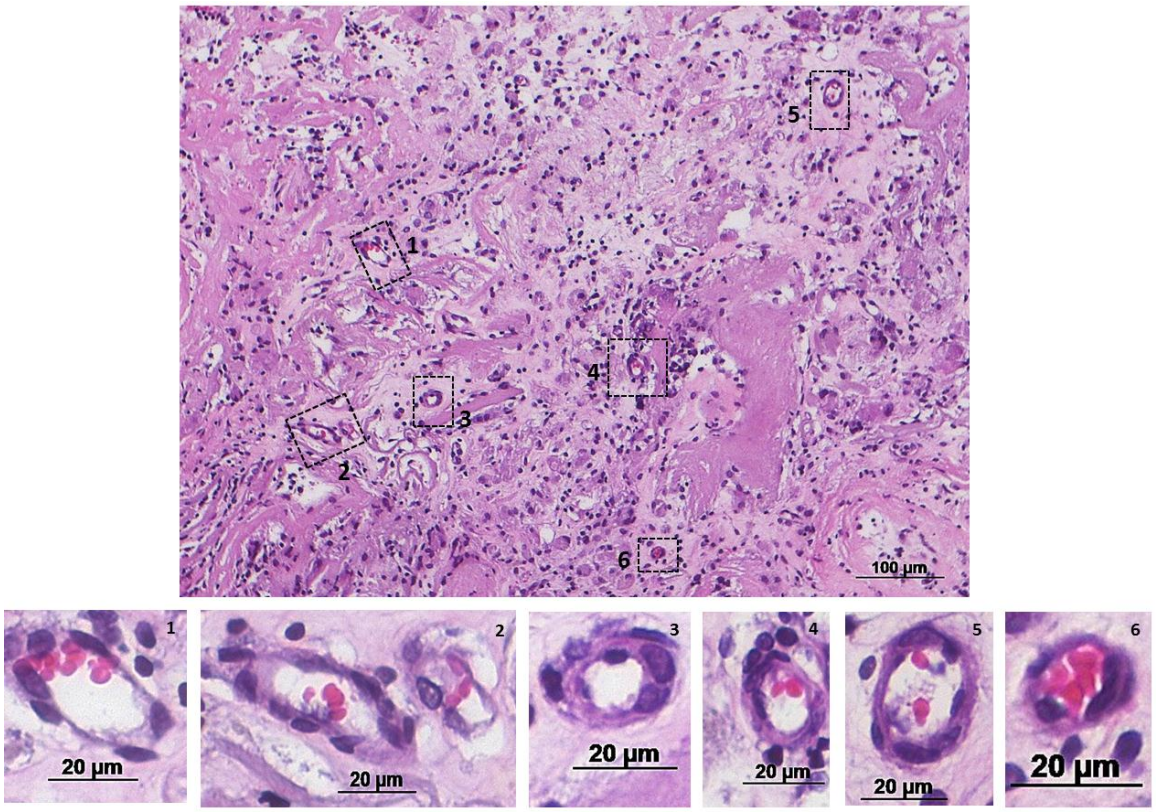

Figure 61: 4 Week Construct Vasculature. An evenly distributed network of blood vessels was observed within the constructs. These vessels were roughly the same size as the average healthy brain vessels.

Cellular Analysis

IHC for neural markers Nestin, Map-2, and GFAP revealed both Nestin and Map-2 staining within the construct regions at 4 weeks. However, no GFAP expression was observed. Both Nestin and Map-2 expression appeared in cell bodies as well as in the matrix surrounding the cells.

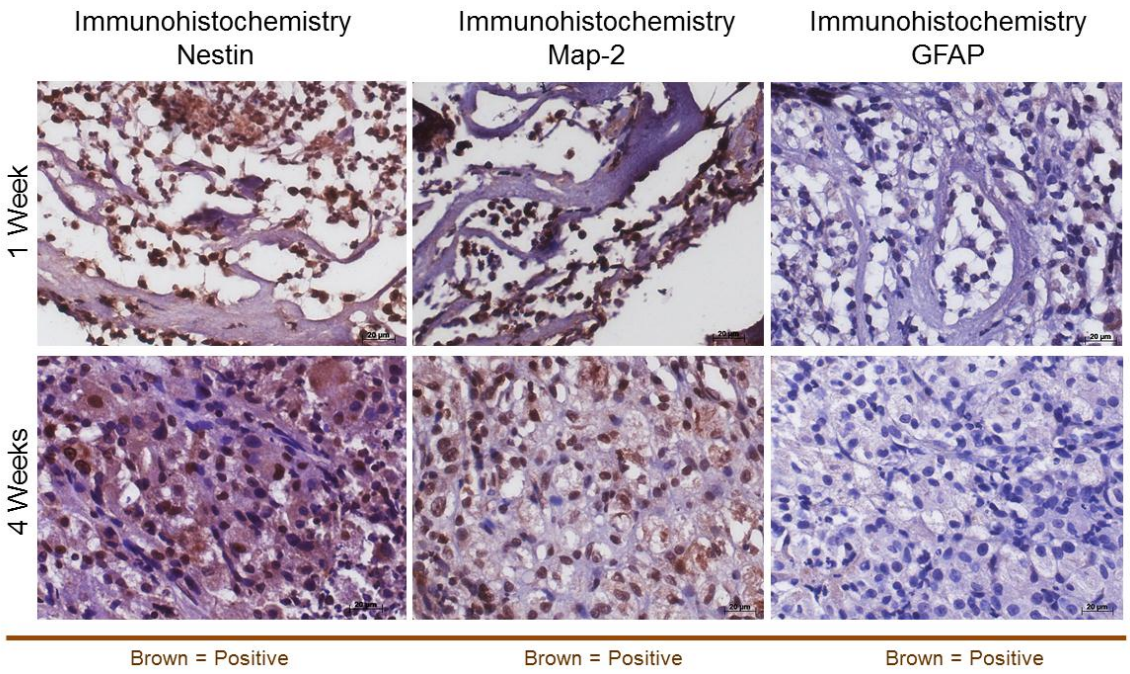

Figure 62: IHC for Neural Markers. Expression of Nestin and Map-2 was observed throughout the construct area. No GFAP expression was seen in the construct.

As illustrated in figure 63, quantitative assessment of marker expression revealed a statistical increase in the number of cells expressing neural markers over time, with the exception of no GFAP expression at either time point.

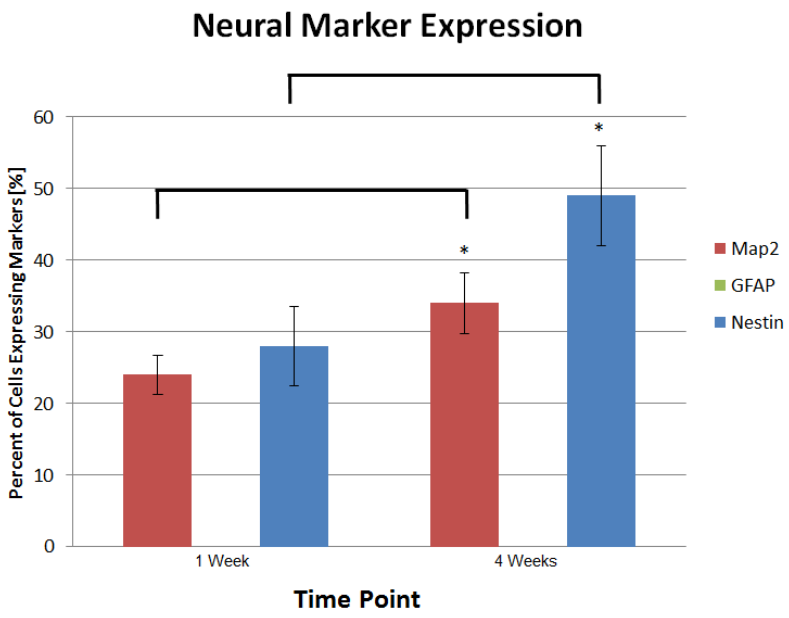

Figure 63: Quantitative Neural marker Expression. Expression of Nestin ($P<0.0005$) and Map-2 ($P<0.001$) increased from 1 to 4 weeks. No GFAP expression observed at either time point.

In depth analysis of cell types present in the construct area at 4 weeks was obtained through high magnification of H&E staining. Six prominent cell types were

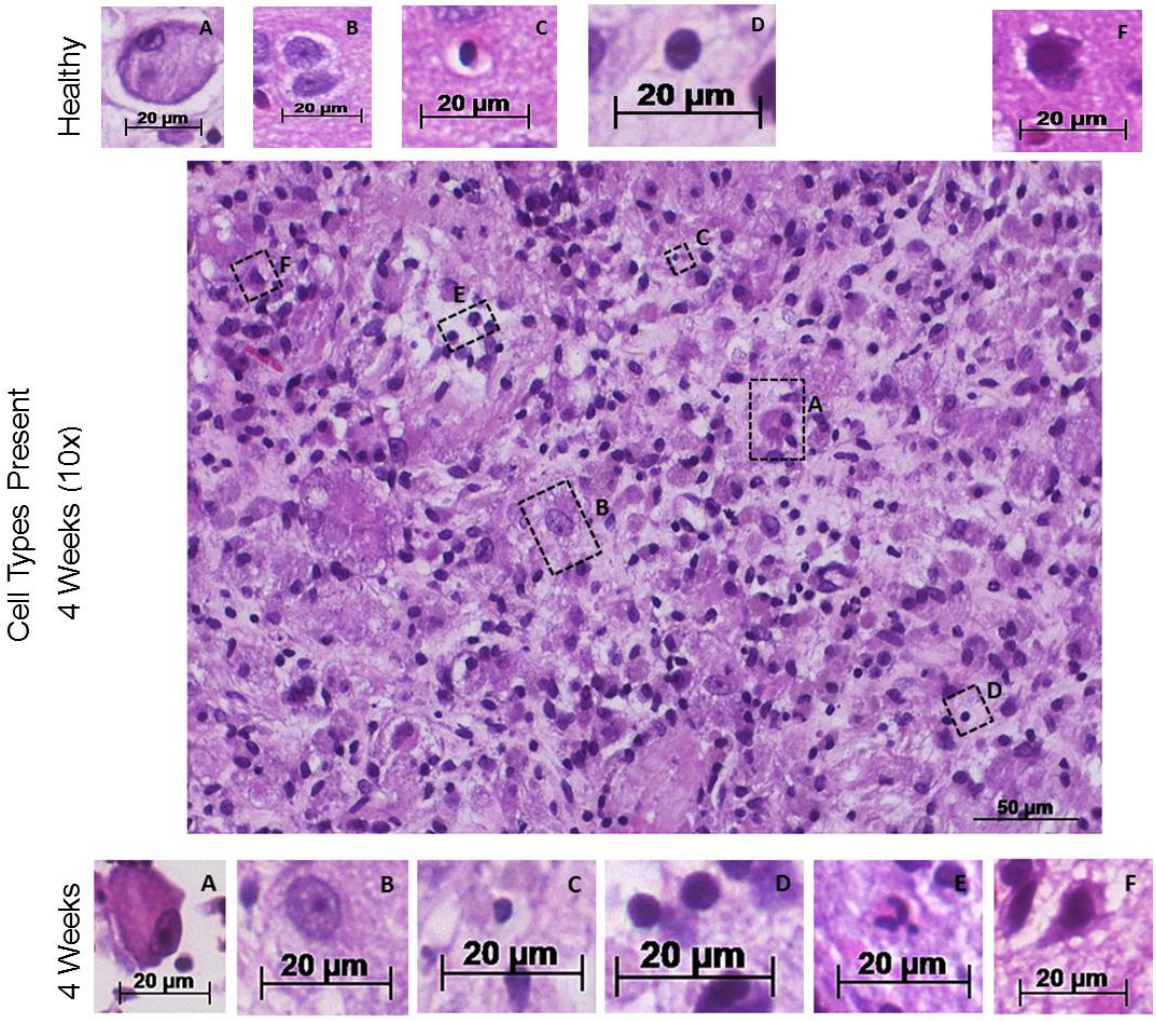

Figure 64: Cell Phenotype Analysis. Middle, a low magnification H&E image with boxes indicating different cell types observed within the construct area. Bottom, high magnification images representative of these cell types. Top, the equivalent cell type found within a healthy rat brain. Note: cell type E was not observed in the healthy brain.

observed, named A-F. Morphologically similar cells were identified in the healthy brain; however, cell type E was not located. Morphological analysis reveals cell types A, B, and F match a neuron phenotype. Cell types C and D appeared to be a form of accessory cell. Lastly, cell type E appeared to be a leukocyte.

In depth analysis was performed on potential neural cell types in an attempt to confirm their identity. Analysis of cell types A, B, and F is seen below. Cell types A, B,

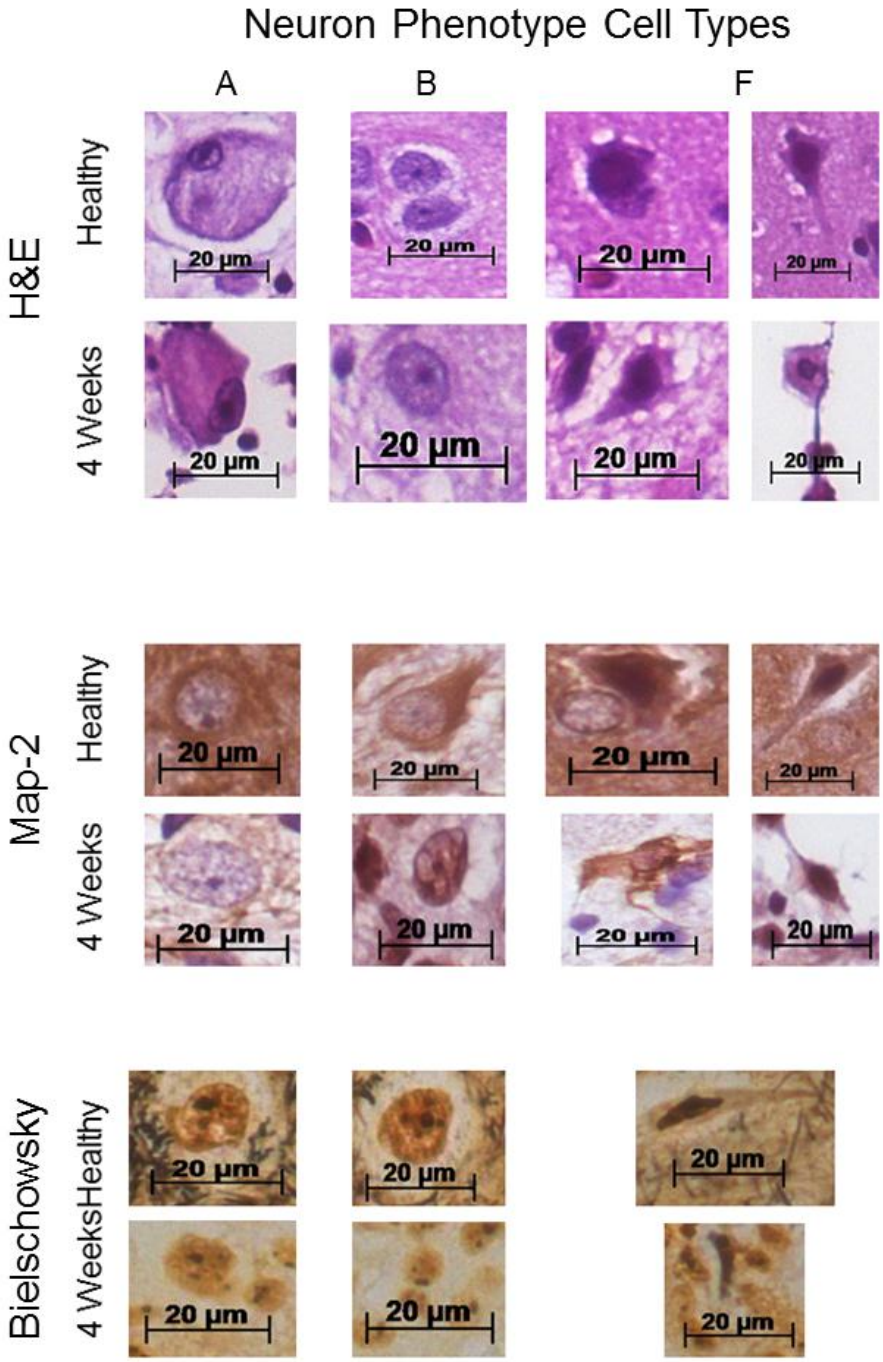

Figure 65: Analysis of Cells of Neuron Phenotype. Through H&E cells morphologically appeared to be neurons. Map-2 staining confirms expression of Map-2 is all these cell types. Bielschowsky staining confirms cell types A and B possess Nissil bodies.

and F are morphologically characteristic of neurons. Cell type F, the stereotypically recognized neuron has two orientations, both are represented in the H&E and Map-2 stains. These neurons stained very darkly and did not necessarily have a visible nucleus and or nucleolus. They did have visible projections, stained for Map-2 along the length of the cell, but they did not stain for Nissil bodies. Cell type B is characteristic of a cross section of an axon, where the axon appears rather centrally and is surrounded by Nissil bodies. Both cell type A and B tended to have concentric Map-2 staining around the cell body. Cell type A was significantly larger than the other cell types and the nucleus and nucleolus were along the periphery.

Cells with characteristic accessory cell phenotypes underwent similar analysis. Morphologically, cell type C was much smaller than cell type D. Both of these cells were typically found in close proximity to cells phenotypically characterized as

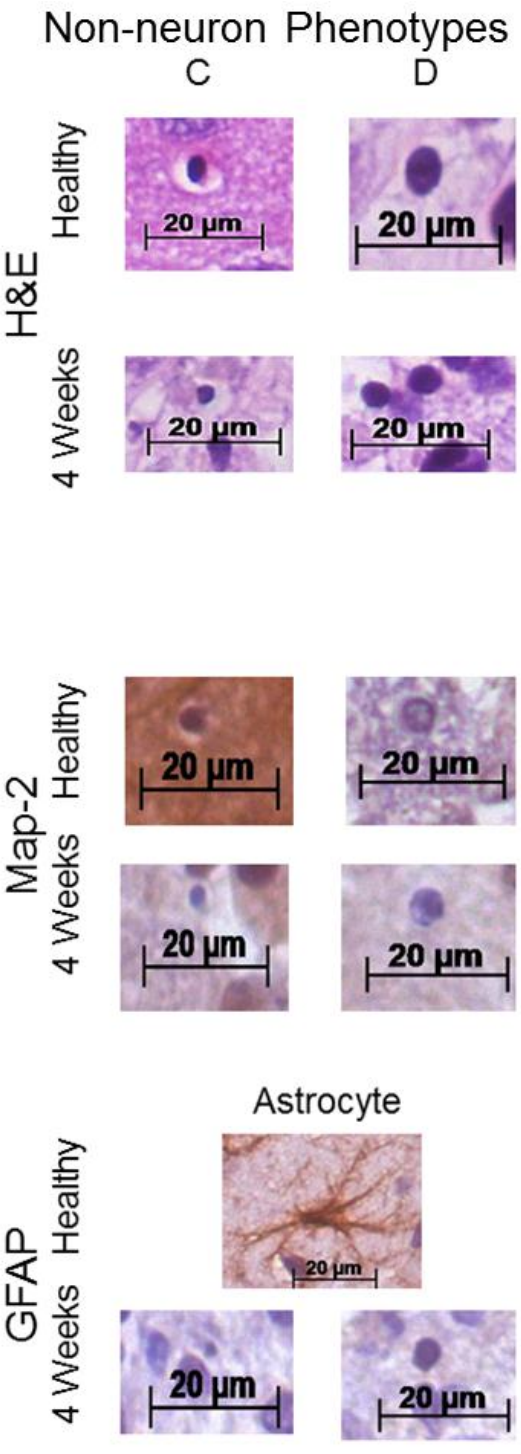

Figure 66: Analysis of Accessory Cell Phenotypes. Both cell types did not express Map-2 or GFAP. An astrocyte is represented and stained with GFAP to allow comparison between cell types C and D and astrocytes.

neurons. As illustrated in figure 66, neither cell type stained for Map-2 or GFAP. In figure 66, an astrocyte from a healthy brain is represented as the healthy cell for GFAP staining to allow comparison between cell types C&D and astrocytes.

HADSCs

Explants from both time points underwent double staining immunofluorescence for human mitochondria (expressed by the HADSCs) and Map-2 (expressed by HADSCs seeded onto niche neural constructs prior to implantation).

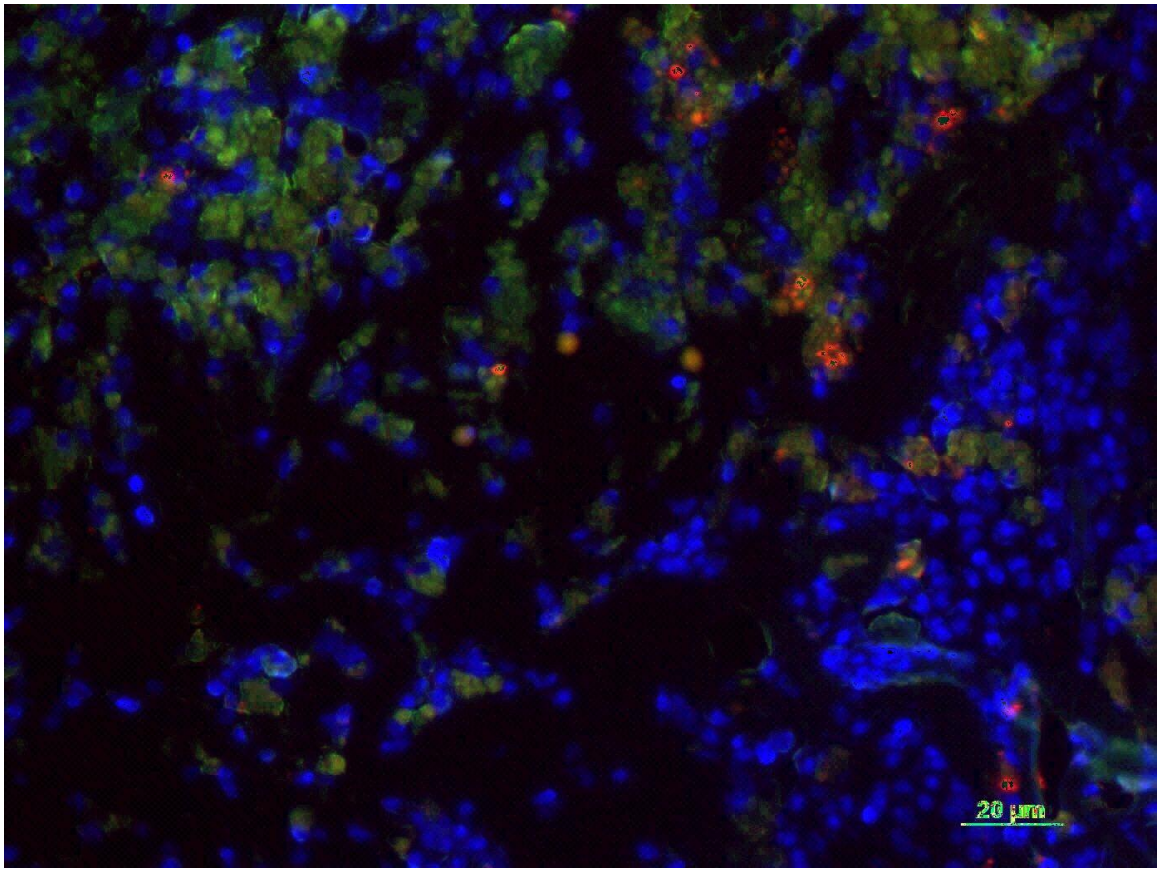

Figure 67: Human mitochondria Map-2 Double Stain. Some individual cells expressed both human mitochondria as well as Map-2. A notable amount of cells also solely expressed Map-2.Green indicates Map-2. Red indicates human mitochondria. Blue indicates DAPI nuclear staining.

Overlays of staining indicated that some individual cells were positive for both Map-2 and human mitochondria. However, a notable number of cells expressed only Map-2. See Appendix A for additional double staining.

The Interface

Analysis of the construct – brain tissue interface revealed no identifiable capsule formation. The construct appeared well integrated with the surrounding host tissue. Additionally, this integrated region was vascularized (indicated by the arrows in figure 68).

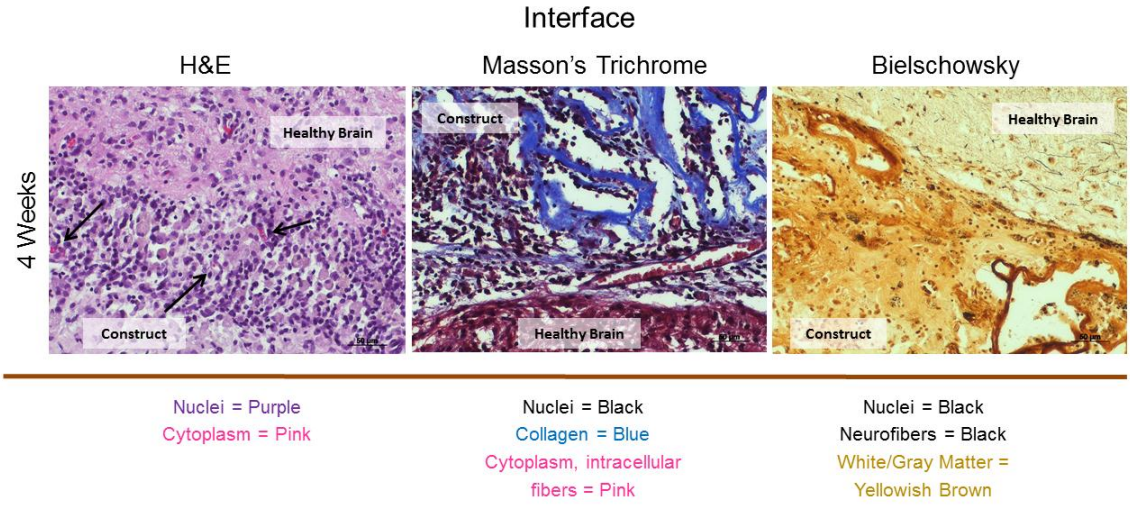

Figure 68: Histological Examination of the Interface. The construct is well integrated with the host tissue with no identifiable fibrous capsule formation. The area is vascularized as indicated by arrows.

Analysis through Movat's Pentachrome and Alcian Blue yielded similar results. In both Movat's and Alcian staining, some cells were oriented orthogonal to the interface, appearing to bridge the gap between construct and host tissue. Additionally, high magnification Alcian Blue staining showed neurons (indicated by arrows) at and on both sides of the interface.

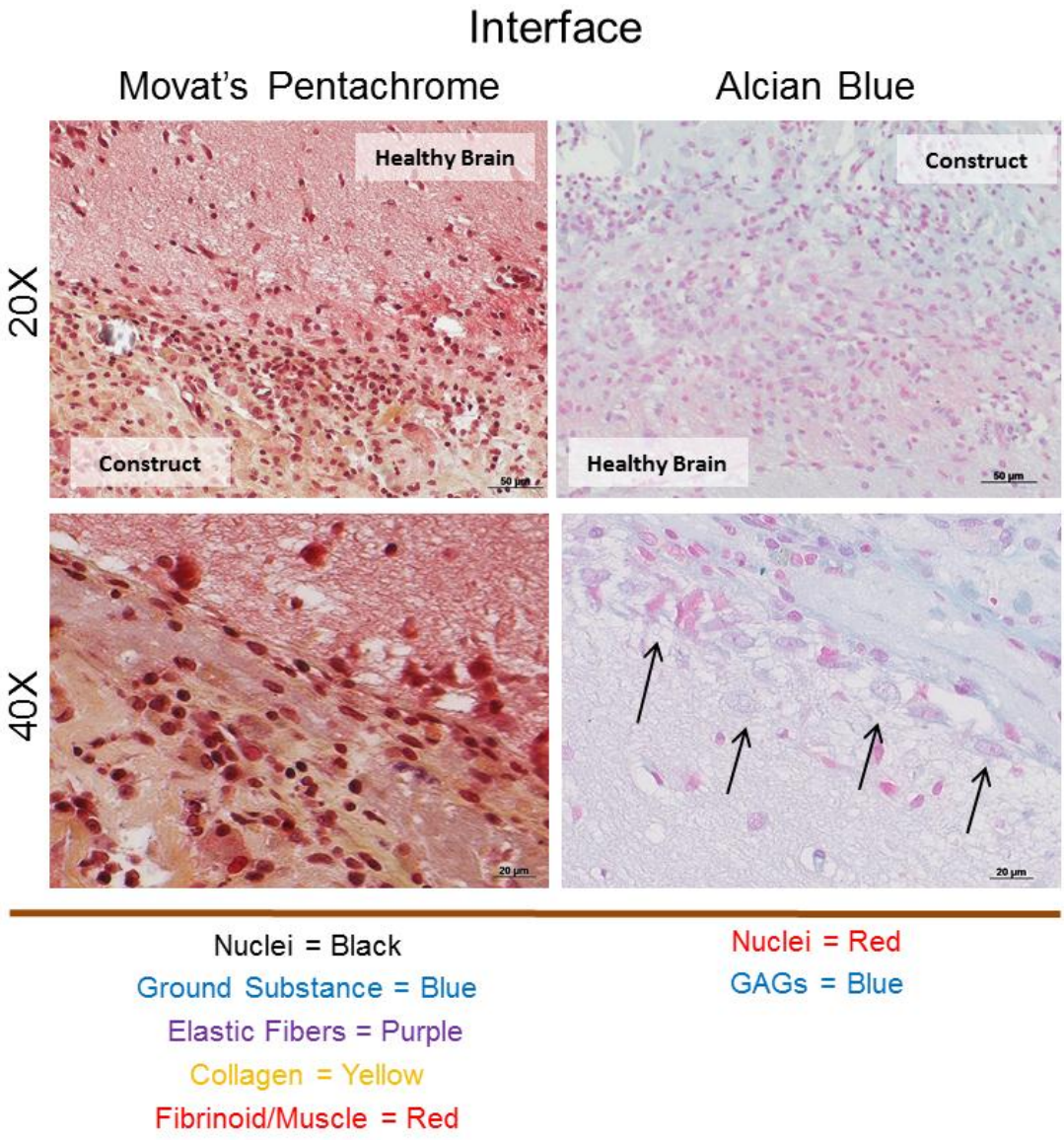

Figure 69: Histological Examination of the Interface Continued. Some cell bodies were orthogonal to the interface, bridging the construct and host tissue. High magnification Alcian Blue staining showed neurons at and on both sides of the interface.

IHC for neural markers confirmed that the majority of cells at and on both sides of the interface stained positively for Nestin and Map-2. GFAP expression was only visible on the host tissue side of the interface.

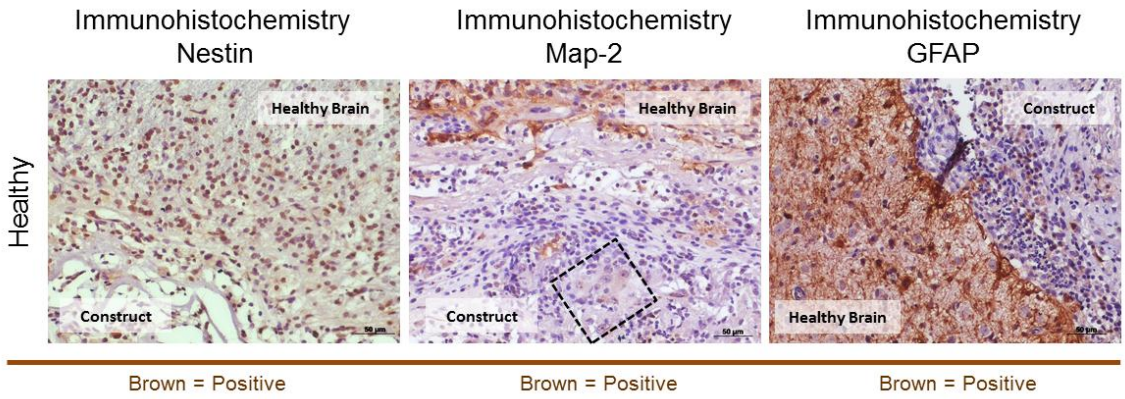

Figure 70: IHC for Neural Markers at the Interface. The majority of cells at and surrounding the interface expressed Nestin and Map-2. Specifically, neurons were visible at the interface (indicated by the box). GFAP expression was only observed on the host-tissue side of the interface

Significantly, there was no evidence suggesting reactive astrocytes had formed a glial scar surrounding the construct. The number of astrocytes nearing the interface was consistent with healthy brain tissue.

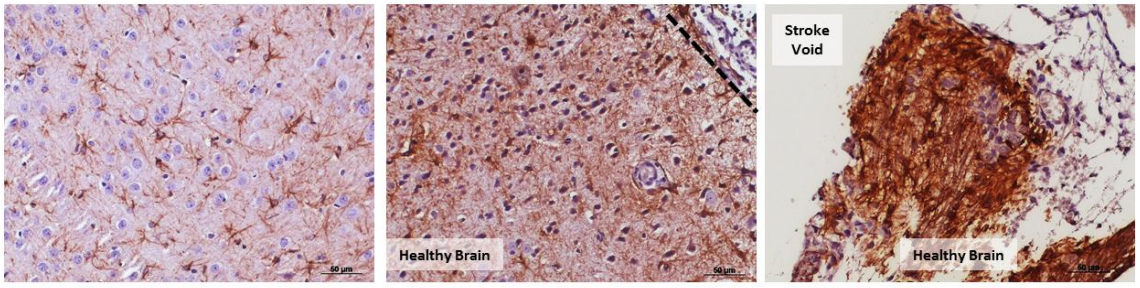

Figure 71: GFAP Expression at the Interface. The number of cells expressing GFAP near the interface (middle) is consistent with that of healthy brain tissue (left). (Right) Extremely high levels of GFAP expression near the edge of a 4 week control group explant.

CHAPTER 5: ANALYSIS AND DISCUSSION

5.1 Neural Scaffolds

A neural scaffold was successfully created through the Decellularization of a porcine brain. As expected, though this process the scaffold lost significant mass, and both qualitative and quantitative analysis confirmed a significant reduction in DNA. Additionally, IHC staining for neural cell markers confirmed complete lack of expression indicating no cellular or protein remnants in the decellularized scaffolds.

Histological characterization of the scaffolds immediately confirmed an intact matrix with the absence of all cell bodies, nuclei, and neural fibers. Both Masson's Trichrome staining and Movat's Pentachrome staining indicated the scaffold's primary composition was collagen. However, Movat's staining revealed retention of the fibrous protein elastin and GAGs (confirmed with Alcian Blue staining).

Lastly, IHC for basement membrane proteins confirmed the retention of collagen IV and Laminin within the matrix. Staining primarily occurred around what appear to be intact blood vessels. All scaffold characterization and analyses support the scaffold's ability to serve as a non-cytotoxic niche for stem cells.

5.2 Niche Neural Constructs

To replicate the gold standard in neural induction, Woodbury's NIM protocol was utilized. This protocol calls for a 24-hour pre-induction step consisting of DMEM, 20% fetal bovine serum, and 1mM β-mercaptoethanol. However, after 24 hours in this medium cells had aggregated and detached from the plastic. Subsequent studies did not utilize this pre-induction step with seemingly no differentiation repercussions. Woodbury

did not monitor cell viability over the course of his study, so our results were compared to Safford and Qian, two publications with induction mediums very similar to the one utilized in this research. By 5 days, Safford reported 35% viability and by 7 days Qian reported 5% viability. The viability results represented in tables 2-4 are slightly lower than Safford by 5 days likely due to the fact that Safford did not employ DMSO, a known cytotoxic cellular environment, in his induction approach. Overall, the values presented in this research fall within close proximity to published results.

The immunofluorescence results for cells seeded onto plastic showed significant morphological changes as early as 24 hours post-induction. Expression of all markers was observed at this time point, but due to almost complete cell death it is unknown if this expression was maintained to day 5. Overall, the efficacy of the NIM protocol was confirmed and a baseline for construct assessments established.

To our knowledge, no publication has examined the effect of changing out the NIM on a regular basis throughout a short-term study. Our hypothesis was that the extremely poor viability associated with NIM induction may be due to a lack of nutrient supply, and that the cells may be dying for these reasons and not solely due to the harshness of the chemical environment. Our hypothesis was proven false, as replacing the NIM resulted in even poorer cell viability. By day 5 statistical difference between NIM and NIM replaced groups was observed. Additionally, the overall neural differentiation of these cells past 4 hours was quite poor. It is likely that the waning viability of the cells contributed to this lack of morphological change and cellular interaction.

Since neural induction is a widely characterized and established approach in the neural regeneration field, it was necessary to determine if this approach is compatible with our neural scaffolds. This also helped establish claims that the scaffold was in fact

capable of maintaining neural-like cell life. Scaffolds were successfully seeded with NIM induced cells. Initially there was no deviation in cell viability from groups seeded onto plastic. However, as early as 24 hours there was statistical difference between the viability of cells seeded onto scaffold vs. cells seeded onto plastic. Significantly, over 90% of these cells had remained viable. Contrary to the established inverse relationship between cell viability and quality of induced differentiation, the quality of differentiation of these cells was not lessened. From 4 hours to 5 days, expression of all markers had been maintained. By 5 days, there is a >8x increase in viability observed when cells are seeded onto scaffolds. Again, the success of differentiation was not hindered as a result of this viability. Most significantly, the Map-2 expression observed was still cytosolic indicating cells were progressing towards a neuron lineage.

We then hypothesized that changing out the NIM would have similar negative effects seen with cells seeded on plastic, but that the scaffold could mitigate some of these effects, still showing an increase in cell viability with less compromised quality of differentiation. As figure 28 illustrates, there was similar viability between scaffold seeded NIM and scaffold seeded NIM replaced groups at 24 hours, but by 5 days statistical difference was observed. However, by 5 days, the scaffold seeded NIM replaced group was still 7x greater than either group where cells were seeded onto plastic. This indicates that the scaffold does mitigate but not completely alleviate the viability limitations of replacing the NIM. The quality of differentiation of these cells was also mitigated but not completely maintained. By 5 days, marker expression was faint but still present (compared to completely absent in plastic seeded groups), specifically cytosolic Map-2 expression was no longer present.

HADSCs with no induction step were seeded onto scaffolds and maintained with their manufacture recommended media to examine the stem cell niche potential of the scaffold. We hypothesized these cells would show significantly higher viability than any of the previous groups at all time points. Some decrease in viability was expected due to a lack of nutrient supply. Additionally, the scaffold should promote unaided differentiation of the seeded cells into neural-like cells. Viability assessments confirmed only a slight decrease in cell viability (to 84%) over the 5 day period. Protein expression analysis confirmed expression of all markers as early as 4 hours. By 24 hours this expression was maintained and Map-2 expression had transitioned from nuclear to cytosolic. In contrast to all previous results, the 5 day time point exhibited the most successful differentiation with all markers being expressed at a higher intensity. Additionally, significant morphological changes, visible as early as the 4 hour time point, had also been maintained. The cells also appeared to exhibit varying forms of alignment. This evidence confirms that the previously described tissue engineered scaffold reseeded with HADSCs produces a niche neural construct.

In an effort to provide optimal conditions for survival of seeded cells, we hypothesized that replacing the MesenPRO medium would result in an increase in overall cell viability without compromising differentiation, morphology, and alignment. An increase from 84% to 93% in cell viability was observed. As expected, the quality of differentiation also appeared to increase with each time point, culminating in the most promising expression at day 5. By 5 days the cells showed cytosolic expression of all markers, significant interaction and alignment, and morphological changes. Interestingly this alignment was occurring at the cell body level as well as occurring with the projections these neural-like cells are developing. Significantly, this evidence indicates:

1) our niche neural construct can produce a >85% viability increase compared to cells seeded onto plastic. 2) These cells are more neural-like, showing a higher quality of differentiation, cellular alignment, and changed morphology compared to cells seeded onto plastic. 3) Successful neural differentiation of HADSCs can occur without the use of the potentially cytotoxic or harmful chemicals utilized in neural induction.

5.3 In Vivo Efficacy

Stroke was successfully induced and a delivery mechanism for our construct was validated. Large amounts of animal death are commonly associated with this procedure, and our animal study was no exception. In future studies we anticipate this death rate to lower based on surgeon and animal care staff familiarity with the procedure. As previously mentioned, treatment delivery typically occurs at one day or seven days post stroke. In future studies, employing a 7 day time point may provide the animals with more recovery time, further improving the survival rate. The construct implantation was ultimately more patient-specific than initially anticipated. Though the average infarcted area determined by TCC staining was used as a general location for implantation, the distinct textural differences between healthy and damaged brain tissue allowed for more targeted treatment delivery.

Behavioral testing indicated the success of this treatment method from a sensory/motor functional recovery perspective. Stroke controls did not show any statistical improvement ($P>0.1$) over the 4 week period. Not only did the treatment group show statistical improvement, but also this improvement was statistically different from control rats as early as 2 weeks post stroke ($P<0.5$). It is also important to note that there was no statistical difference in the week 0 mNSS scores between groups ($P>0.1$). Most

significantly, the treatment group exhibited almost complete recovery by 4 weeks. It is important to note that complete recovery indicates perfect completion of the mNSS analysis; it is not a statement of complete return of all sensory or motor functions. More behavioral tests would be necessary to understand exactly which types of functions have completely recovered and which have not.

Histological examination of the stroke group revealed a visibly damaged area at 1 week post stroke. This tissue was extremely fragmented and overall does not stain well – indicating significantly compromised tissue health. There is also significant hemorrhage observed throughout this area. As dictated by the previously described stroke pathology, this damaged tissue area eventually degraded resulting in a physical void within the brain. This has been reported as early as 7 days in rat models.[16] In our study, this characteristic behavior was observed in the presented stroke controls by 4 weeks.

At 1 week post craniotomy, the treatment group showed significant cell presence throughout the construct. Masson's Trichrome and Movat's staining confirmed very little remodeling had occurred, as the majority of the construct was still comprised of collagen. Some red blood cells remaining from stroke or craniotomy-related hemorrhage were also observed. Alcian Blue staining showed initial tissue ingrowth occurring between the folds of the construct; this tissue was almost exclusively GAGs.

Extensive and widespread tissue ingrowth occurred by 4 weeks. This tissue appeared not well organized and was heavily populated by cells. The composition of this newly formed matrix was not collagen, indicating a degree of scaffold degradation prior to tissue ingrowth. Significantly, there was a large amount (relatable to fresh tissue) of

GAG formation. Overall, this newly formed tissue greatly resembles granulation tissue, the initial tissue type formed during the wound healing process.

The large population of cells necessitated an examination of neovascularization within the construct area to determine if these cells were getting oxygen and general nutrient supply. As figure 61 illustrates, vessels primarily 20μm in diameter were widely spread throughout the newly formed matrix within the construct area. These vessels showed distinct endothelial cell linings with a lumen filled with red blood cells, a strong indication of the biocompatibility and integration of the construct by the host.

Further indications of integration and maintenance of the construct area as a viable tissue result from in depth analysis of the cell types observed in this area. Numerous cells throughout the construct stained positively for Nestin and Map-2, indicating cells committing to neuron lineages. Interestingly, expression of both these markers increases from 1 to 4 weeks. This could support the mechanism proposed by Borlongan that stem cells act as bridges, providing a pathway for host neural cells to migrate into damaged tissue areas. Contrastingly, no cells stain for GFAP confirming that this area is not a host to reactive astrocytes and therefore no further analysis relating to glial scarring was done. However, another measure to increase the validity of this claim would be analysis of chondroitin sulfate.

Figure 64 shows an in depth analysis of the representative cell types populating the scaffold area. Cell type A contains a larger cell body with a non-centered nucleus and a visible nucleolus. These cells express Map-2 and contain Nissil bodies indicating these cells are in fact a neuron. However, these cells were not observed in high populations. Cell type B is very characteristic of a neuron. These cells contain Nissil bodies, express Map-2 in a concentric ring around the cell body, and have a centrally

located axon (in cross section). These cells were observed consistently throughout the construct area and are overall one of the largest cell populations. Cell type F is the stereotypical neuron. This neuron has numerous orientations including a darkly staining area with or without a distinct nucleus/nucleolus. Additionally, the extensions of these cells are visible in some orientations. These cells do stain positively for Map-2, but no Nissil bodies are seen due to their orientation and dark staining.

Cell types C and D are both found in near proximity to the previously described neurons. These cells appear to have no cytoplasm; they appear as one small (type C) or large (type D) nucleus. Morphologically, these cells mimic accessory cell phenotypes. Lack of Map-2 staining confirms these cells are not neurons, and lack of GFAP staining indicates these cells are not astrocytes. They could be oligodendrocytes or another form of accessory cell. Further analysis is required to confirm the identity of these cells.

The presence of cell type F clearly indicates leukocytes have been recruited to the construct area. These cells are presumably macrophages, recruited to degrade the scaffold in the initial phases of a wound healing response ultimately leading to tissue remodeling and regeneration. IHC for rat macrophages confirmed a macrophage presence (not shown). Importantly, no foreign body giant cells were observed anywhere in the explanted tissue at either time point, a strong indicator of biocompatibility. This also supports that the macrophages are present from remodeling mechanisms vs. chronic inflammatory mechanisms.

The fate of the implanted HADSCs was examined through identification and staining of human mitochondria. Figure 67 illustrates that populations of the HADSCs have remained engrafted in the construct area. Though the exact amount of cells was not quantified, there was significant engraftment and retention of these implanted cells to

the damaged area. Most significantly, these cells still express Map-2, indicating these cells have committed to a neuron lineage. To our knowledge this is the first data supporting sustained neural differentiation of stem cells in a stroke animal model. Neural induction has been previously confirmed in traumatic brain injury models; however, the success refers to cells that have committed to a neural but non-neuron phenotype (i.e. astrocytes, oligodendrocytes, and microglia). To our knowledge, this is the first data supporting injected cell commitment to a neuron lineage over a 4 week period. A notable amount of Map-2 expression co-localized with cell nuclei (but not co-localized with human mitochondria staining) is observed throughout the construct area. This is another indication that this research supports implanted cells recruiting host neural cells via paracrine effects. However, as previously mentioned, HADSCs have maintained neural protein expression and remained in the construct area indicating that mechanistically the HADSCs' functions are beyond strictly paracrine.

Histological analysis of the interface served as a final assessment of construct integration and biocompatibility. Overall, there were no indications of fibrous encapsulation. There is no gap between the host tissue and construct tissue. There is a strong presence including cells that are oriented orthogonal to the interface. The area is contains extensive cell populations including neurons. Cells on both sides of the interface express Nestin and Map-2 indicating a strong neuron and neural cell presence in the area. No GFAP expression was observed within the construct and the quantities of GFAP positive cells on the host side of the interface was consistent with the numbers found in healthy brain tissue. More in depth examination of the host-side of the interface reveals no glial encapsulation, indicating the scaffold is not contributing to or promoting anti-regenerative astrocyte activity. Lastly, this are is well vascularized (see figure 68).

CHAPTER 6: CONCLUSIONS

A novel neural scaffold was successfully created and characterized using a tissue engineering approach. Specifically this scaffold showed an intact matrix, almost no DNA remnants, no cellular remnants, and retained basement membrane proteins.

In vitro cell seeding studies confirmed the ability of this scaffold to support and maintain the viability and neural protein marker expression of both NIM-induced and non-induced cell types up to 5 days. Most significantly, the scaffold does promote the unaided differentiation of HDSCs into cells of great neural likeness and maintains these cells, indicating the scaffold is in fact a stem cell niche.

Niche neural constructs were successfully implanted into stroke-afflicted rats resulting in significant sensory/motor functional recovery as well as the continual support of life and neural likeness of HADSCs as well as host neural cells. After 4 weeks, implanted HADCSs remained in the construct area and appeared to be committed to a neuron lineage. To our knowledge, this is the first evidence suggesting significant retention of implanted stem cells to damaged stroke areas as well as the first evidence validating neural induction in animal stroke models. There was significant evidence suggesting this construct was integrating with host tissue. There was no evidence of fibrous encapsulation at the interface, which was vascularized and the host of numerous neurons among other cell types. Additionally, the construct had begun to degrade to make way for a newly formed vascularized neural matrix. Overall, these results support the future use of this niche neural construct for the next generation of stroke treatments.

CHAPTER 7: RECOMMENDATIONS

Though the niche potential of this scaffold was confirmed to 5 days, longer studies are needed since any clinical application would necessitate use past 5 days. Also, HADSCs have been proven to revert from a neural lineage after the neural induction process. Longer studies are required to ensure the non-induced group does not show this same behavior as the viability of the cells wanes. Additionally, I would suggest combinations of NIM and MesenPRO media be utilized in the in vitro conditioning of the niche neural constructs. The evidence presented in this work shows significant evidence suggesting NIM induction yields faster differentiation while the non-induced cells exhibit maintained differentiation and viability percentages nearing clinical relevance. A combination of these (ex. 1 day exposure to NIM followed by MesenPRO) may lead to more efficient niche neural construct preparation.

The goal of this research was to establish preliminary efficacy of this niche neural construct in stroke treatment applications. More in depth analyses are required to further confirm sensory/motor recovery and understand the regeneration observed in the construct region. More involved behavioral tests such as the adhesive removal test, food grabbing test, and NSS scoring system could be employed to achieve a better and more thorough representation of damage. Additionally, the researcher performing these analyses must be blind to the condition of the rats. Another important consideration in the framework of the study is to include more control groups (scaffold only, and sham craniotomy) and overall larger animal numbers in order to achieve a higher degree of statistical relevance. Since there is significant evidence suggesting new matrix formation, analysis of neurotrophic factors and other neural matrix proteins would confirm that this newly formed matrix is actually brain matrix. A much longer study would

also allow for the establishment of a neural regeneration timeline. For example, a two-week timeline is appropriate for analysis of skin regeneration; due to very minimal success in this area neural matrix regeneration has no generally accepted timeline. The vast abundance of neurons in the regenerated area begs the question: are these functional neurons. This research preliminarily suggests that are, but examination of more neuron-specific proteins such as sox2 and NeuN as well as an electrical examination or neurotransmitter release would prove very useful.

To further advance this research towards a translational application, I would suggest at least one study be completed where the niche neural constructs are prepared using autologous cells as opposed to human adipose derived stem cells. I would also suggest that minimally invasive methods of delivery be investigated, as minimally invasive procedures would be safer and overall more appealing to patient populations. Additionally, turning this scaffold into a manufacturable product will require further research, specifically investigating a shorter time line of decellularization. Initial efforts I would suggest include changing variables such as agitation speed as well as the shapes of the containers employed during decellularization.

REFERENCES

Contextual

1. Novak U, Kaye AH. Extracellular matrix and the brain: Components and function. *Journal of clinical neuroscience : official journal of the Neurosurgical Society of Australasia*. 2000;7:280-290

2. Carulli D, Laabs T, Geller HM, Fawcett JW. Chondroitin sulfate proteoglycans in neural development and regeneration. *Current opinion in neurobiology*. 2005;15:116-120

3. Park DS, Park JS, Yeon DS. The effects of laminin on the characteristics and differentiation of neuronal cells from epidermal growth factor-responsive neuroepithelial cells. *Yonsei medical journal*. 1998;39:130-140

4. Strong K, Mathers C, Bonita R. Preventing stroke: Saving lives around the world. *Lancet neurology*. 2007;6:182-187

5. Heidenreich PA, Trogdon JG, Khavjou OA, Butler J, Dracup K, Ezekowitz MD, Finkelstein EA, Hong Y, Johnston SC, Khera A, Lloyd-Jones DM, Nelson SA, Nichol G, Orenstein D, Wilson PW, Woo YJ. Forecasting the future of cardiovascular disease in the united states: A policy statement from the american heart association. *Circulation*. 2011;123:933-944

6. Kochanek KD XJ, Murphy SL, Minino AM, Kung HC. Deaths:Final data from 2009. *National Vital Statistics Report*. 2011;60

7. Sacco RL, Kasner SE, Broderick JP, Caplan LR, Connors JJ, Culebras A, Elkind MS, George MG, Hamdan AD, Higashida RT, Hoh BL, Janis LS, Kase CS, Kleindorfer DO, Lee JM, Moseley ME, Peterson ED, Turan TN, Valderrama AL, Vinters HV. An updated definition of stroke for the 21st century: A statement for healthcare professionals from the american heart association/american stroke association. *Stroke; a journal of cerebral circulation*. 2013;44:2064-2089

8. Bible E, Chau DY, Alexander MR, Price J, Shakesheff KM, Modo M. The support of neural stem cells transplanted into stroke-induced brain cavities by plga particles. *Biomaterials*. 2009;30:2985-2994

9. Martino G, Pluchino S, Bonfanti L, Schwartz M. Brain regeneration in physiology and pathology: The immune signature driving therapeutic plasticity of neural stem cells. *Physiological reviews*. 2011;91:1281-1304

10. Rosado-de-Castro PH, Pimentel-Coelho PM, Barbosa da Fonseca LM, de Freitas GR, Mendez-Otero R. The rise of cell therapy trials for stroke: Review of published and registered studies. *Stem cells and development*. 2013;22:2095-2111

11. Rossi F, Cattaneo E. Opinion: Neural stem cell therapy for neurological diseases: Dreams and reality. *Nature reviews. Neuroscience*. 2002;3:401-409

12. Gimble JM, Katz AJ, Bunnell BA. Adipose-derived stem cells for regenerative medicine. *Circulation research*. 2007;100:1249-1260

13. Ning H, Lin G, Lue TF, Lin CS. Neuron-like differentiation of adipose tissue-derived stromal cells and vascular smooth muscle cells. *Differentiation; research in biological diversity*. 2006;74:510-518

14. Ahmadi N, Razavi S, Kazemi M, Oryan S. Stability of neural differentiation in human adipose derived stem cells by two induction protocols. *Tissue and Cell*. 2011

15. Safford KM, Safford SD, Gimble JM, Shetty AK, Rice HE. Characterization of neuronal/glial differentiation of murine adipose-derived adult stromal cells. *Experimental neurology*. 2004;187:319-328

16. Guan J, Zhu Z, Zhao RC, Xiao Z, Wu C, Han Q, Chen L, Tong W, Zhang J, Han Q, Gao J, Feng M, Bao X, Dai J, Wang R. Transplantation of human mesenchymal stem cells loaded on collagen scaffolds for the treatment of traumatic brain injury in rats. *Biomaterials*. 2013;34:5937-5946

17. Zhang Y, Xiong Y, Mahmood A, Meng Y, Liu Z, Qu C, Chopp M. Sprouting of corticospinal tract axons from the contralateral hemisphere into the denervated side of the spinal cord is associated with functional recovery in adult rat after traumatic brain injury and erythropoietin treatment. *Brain research*. 2010;1353:249-257

18. Chen J, Sanberg PR, Li Y, Wang L, Lu M, Willing AE, Sanchez-Ramos J, Chopp M. Intravenous administration of human umbilical cord blood reduces behavioral deficits after stroke in rats. *Stroke; a journal of cerebral circulation*. 2001;32:2682-2688

19. Leong WK, Lewis MD, Koblar SA. Concise review: Preclinical studies on human cell-based therapy in rodent ischemic stroke models: Where are we now after a decade? *Stem Cells*. 2013;31:1040-1043

20. Yan ZJ, Zhang P, Hu YQ, Zhang HT, Hong SQ, Zhou HL, Zhang MY, Xu RX. Neural stem-like cells derived from human amnion tissue are effective in treating traumatic brain injury in rat. *Neurochemical research*. 2013;38:1022-1033

21. DeQuach JA, Yuan SH, Goldstein LSB, Christman KL. Decellularized porcine brain matrix for cell culture and tissue engineering scaffolds. *Tissue Engineering Part A*. 2011;17:2583-2592

22. Qian DX, Zhang HT, Ma X, Jiang XD, Xu RX. Comparison of the efficiencies of three neural induction protocols in human adipose stromal cells. *Neurochemical research*. 2010;35:572-579

23. Dhar S, Yoon ES, Kachgal S, Evans GR. Long-term maintenance of neuronally differentiated human adipose tissue-derived stem cells. *Tissue engineering*. 2007;13:2625-2632

24. Woodbury D, Schwarz EJ, Prockop DJ, Black IB. Adult rat and human bone marrow stromal cells differentiate into neurons. *Journal of neuroscience research*. 2000;61:364-370

25. Chen J, Li Y, Chopp M. Intracerebral transplantation of bone marrow with bdnf after mcao in rat. *Neuropharmacology*. 2000;39:711-716

26. Badylak SF, Taylor D, Uygun K. Whole-organ tissue engineering: Decellularization and recellularization of three-dimensional matrix scaffolds. *Annual review of biomedical engineering*. 2011;13:27-53

27. Crapo PM, Gilbert TW, Badylak SF. An overview of tissue and whole organ decellularization processes. *Biomaterials*. 2011;32:3233-3243

28. Crapo PM, Medberry CJ, Reing JE, Tottey S, van der Merwe Y, Jones KE, Badylak SF. Biologic scaffolds composed of central nervous system extracellular matrix. *Biomaterials*. 2012;33:3539-3547

29. Freytes DO, Martin J, Velankar SS, Lee AS, Badylak SF. Preparation and rheological characterization of a gel form of the porcine urinary bladder matrix. *Biomaterials*. 2008;29:1630-1637

30. Delcroix GJ, Schiller PC, Benoit JP, Montero-Menei CN. Adult cell therapy for brain neuronal damages and the role of tissue engineering. *Biomaterials*. 2010;31:2105-2120

31. Langer R, Vacanti JP. Tissue engineering. *Science*. 1993;260:920-926

32. Gilbert TW, Sellaro TL, Badylak SF. Decellularization of tissues and organs. *Biomaterials*. 2006;27:3675-3683

33. Ochoa ER, Vacanti JP. An overview of the pathology and approaches to tissue engineering. *Annals of the New York Academy of Sciences*. 2006;979:10-26

34. Chen ST, Hsu CY, Hogan EL, Maricq H, Balentine JD. A model of focal ischemic stroke in the rat: Reproducible extensive cortical infarction. *Stroke; a journal of cerebral circulation*. 1986;17:738-743

35. Longa EZ, Weinstein PR, Carlson S, Cummins R. Reversible middle cerebral artery occlusion without craniectomy in rats. *Stroke; a journal of cerebral circulation*. 1989;20:84-91

36. Shimamura N, Matchett G, Tsubokawa T, Ohkuma H, Zhang J. Comparison of silicon-coated nylon suture to plain nylon suture in the rat middle cerebral artery occlusion model. *Journal of neuroscience methods*. 2006;156:161-165

37. Takano K, Tatlisumak T, Bergmann AG, Gibson DG, 3rd, Fisher M. Reproducibility and reliability of middle cerebral artery occlusion using a silicone-coated suture (koizumi) in rats. *Journal of the neurological sciences*. 1997;153:8-11

38. Belayev L, Alonso OF, Busto R, Zhao W, Ginsberg MD. Middle cerebral artery occlusion in the rat by intraluminal suture. Neurological and pathological evaluation of an improved model. *Stroke; a journal of cerebral circulation*. 1996;27:1616-1622; discussion 1623

39. Kang SK, Lee DH, Bae YC, Kim HK, Baik SY, Jung JS. Improvement of neurological deficits by intracerebral transplantation of human adipose tissue-derived stromal cells after cerebral ischemia in rats. *Experimental neurology*. 2003;183:355-366

40. Chen J, Li Y, Wang L, Lu M, Zhang X, Chopp M. Therapeutic benefit of intracerebral transplantation of bone marrow stromal cells after cerebral ischemia in rats. *Journal of the neurological sciences*. 2001;189:49-57

41. Tupper DE, Wallace RB. Utility of the neurological examination in rats. *Acta neurobiologiae experimentalis*. 1980;40:999-1003

42. Shohami E, Novikov M, Bass R. Long-term effect of hu-211, a novel non-competitive nmda antagonist, on motor and memory functions after closed head injury in the rat. *Brain research*. 1995;674:55-62

43. Andrews EM, Tsai SY, Johnson SC, Farrer JR, Wagner JP, Kopen GC, Kartje GL. Human adult bone marrow-derived somatic cell therapy results in functional recovery and axonal plasticity following stroke in the rat. *Experimental neurology*. 2008;211:588-592

44. Li X, Blizzard KK, Zeng Z, DeVries AC, Hurn PD, McCullough LD. Chronic behavioral testing after focal ischemia in the mouse: Functional recovery and the effects of gender. *Experimental neurology*. 2004;187:94-104

45. Zhao LR, Duan WM, Reyes M, Keene CD, Verfaillie CM, Low WC. Human bone marrow stem cells exhibit neural phenotypes and ameliorate neurological deficits after grafting into the ischemic brain of rats. *Experimental neurology*. 2002;174:11-20

Figures

Figure 1: Cell Types of the central Nervous System

Biosciences (2011). "Overview of microglial cells in the CNS." www.mdbiosciences.com Retrieved September 20, 2013, from http://www.mdbiosciences.com/blog/bid/76291/Overview-of-microglial-cells-in-the-CNS

Figure 2: Type of Stroke

Wood, D. "Stroke." www.westwickhamfitness.com Retrieved September 20, 2013, from http://westwickhamfitness.com/1124/stroke/

Figure 3: Stroke Progression

"Brain Tumor." www.healthinplainenglish.com Retrieved September 20, 2013, from http://www.healthinplainenglish.com/health/cancer/brain_tumor/index.htm

Davis, C.P. "Stroke Continued." www.emedicinehealth.com Retrieved September 20, 2013, from http://www.emedicinehealth.com/stroke/page13_em.htm

Figure 4: Current Clinical Scenario

1. Rowley, H.A. "Comprehensive Stroke Imaging: The Time is Now." www.americanheartassociation.org Retrieved September 20, 2013, from chttp://my.americanheart.org/professional/General/Comprehensive-Stroke-Imaging-The-Time-is-Now_UCM_432617_Article.jsp

Figure 5: HADSCs

Gimble JM, Katz AJ, Bunnell BA. Adipose-derived stem cells for regenerative medicine. *Circulation research*. 2007;100:1249-1260

Figure 6: Markers of Neural Differentiation

Millipore. Anti-Nestin Anitbody, clone rat-401, Alexa Fluor 488 conjugate. www.millipore.com Retrieved September 20, 2013, from http://www.millipore.com/catalogue/item/mab353a4#

Abcam. Anti-MAP2 antibody [AP-20] – Neuronal Marker (ab11268). www.abcam.com Retrieved September 20, 2013, from http://www.abcam.com/map2-antibody-ap-20-neuronal-marker-ab11268.html#description_images_3

Science Cell Research Laboratories. Mouse Astrocytes (MA). www.scienceonline.com Retrieved September 20, 2013, from http://www.sciencellonline.com/site/productInformation.php?keyword=M1800

Figure 8: Collagen Scaffold

Guan J, Zhu Z, Zhao RC, Xiao Z, Wu C, Han Q, Chen L, Tong W, Zhang J, Han Q, Gao J, Feng M, Bao X, Dai J, Wang R. Transplantation of human mesenchymal stem cells loaded on collagen scaffolds for the treatment of traumatic brain injury in rats. *Biomaterials*. 2013;34:5937-5946

Figure 9: Tissue Engineered Gel

DeQuach JA, Yuan SH, Goldstein LSB, Christman KL. Decellularized porcine brain matrix for cell culture and tissue engineering scaffolds. *Tissue Engineering Part A*. 2011;17:2583-2592

APPENDIX A: Extra Figures

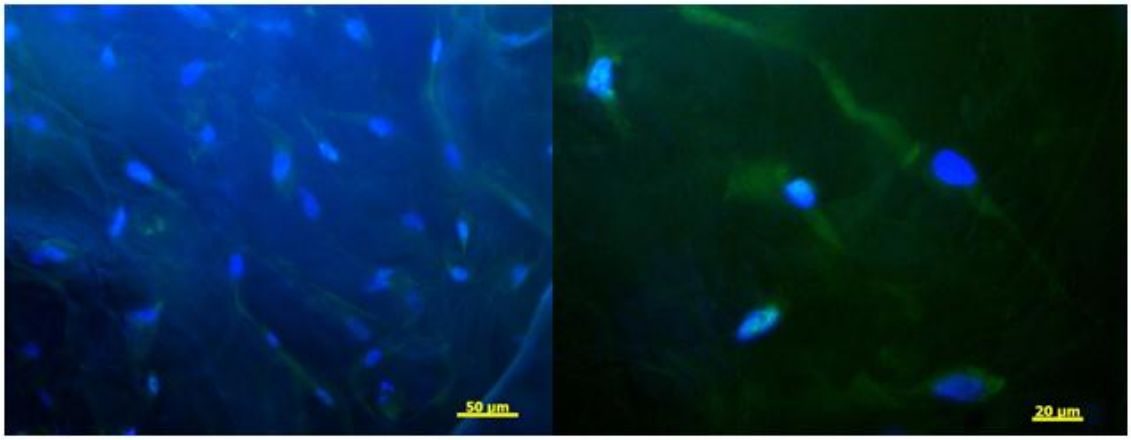

Extra Figure 1: Map-2 staining overlayed with DAPI nuclear stain to demonstrate staining is in fact co-localized with cell nuclei.

Extra figure 1 clearly illustrates that the Map-2 expression previously shown is in fact co-localized with a cell nucleus. These images were provided as an additional measure to ensure the green fluorescence observed is in fact positive staining. This further confirms our previous conclusions that these cells are in fact expressing and maintaining the expression of the neuron marker Map-2.

Extra figures 2 and 3 were provided to enable the viewer to directly compare the neural marker expression between groups. At lower magnification, it is clear the previously represented expression is representative. Extra figure 3 clearly portrays the developing extensions and projections of the cells and provides clearer evidence that the cells have maintained marker expression.

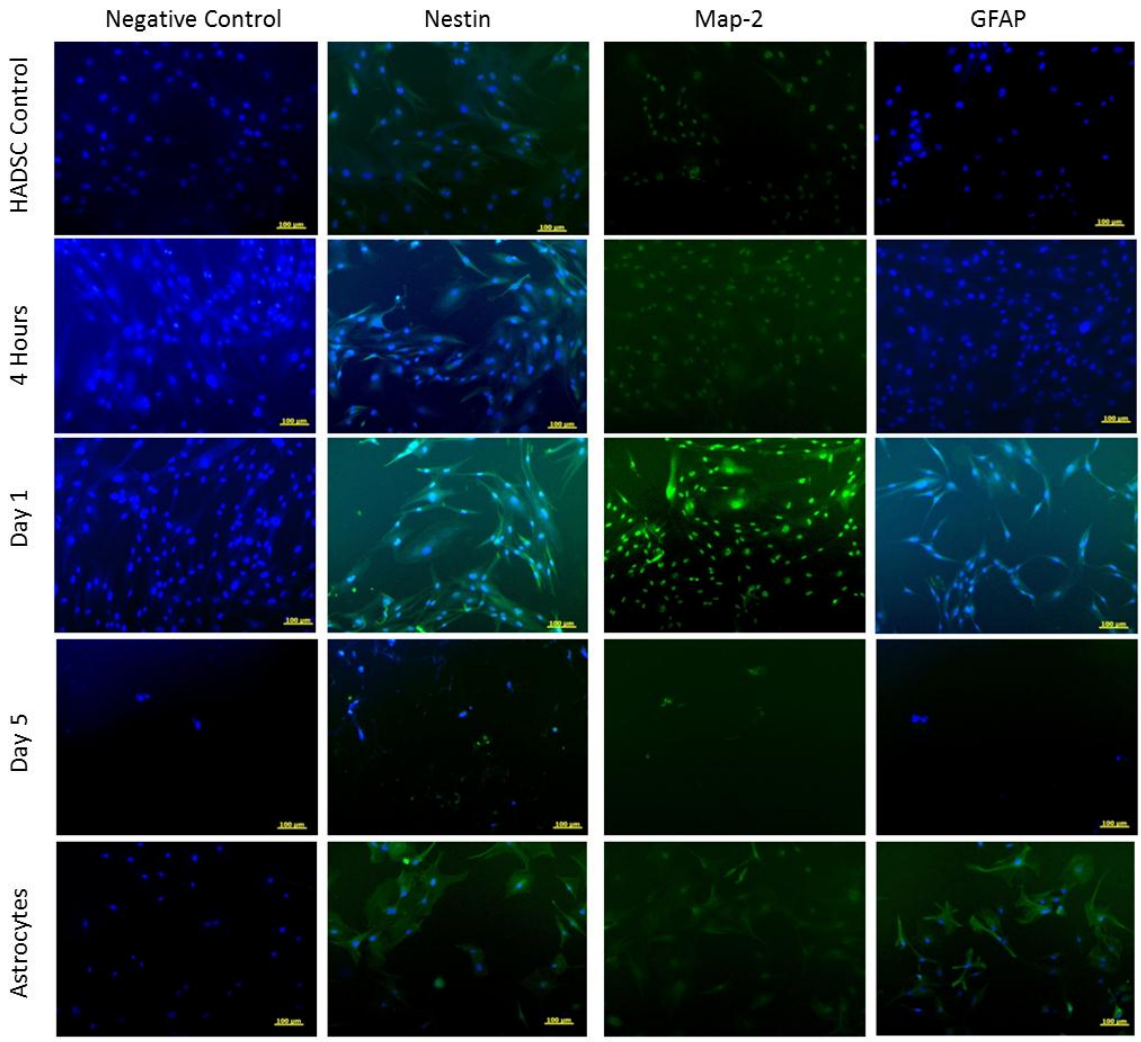

Extra Figure 2: Comparative matrix of in vitro studies at lower magnification to demonstrate representativeness of staining.

Both figures 2 and 3 support the previously reported conclusions that we have replicated the neural induction process for human adipose derived stem cells seedded onto plastic. Up to the 5 day timepoint, these cells are morphologically changing and expressing key neural proteins. However, by day 5 a lack of viable cell presence hinders analysis of protein marker expression, although extra figure 2 seems to indicate a degree of expression was still maintained.

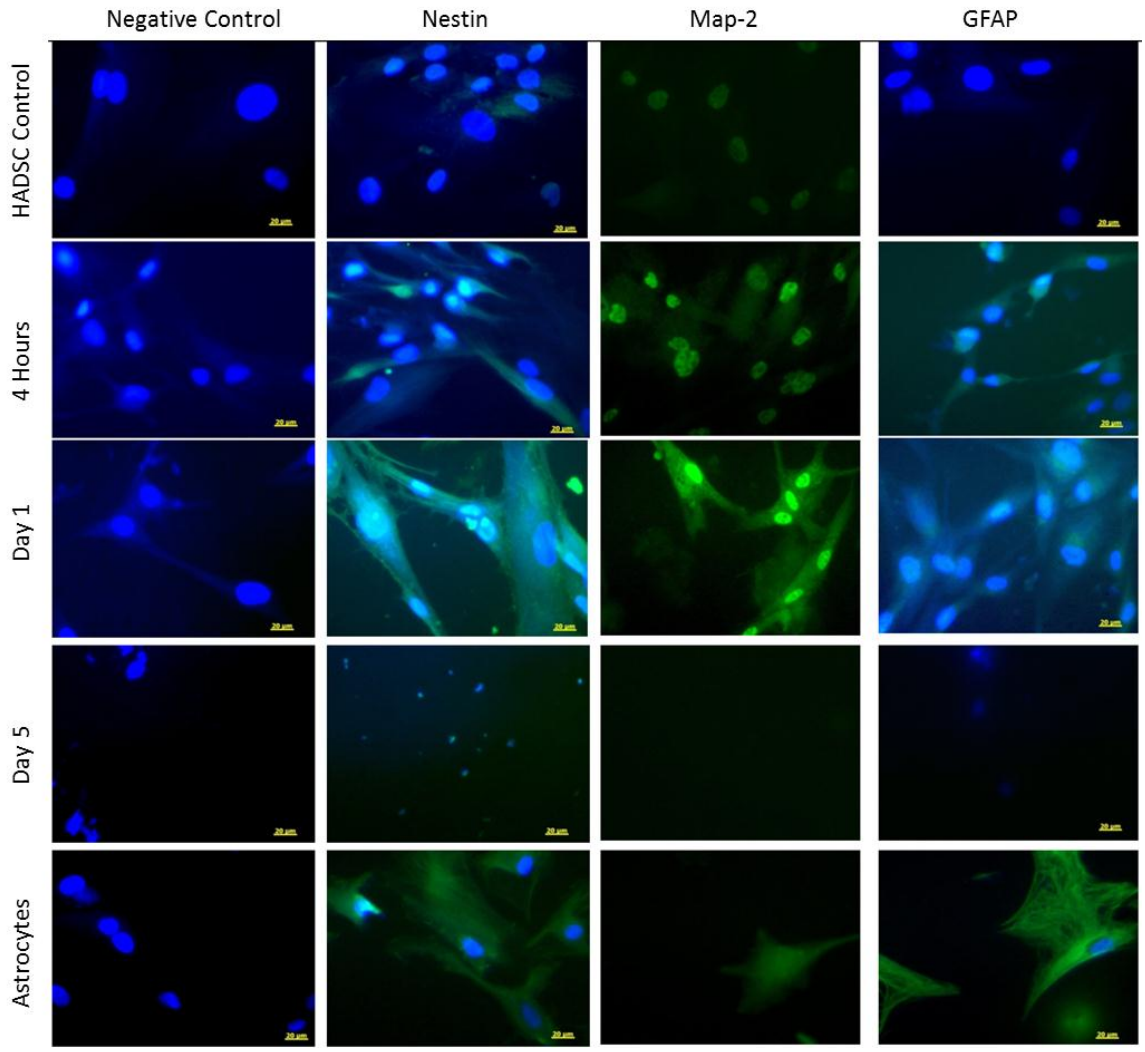

Extra Figure 3: Comparative matrix of in vitro studies at higher magnification. Morphological changes as well as the extent of co-localized staining is more readily apparent.

Extra figure 4 illustrates the extreme morphological changes observed within the niche neural constructs. Cells appear to consist of one large cell body with extensive projections. These projections extend up to 450μm in some cases. The arrows point to such projections. The box at the right, outlines an entire cell, which morphological analysis dictates is phenotypically a neuron. This analysis further bolsters our claims that this niche neural construct can produce and maintain neurons.

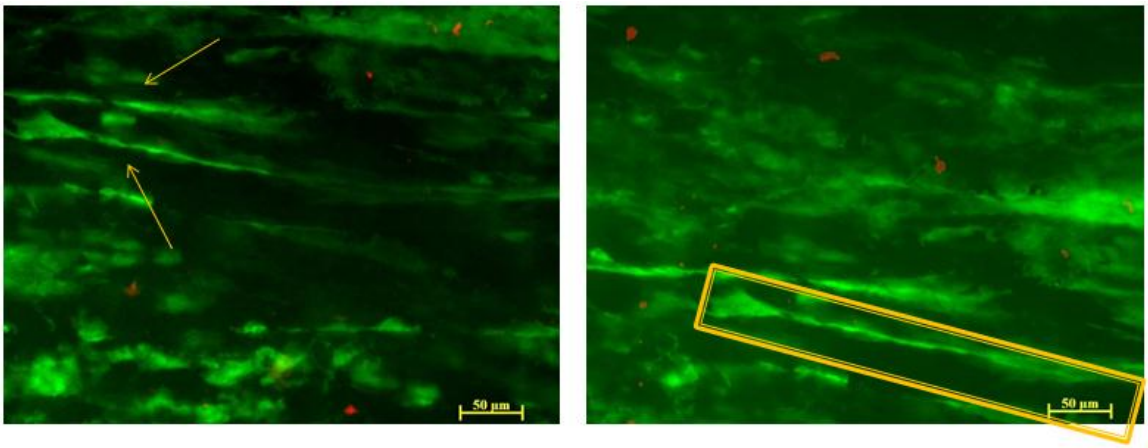

Extra Figure 4: Live/Dead staining of niche neural constructs (representative of study 6, cells seeded onto scaffolds with no induction step where the media was replaced daily). The cells have formed large cell bodies with projections that elongate as much as 450µm.

Extra figures 5 and 6 provide further in depth analysis of the fate of the implanted HADSCs. Consistent with the previously presented IHC staining, there is no GFAP expression within the construct area. More significantly, we have confirmed the implanted HADSCs have not committed to an astrocyte lineage. As previously described

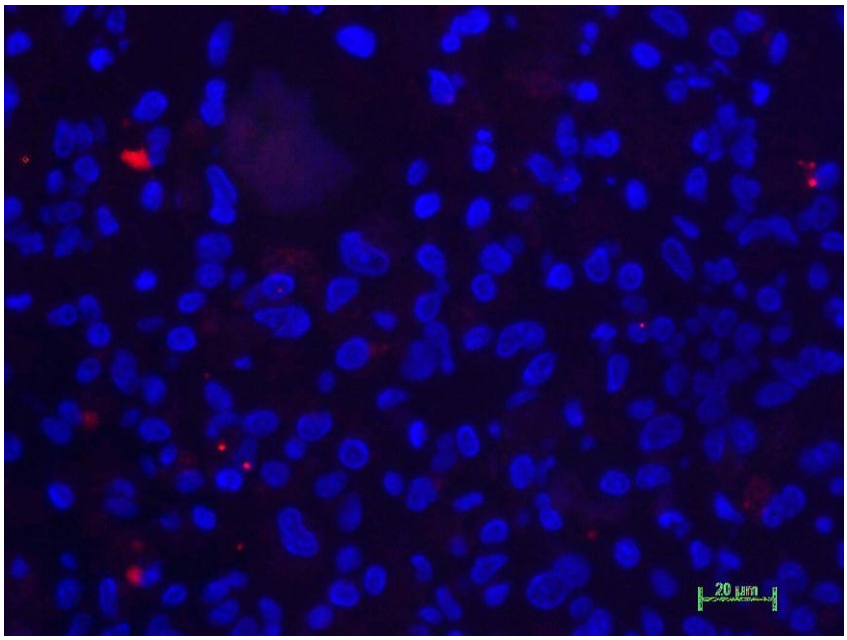

Extra Figure 5: Human mitochondria - GFAP Double Staining. Results are consistent with the IHC results presented in figure 62.Green indicates GFAP. Red indicates human mitochondria. Blue indicates DAPI nuclear staining.

a large portion of these implanted HADSCs express Map-2, indicative of commitment to a neuron lineage. To further confirm this and to very preliminarily assess the functionality of these neurons, expression of Synapsin I, a key protein involved in synaptic connections, was analyzed. As seen below, a significant amount of Synapsin I expression is observed, further confirming a neuron presence within the construct area indicating a degree of functionality of these neurons.

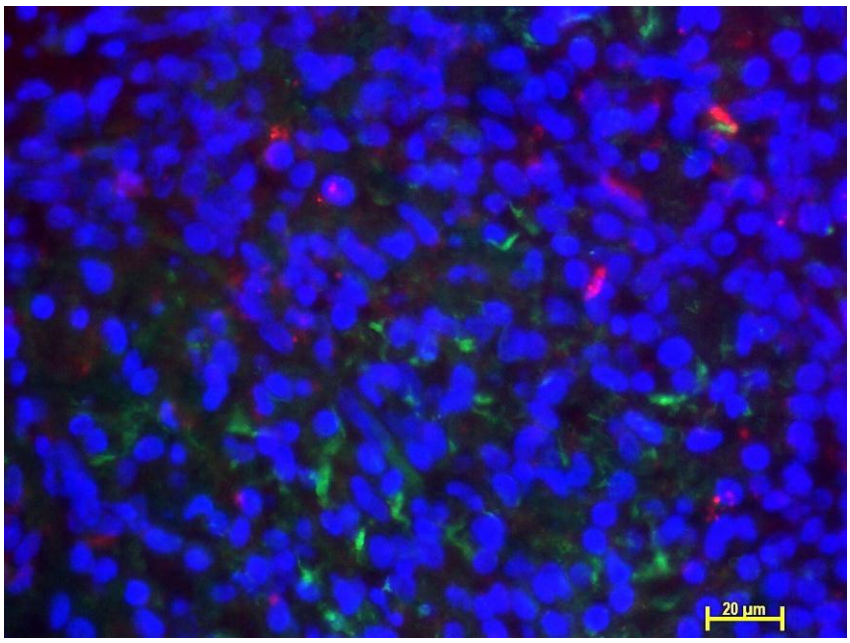

Extra Figure 6: Human mitochondria – Synapsin I Double Staining. Explants were stained for Synapsin I, a key protein of synaptic connections, as a preliminary assessment of the functionality of the neurons observed within the construct area. Green indicates Synapsin I. Red indicates human mitochondria. Blue indicates DAPI nuclear staining.

Staining for myelin was another measure employed as a preliminary functional assessment of the neurons within the construct area. The patchy nature and overall faintness of the staining observed in the construct area does not permit any myelin-based conclusions at this time.

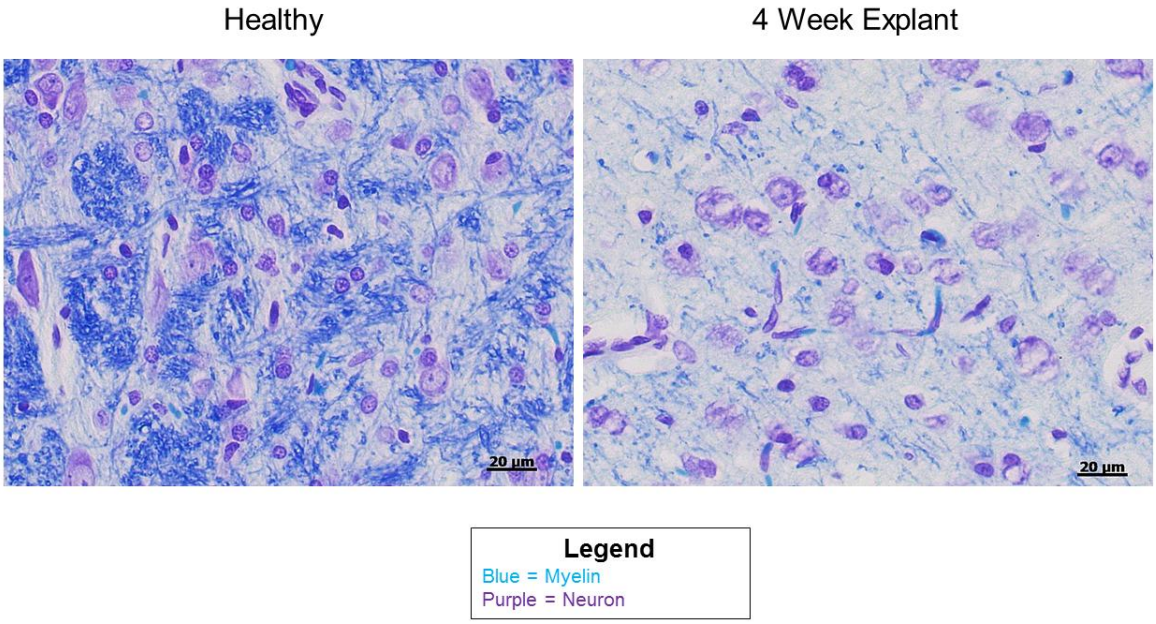

Extra Figure 7: Luxol Fast Blue Staining for Myelin. Explants exhibit blue staining; however, the inconsistent and faint nature of staining could indicate a false positive or background staining. Overall, this preliminary myelin assessment is inconclusive.